nagra.

Arbeitsbericht NAB 21-20

TBO Marthalen-1-1: Data Report

Dossier IV
Microfacies, Bio- and Chemo-stratigraphic Analysis

September 2021

S. Wohlwend, H.R. Bläsi, S. Feist-Burkhardt,
B. Hostettler, U. Menkveld-Gfeller,
V. Dietze & G. Deplazes

National Cooperative
for the Disposal of
Radioactive Waste

Hardstrasse 73
P.O. Box 280
5430 Wettingen
Switzerland
Tel. +41 56 437 11 11

www.nagra.ch

nagra.

Arbeitsbericht NAB 21-20

TBO Marthalen-1-1: Data Report

Dossier IV Microfacies, Bio- and Chemo-stratigraphic Analysis

September 2021

S. Wohlwend[1], H.R. Bläsi[2], S. Feist-Burkhardt[3,4], B. Hostettler[5], U. Menkveld-Gfeller[5], V. Dietze[6] & G. Deplazes[7]

[1] Geological Institute, ETH Zurich
[2] Geo-Consulting, Wünnewil, Switzerland
[3] SFB Geological Consulting & Services, Ober-Ramstadt, Germany
[4] Département des Sciences de la Terre, Université de Genève
[5] Natural History Museum Bern
[6] Nördlingen, Germany
[7] Nagra

Keywords:
MAR1-1, Zürich Nordost, TBO, deep drilling campaign, microfacies, lithostratigraphy, biostratigraphy, ammonite stratigraphy, palynostratigraphy, chemostratigraphy, dinoflagellate cysts, stable carbon isotopes

National Cooperative for the Disposal of Radioactive Waste

Hardstrasse 73
P.O. Box 280
5430 Wettingen
Switzerland
Tel. +41 56 437 11 11

www.nagra.ch

Nagra Arbeitsberichte ("Working Reports") present the results of work in progress that have not necessarily been subject to a comprehensive review. They are intended to provide rapid dissemination of current information.

This NAB aims at reporting drilling results at an early stage. Additional borehole-specific data will be published elsewhere.

In the event of inconsistencies between dossiers of this NAB, the dossier addressing the specific topic takes priority. In the event of discrepancies between Nagra reports, the chronologically later report is generally considered to be correct. Data sets and interpretations laid out in this NAB may be revised in subsequent reports. The reasoning leading to these revisions will be detailed there.

This Dossier was prepared by a project team consisting of:
S. Wohlwend (sampling, chemostratigraphy, conceptualisation and compilation)
H.R. Bläsi (microfacies)
S. Feist-Burkhardt (palynostratigraphy)
B. Hostettler, U. Menkveld-Gfeller, V. Dietze (ammonite stratigraphy)
G. Deplazes (project management and conceptualisation)

Editorial work: P. Blaser and M. Unger

The Dossier has greatly benefitted from technical discussions with, and reviews by, external and internal experts. Their input and work are very much appreciated.

Table of Contents

List of Tables

List of Figures

List of Appendices

1 Introduction

1.1 Context

To provide input for site selection and the safety case for deep geological repositories for radioactive waste, Nagra has drilled a series of deep boreholes ("Tiefbohrungen", TBO) in Northern Switzerland. The aim of the drilling campaign is to characterise the deep underground of the three remaining siting regions located at the edge of the Northern Alpine Molasse Basin (Fig. 1-1).

In this report, we present the results from the Marthalen-1-1 borehole.

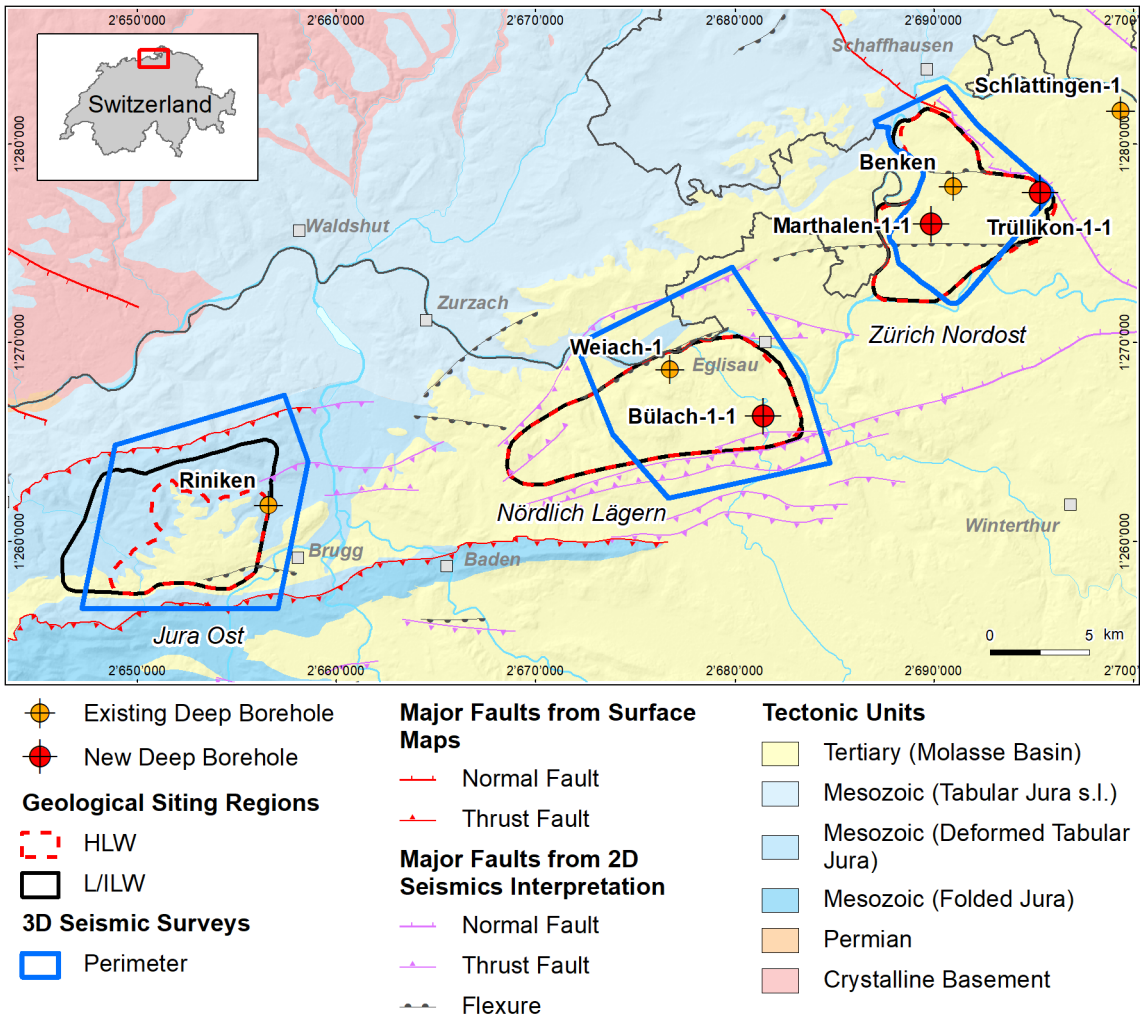

Fig. 1-1: Tectonic overview map with the three siting regions under investigation

1.2 Location and specifications of the borehole

The Marthalen-1-1 (MAR1-1) exploratory borehole is the third borehole drilled within the framework of the TBO project. The drill site is located in the western part of the Zürich Nordost siting region (Fig. 1-2). The vertical borehole reached a final depth of 1'099.25 m (MD)[1]. The borehole specifications are provided in Tab. 1-1.

Tab. 1-1: General information about the MAR1-1 borehole

Siting region	Zürich Nordost
Municipality	Marthalen (Canton Zürich / ZH), Switzerland
Drill site	Marthalen-1 (MAR1)
Borehole	Marthalen-1-1 (MAR1-1)
Coordinates	LV95: 2'689'889.946 / 1'275'956.932
Elevation	Ground level = top of rig cellar: 399.48 m above sea level (asl)
Borehole depth	1'099.25 m measured depth (MD) below ground level (bgl)
Drilling period	9th February 2020 – 14th July 2020 (spud date to end of rig release)
Drilling company	Daldrup & Söhne AG
Drilling rig	Wirth B 152t
Drilling fluid	Water-based mud with various amounts of different components such as[2]: 55 – 460 m: Bentonite & polymers 460 – 881 m: Potassium silicate & polymers 881 – 961 m: Sodium silicate & polymers 961 – 1'099.25 m: Sodium chloride & polymers

The lithostratigraphic profile and the casing scheme are shown in Fig. 1-3. The main lithostratigraphic boundaries in the MAR1-1 borehole are shown in Fig. 1-4.

[1] Measured depth (MD) refers to the position along the borehole trajectory, starting at ground level, which for this borehole is the top of the rig cellar. For a perfectly vertical borehole, MD below ground level (bgl) and true vertical depth (TVD) are the same. In all Dossiers depth refers to MD unless stated otherwise.

[2] For detailed information see Dossier I.

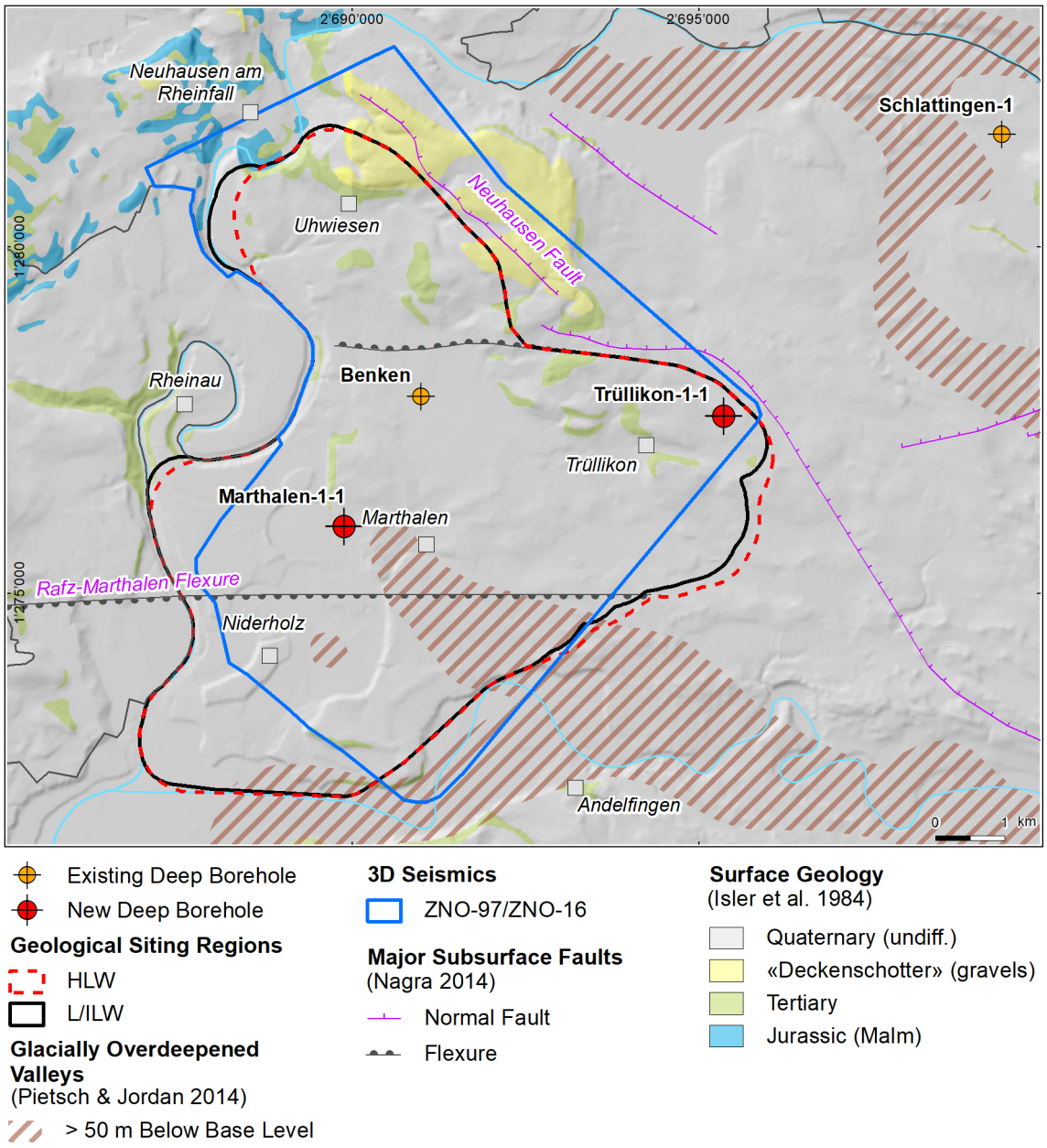

Fig. 1-2: Overview map of the investigation area in the Zürich Nordost siting region with the location of the MAR1-1 borehole in relation to the boreholes Benken, Schlattingen-1 and TRU1-1

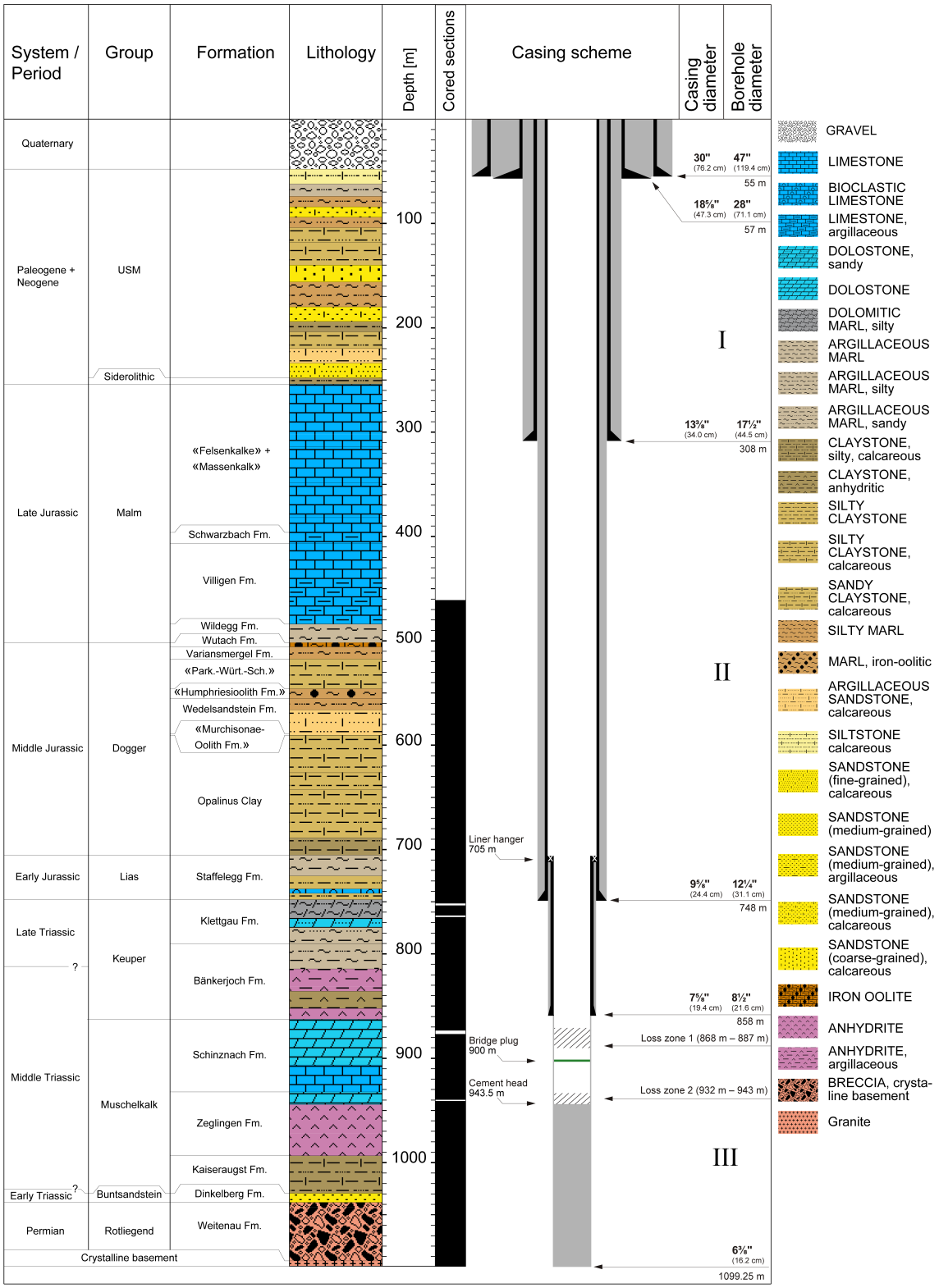

Fig. 1-3: Lithostratigraphic profile and casing scheme for the MAR1-1 borehole[3]

[3] For detailed information see Dossier I and III.

1.3 Documentation structure for the MAR1-1 borehole

NAB 21-20 documents the majority of the investigations carried out in the MAR1-1 borehole, including laboratory investigations on core material. The NAB comprises a series of stand-alone dossiers addressing individual topics and a final dossier with a summary composite plot (Tab. 1-2).

This documentation aims at early publication of the data collected in the MAR1-1 borehole. It includes most of the data available approximately one year after completion of the borehole. Some analyses are still ongoing (e.g. diffusion experiments, analysis of veins, hydrochemical interpretation of water samples) and results will be published in separate reports.

The current borehole report will provide an important basis for the integration of datasets from different boreholes. The integration and interpretation of the results in the wider geological context will be documented later in separate geoscientific reports.

Tab. 1-2: List of dossiers included in NAB 21-20

Black indicates the dossier at hand.

Dossier	Title	Authors
I	TBO Marthalen-1-1: Drilling	P. Hinterholzer-Reisegger & B. Garitte
II	TBO Marthalen-1-1: Core Photography	D. Kaehr & M. Gysi
III	TBO Marthalen-1-1: Lithostratigraphy	P. Jordan, P. Schürch, H. Naef, M. Schwarz, R. Felber, T. Ibele & M. Gysi
IV	TBO Marthalen-1-1: Microfacies, Bio- and Chemostratigraphic Analyses	S. Wohlwend, H.R. Bläsi, S. Feist-Burkhardt, B. Hostettler, U. Menkveld-Gfeller, V. Dietze & G. Deplazes
V	TBO Marthalen-1-1: Structural Geology	A. Ebert, L. Gregorczyk, E. Hägerstedt, S. Cioldi & M. Gysi
VI	TBO Marthalen-1-1: Wireline Logging and Micro-hydraulic Fracturing	J. Gonus, E. Bailey, J. Desroches & R. Garrard
VII	TBO Marthalen-1-1: Hydraulic Packer Testing	R. Schwarz, S.M.L. Hardie, H.R. Müller, S. Köhler, A. Pechstein
VIII	TBO Marthalen-1-1: Rock Properties, Porewater Characterisation and Natural Tracer Profiles	L. Aschwanden, L. Camesi, T. Gimmi, A. Jenni, M. Kiczka, U. Mäder, M. Mazurek, D. Rufer, H.N. Waber, P. Wersin, C. Zwahlen & D. Traber
IX	TBO Marthalen-1-1: Rock-mechanical and Geomechanical Laboratory Testing	E. Crisci, L. Laloui & S. Giger
X	TBO Marthalen-1-1: Petrophysical Log Analysis	S. Marnat & J.K. Becker
	TBO Marthalen-1-1: Summary Plot	Nagra

1.4 Scope and objectives of this dossier

The dossier at hand complements the lithostratigraphic report (Dossier III) on the MAR1-1 borehole. The report documents data on microfacies analysis, ammonite- and palynostratigraphy as well as detailed geochemical (C, O and N isotopes) analyses. Preliminary results of these analyses already existed at data-freeze (14.09.2020), two months after the end of drilling operations and were integrated into the lithostratigraphic discussion and lithostratigraphic boundary definition (Dossier III).

The objectives of this report focusing on the Opalinus Clay and its confining units are:

- to specify the macroscopic description by a detailed microfacies analysis (components, matrix, cements),
- to allow a microfacies comparison of specific horizons, for example hardgrounds of the upper Opalinus Clay,
- to provide additional data on the diagenetic history of the sediment,
- to recover macrofossils from the stratigraphic interval of interest which are significant for facies changes and chronostratigraphic data,
- to compile an additional independent dataset of palynomorphs for chronostratigraphic data,
- to provide detailed geochemical (C, O and N isotopes) analyses with one metre spacing from the stratigraphic interval of interest,
- to allow a chemostratigraphic correlation (stable isotopes) with other deep boreholes in the three siting regions,
- to support the definition of the lithostratigraphic units.

The detailed stratigraphy of the MAR1-1 borehole with core depth in metres can be found in Fig. 1-4. The stratigraphic intervals of interest for the different investigations (microfacies analysis, ammonite- and palynostratigraphy and geochemical analyses) and their specific sampling intervals are visualised in Fig. 1-5 with respect to the 1:5'000 lithostratigraphic profile.

All depths labelled with metres [m] in this report refer to "m MD core depth" if not stated otherwise.

TBO MARTHALEN-1-1

System / Period		Group	Formation	Metres MD	Member / Sub-unit
Quaternary				48	
Paleogene / Neogene		USM		248	
		Siderolithic		254	
Jurassic	Late	Malm	«Felsenkalke» + «Massenkalk»	396.1	
			Schwarzbach Fm.	406.9	
			Villigen Fm.	484.02	
			Wildegg Fm.	500.69	Effingen Mb.
				501.80	Birmenstorf Mb. and «Glaukonitsandmergel Bed»
	Middle	Dogger	Wutach Fm.	505.75	
			Variansmergel Fm.	517.43	
			«Parkinsoni-Württembergica-Sch.»	545.93	
			«Humphriesioolith Fm.»	550.66	
				554.46	
				555.23	
			Wedelsandstein Fm.	589.17	
			«Murchisonae-Oolith Fm.»	590.35	
			Opalinus Clay	626.41	«Sub-unit with silty calcareous beds»
				642.77	«Upper silty sub-unit»
				688.88	«Mixed clay-silt-carbonate sub-unit»
				705.40	«Clay-rich sub-unit»
	Early	Lias	Staffelegg Fm.	712.10	Gross Wolf Mb.
				721.48	Rietheim Mb.
				724.08	Breitenmatt Mb. and Rickenbach Mb.
				725.13	Grünschholz Mb.
				737.74	Frick Mb.
				741.98	Beggingen Mb.
				747.83	Schambelen Mb.
Triassic	Late	Keuper	Klettgau Fm.	765.75	Gruhalde Mb.
				774.71	Seebi Mb.
				782.46	Gruhalde Mb.
				784.02	Gansingen Mb.
				790.12	Ergolz Mb.
	?812		Bänkerjoch Fm.	814.28	«Claystone with anhydrite nodules»
				835.66	«Cyclic sequence»
				852.34	«Thin-layered anhydrite and claystone sequence»
				862.52	«Dolomite and anhydrite» and «Banded massive anhydrite»
	Middle	Muschelkalk	Schinznach Fm.	867.61	Asp Mb.
				906.44	Stamberg Mb.
				910.27	Liedertswil Mb.
				932.24	Leutschenberg Mb. and Kienberg Mb.
			Zeglingen Fm.	944.29	«Dolomitzone»
				993.50	«Sulfatzone»
			Kaiseraugst Fm.	1'001.90	«Orbicularismergel»
				1'022.44	«Wellenmergel»
	?1030			1'029.45	«Wellendolomit»
	E.	Bsst.	Dinkelberg Fm.	1'037.98	
Permian		Rotlieg.	Weitenau Fm.	1'094.08	
			Crystalline basement	1'099.25	Final depth

Fig. 1-4: Marthalen-1-1 stratigraphy with core depth in metres [m MD]

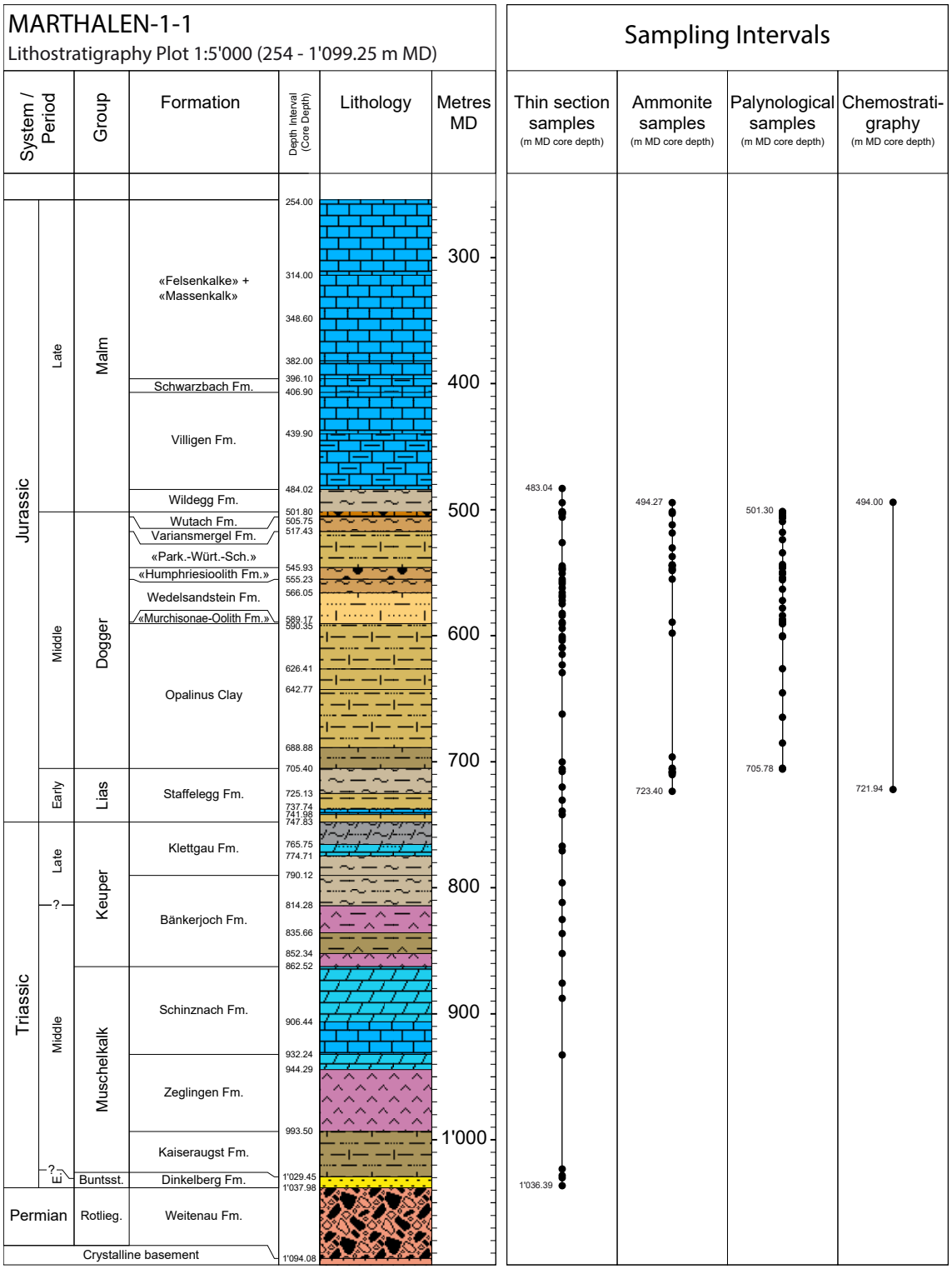

Fig. 1-5: Lithostratigraphy plot (1:5'000) from the Mesozoic succession with the individual sampling intervals for thin sections, macrofossils, palynological analysis and chemostratigraphy

1:5'000 stratigraphic plot modified from Dossier III.

2 Methods

2.1 Microfacies

Thin section preparation

All thin sections (TS) were cut edgewise from the core so that the long side is parallel to the coring direction and therefore covers as much of the stratigraphy as possible. The mean depth of the thin section corresponds to the Sample ID. Therefore, thin sections containing lithological boundaries may have Sample IDs that fall into only one of the two described intervals. However, the lower or upper range on the thin section still covers the interval. A list of all thin sections with their sampling range and Sample ID can be found in Appendix A1 of this report.

The thin sections from calcareous lithologies with a standard length of 4 cm were prepared at the University of Basel. Lithologies sensitive to water such as claystones and argillaceous sediments (swelling of clay minerals) or evaporates (dissolution of evaporitic minerals) were prepared by the Thin Section Lab (TSL) using petroleum. Thin sections prepared by TSL are only 3 cm long. For better identification of the carbonate minerals calcite, Fe-calcite and Fe-dolomite, the left half of the thin sections was stained applying the technique of Dickson (1965). Thin sections with a macroscopic porosity were impregnated during preparation using a blue coloured epoxy resin to estimate the percentage of their porosity.

Thin section analyses

57 thin sections were analysed using a Zeiss polarisation microscope. First, all allochemical components, biogenic particles, siliciclastics, matrix and diagenetic alterations as neomorphic minerals, cements and replacements were studied. Then, to obtain the percentage of the components etc., 100 points were counted with a net micrometer ocular. For detrital quartz-bearing thin sections, the average grain size was evaluated in millimetres. To count inhomogeneous sediments, two different sections were looked at and averaged. A selection of 24 thin section photographs for microfacies analysis is documented in Appendix B (Figs. B-1 to B-24).

Components, matrix and cements (definitions)

To describe thin sections, several allochemical components (described below) were counted, and their numbers are documented in Section 3.1 ('Microfacies'). Some of the specific terms used for the components or matrix are explained as follows:

Clay matrix, micrite, microsparite (or pseudosparite): Sedimented mud consisting of clay minerals, other very small silicate grains (i.e. clay matrix) and/or microcrystalline carbonate ooze (i.e. micrite). Microsparite is defined as a mosaic of small calcite crystals formed by aggrading neomorphism; originally, it was micrite and not a diagenetic pore-filling cement. Alternatively, microsparite could also be the product of dedolomitisation as seen in the «Felsenkalke» and «Massenkalk» in thin sections of BUL1-1 (Wohlwend et al. 2021a).

Dolomitic matrix: primary microcrystalline dolostone ooze.

Limonitic matrix: Calcite micrite mixed with microcrystalline limonitic grains grown during diagenesis.

Limonitic echinoderms, limonitic bivalves: Fragments, parts of echinoderms and bivalves, with limonite filling the skeletal structure of the fossil.

Fe-stromatolites and stromatolitic clasts: Iron-mineralised microbial mats and/or microbial clasts.

Fe-ooids or iron-ooids: Limonitic/goethitic or chamositic ooids, with a visible concentric structure; some iron-ooids are replaced by calcite (calcitic iron-ooids), a few of them show relicts of iron mineral layers (MAR1-1-589.23).

Intraclasts: Rock fragments of early diagenetic cemented sediment, reworked and sedimented in the same sedimentary environment.

Calcite cement (sparite): "Normal" cement, calcite crystals grown – filled in – within the primary pore space or in leached components. In this column, the amount of calcite crystal pseudomorphs after gypsum was noted.

"Stellate cement": Calcite "cement" grown within the matrix and not filling primary or secondary pore space (e.g. MAR1-1-741.95). The calcite crystals form small "stellates", i.e. a habitus typical for "hiatus beds" (firm-, hardgrounds) (Wetzel & Allia 2000) or "hiatus concretions" (Voigt 1968).

Cone-in-cone calcite: Rows of piled calcite cones grown during diagenesis which were named "Tutenmergel" in the Swabian realm.

(Fe)-Dolomite: Normally dolomite rhombohedrons that originated during diagenesis; in special cases, the dolomite replaces gypsum crystals that were sedimented as detritical gypsum crystals. In some cases, the rhombohedrons consist of iron-dolomite, which are stained blue after the thin section staining.

Dedolomite: Calcite replacement of dolomite: each single dolomite rhombohedron is replaced by a few smaller calcite crystals. When it was a total dolostone and the calcitic replacement has been completed, the result is a thoroughly crystalline, sparitic/ microsparitic limestone; e.g. TS from TRU1-1 (Wohlwend et al. 2021b). In addition, another dedolomite type exists with larger calcite crystals jointly replacing a few dolomite crystals, thus forming a calcite mosaic similar to marble.

Anhydrite: Present in various forms: as a rock-forming mineral, as a vein mineral, mainly replacing "Fasergips", and as cement in sandstones (e.g. Ergolz Member of the Klettgau Formation; e.g. TS from TRU1-1; Wohlwend et al. 2021b).

Quartz cement: Authigenic quartz rims grown during diagenesis around detrital quartz grains; also quartz/chalcedony in silicified bivalves (MAR1-1-569.18).

Porosity: Thin sections with a macroscopic porosity were impregnated during preparation using a blue coloured epoxy resin to estimate the volume percentage (vol.-%) of their porosity.

Hardground: Thin sections from hardgrounds document synsedimentarily cemented and lithified carbonate layers which have been exposed on the seafloor. During that time period, the hardgrounds are therefore mostly encrusted and bored by organisms and may consist of early marine calcite cements and are in parts mineralised by iron and manganese oxides or calcium phosphates.

2.2 Ammonite preparation

The MAR1-1 cores were carefully examined for macrofossils at the Würenlingen (Canton Aargau) core storage facility. The cores were examined for ammonites and other macrofossils on the bedding and fractured surfaces as well as on the outer surface of the core; the core itself was not broken open. A list of all samples with their sampling range and Sample ID can be found in Appendix A2 of this report. In addition to ammonites, other conspicuous fossils were identified to the extent possible and entered in the list (Appendix A3), even when they were not subsequently, or only occasionally, recovered. The ammonites were then secured from the core and brought to the Natural History Museum in Bern, where they were prepared, documented, and afterwards archived in the earth sciences collection.

For the preparation, we used mechanical methods such as air tools and fine sandblasting equipment as well as a chemical etching method using potassium hydroxide (KOH). Sodium hydrogen carbonate was mainly used as abrasive. In one case, also some biloxite (corundum) was utilised (specimen from 546.40 m). Residual material from sawing and preparing six ammonite samples (marked in grey in Appendix A4) was used as material for palynological samples. Before being photographed, we applied ammonium chloride steam to the fossils to make the fine structure more visible. A selection of ammonites is documented on four plates (Plate I – IV) in Appendix C.

The names of several ammonite taxa are followed by a question mark, for example in *Pleydellia*? sp. The question mark after the genus name was used to indicate a question regarding the correct taxonomical assignment of the species to the genus.

2.3 Palynological sample preparation and quantitative analysis

Palynolgical processing of the rock samples was carried out by PLS Palynological Laboratory Services Ltd. (Holyhead, Anglesey, UK). Processing follows the standard protocol (Wood et al. 1996) using concentrated HCl and concentrated HF, followed by a short oxidation with HNO_3 and, if necessary, treatment with ultrasound. The residues are sieved at a mesh size of 15 µm. Residues are mounted on microscope slides and analysed using transmitted light microscopy. A list of all samples with their sampling range and Sample ID can be found in Appendix A4 of this report.

Two consecutive counts were carried out in the quantitative microscopic analysis. In a first count 200 grains of all palynomorphs were counted and the number of dinoflagellate cysts is noted (column 'DA *Dinocysts (count 1)*' in Appendix D1). In a second count, only dinoflagellate cysts are counted until a total of 100 dinoflagellate cysts is reached. The reminder of the slide is checked for additional, out-of-count species. Taxa recorded out of count are marked with a '+' in the range chart. Taxa only questionably identified are marked with a '?' in the range chart. Occurrences of fungal remains are recorded semi-quantitatively (R = Rare, O = Occasional, C = Common, A = Abundant, S = Superabundant).

Results are illustrated using the software package StrataBugs v2.1 (Appendices D1 and D2). Numerical age dates used for the Composite Standard and the Depth/Age plot are in line with those of the *Geologic Time Scale 2016* (Ogg et al. 2016). On the range chart Appendix D1 several abbreviations are used (AC = Acritarchs, ALBO = Algae, *Botryococcus* and *Pediastrum*, ALPR = Algae, Prasinophytes, ALZY = Algae, Zygnematophyceae, DA = Dinocyst abundance, DC = Dinoflagellate cysts, FT = Foraminiferal test linings, FU = Fungi, MP = Miscellaneous palynomorphs, SP = Spores and pollen. Several dinoflagellate cyst taxa contain a question mark in the name, as for example in *Evansia*? *eschachensis*. The question mark after the genus name indicates uncertainty regarding the correct taxonomical assignment of the species to the genus.

2.4 Chemostratigraphy

Sampling

The sampling of the MAR1-1 borehole focused primarily on the Dogger and Lias Groups and therefore primarily on clay mineral-rich layers of the Opalinus Clay. The sampling resolution was one metre, except for some intervals with denser sampling density (mainly hardgrounds, condenced intervals and the Rietheim Member of the Staffelegg Formation). All 330 samples were drilled with a micro-drill. In general clay mineral-rich lithologies were sampled. Diagenetic calcite and siderite veins and nodules were avoided. The drilled powder amounted to around 1 g of material. A list of specific samples (n = 40) with results from calcareous beds, calcareous concretions, and macrofossils (e.g. belemnites) can be found in Appendix E1 of this report.

Inorganic (carbonate) analyses

The 329 samples were analysed for **stable carbon** ($\delta^{13}C_{carb}$) and **oxygen isotope** ($\delta^{18}O_{carb}$) of bulk carbonate, 283 continuous samples (roughly in metre resolution) and additional 46 samples from specific calcareous beds in the Opalinus Clay and its confining units (Appendix E1). Varying amounts of powder to reach approximately 120 µg of carbonate in the vial were weighed using a Mettler Toledo MT5 Fact microbalance in 12 ml vacutainers. The headspace was flushed with pure He, and then the samples were reacted with 100% phosphoric acid at 72 °C in a ThermoFisher GasBench II carbonate device connected to a ThermoFisher Delta V PLUS mass spectrometer. The instrument is calibrated with international carbonate standards NBS19 and NBS18 distributed by the International Atomic Energy Agency (IAEA), Vienna and internal standards (MS2 "Carrara marble"; $\delta^{13}C_{carb}$ = 2.16‰, $\delta^{18}O_{carb}$ = -1.85‰). The reproducibility of the measurements based on replicated standards was ± 0.05‰ for $\delta^{13}C_{carb}$ and ± 0.06‰ for $\delta^{18}O_{carb}$. All isotope measurements were performed at the Stable Isotope Laboratory of the ETH Zurich (Geological Institute). The isotope values are reported in the conventional delta notation with respect to the Vienna Pee Dee Belemnite (VPDB).

The **Total Carbonate content** (TCarb) was calculated based on a calibration using extracted CO_2 from the known weight of the internal standard material (MS2), which is composed to 100% of carbonate (calcite). The mean area of the m/z 44 peak (corresponding to the most abundant isotopologue $^{12}C^{16}O_2$) in the mass spectrometer allows the carbonate content to be estimated from the individual bulk rock samples. The individual uncertainty for TCarb, represents the average from all standard deviations from the MS2 and is ± 5.83%. However, the TCarb values calculated from the reaction of the phosphoric acid with the bulk rock, only reflect the carbonate that was able to react during the reaction time (~ 60 min). However, ankerite and especially siderite, for example, roughly require 60 h reaction time for full dissolution at 70 °C (Fernandez et al. 2016). Therefore, the calculated carbonate content (TCarb) does not completely represent the total amount of all different carbonates. The data reflect a mixed signal composed mostly of calcite and dolomite with a smaller component of the other more resistant carbonates (see also Wohlwend et al. 2019a).

Organic analyses

The powders remaining after inorganic analysis from 217 samples were decarbonated in quantities of less than 1 g in 10 ml of 3 M HCl for 12 h in 15 ml centrifuge tubes, to ensure the complete removal of carbonate. For neutralisation purposes, the residue was subsequently washed three times with deionised water, and then centrifuged and decanted. After drying at 70 °C in an oven for at least 72 h the samples were homogenised with a mortar and pestle. Depending on the

organic carbon content of each specific sample, a different amount was weighed in a tin capsule using a Mettler Toledo MT5 Fact microbalance, so that approximately the same amount of organic carbon was always measured.

$\delta^{13}C_{org}$ and **$\delta^{15}N_{org}$** were measured by flash combustion on a ThermoFisher Scientific FlashEA elemental analyser connected to a Delta V isotope ratio mass spectrometer (IRMS) operated in continuous flow mode. The samples were combusted in an O_2 atmosphere in a quartz reactor at 1'020 °C packed with $(Co_3O_4)Ag$ and Cr_2O_3 to form CO_2, N_2, NO_X and H_2O. These gases were then transferred through a reduction reactor containing elemental Cu at 600 °C to remove excess O_2 and to reduce NO_X to N_2. H_2O and SO_X were subsequently removed using anhydrous $Mg(ClO_4)_2$ and elemental Ag. Then, N_2 and CO_2 were separated in a packed gas chromatographic column and analysed for their isotopic composition using the IRMS. Isotope ratios are reported in conventional delta notation with respect to atmospheric N_2 (AIR) and VPDB standards, respectively. The methods were calibrated with the International Atomic Energy Agency (IAEA)-N1 ($\delta^{15}N$ = 0.45‰), IAEA-N2 ($\delta^{15}N$ = +20.41‰) and IAEA-N3 ($\delta^{15}N$ = +4.72‰) reference materials for nitrogen, and NBS22 ($\delta^{13}C$ = -30.03‰) and IAEA-CH-6 ($\delta^{13}C$ = -10.46‰) for carbon. Reproducibility of the measurements is better than ± 0.2‰ for both nitrogen and carbon. Reproducibility and accuracy of the measurements are based on replicate analyses of the internal laboratory standards atropine, peptone and nicotinamide. All geochemical measurements were performed at the Stable Isotope Laboratory of the ETH Zurich (Geological Institute).

The **Total Organic Carbon** (TOC_{decarb}) and **Total Nitrogen** (TN_{decarb}) contents of the decarbonised samples were calculated based on the known carbon and nitrogen contents of atropine (70.56 wt.-% C, 4.84 wt.-% N). The individual uncertainty for TOC_{decarb} represents the average from all standard deviations from atropine during that calculation and is ± 0.39%, respectively ± 0.06% for the TN_{decarb}. The calculated TN_{decarb} reflects a mixture of bound inorganic and organic nitrogen and therefore also contains ammonium, which substitutes for K^+ in the interlayer exchange sites of illite (Scheffer & Schachtschnabel 1984).

The **Carbon-to-Nitrogen ratio** (C/N ratio) is a ratio of the mass of carbon to the mass of nitrogen. In this study, the ratio was calculated using the TOC_{decarb} and the TN_{decarb}. As mentioned above, the C/N ratios can also be influenced by inorganic nitrogen in the form of soil-derived ammonium (Scheffer & Schachtschnabel 1984). Due to this inorganic nitrogen, the C/N ratios of sediments containing additional inorganic nitrogen will decrease. Therefore, C/N ratios are referred to as organic carbon/total nitrogen (TOC_{decarb}/TN_{decarb}) giving the ratio of the C and N masses of the decarbonised samples (C_{org}/N_{org}). The calculated ratios allow to distinguish between marine (C/N ≤ 10; Parsons 1975) *versus* terrigenous matter (C/N ≥ 12; Kukal 1971) in marine sediments.

$$\frac{C_{org}}{N_{org}} = \frac{TOC_{decarb}}{TN_{decarb}} * \frac{atomic\ mass\ (C)}{atomic\ mass\ (N)} = \frac{TOC_{decarb}}{TN_{decarb}} * \frac{14.007}{12.011}$$

The **Total Organic Carbon** (TOC) of the whole/bulk sample was calculated using the semi-quantitative carbonate content (TCarb) and semi-quantitative TOC_{decarb} content based on the following equation:

$$TOC = (1 - TCarb) * TOC_{decarb}$$

3 Results

3.1 Microfacies

Dinkelberg Formation (MAR1-1-1036.39, 1030.14)

The Dinkelberg Formation is a very heterogeneous sandstone formation: typical attributes are quartz-, calcite- and/or anhydrite-cements, nodules, druses and veins, grown during diagenetic processes. Sample MAR1-1-1036.39, a calcareous sandstone, consists mainly of calcite and chalcedony nodules. That means the thin section shows 45 vol.-% calcite cement (Tab. 3-1), 30 vol.-% authigenic quartz as well as 20 vol.-% detritic quartz grains (incl. siliciclastic rock fragments). Many of the sandstones are poorly sorted, as for example MAR1-1-1030.14 with quartz grains and rock fragments (74 vol.-%) of 0.04 – 5 mm grain-size and clay matrix (24 vol.-%).

Kaiseraugst Formation (MAR1-1-1028.34, 1023.15)

The sample MAR1-1-1028.34 comes from the transition zone of the terrestrial Dinkelberg Formation to the marine Kaiseraugst Formation. The thin section consists of dolomitic sandstone layers alternating with dolomitic microbial mats, that means 18 vol.-% stromatolite (Tab. 3-1), 59 vol.-% quartz and silicate rock fragments and 23 vol.-% dolomite cement.

Then MAR1-1-1023.15 is a purely marine biodetritic limestone (sandy) (Fig. B-1, Appendix B, for all figures in this section) with 17 vol.-% echinoderm plates (Tab. 3-1), 15 vol.-% bivalves and 17 vol.-% coarse-grained quartz with microsparitic matrix (40 vol.-%), few calcite cement rims (5 vol.-%) and dolomite rhombohedrons (6 vol.-%). Few of the grains have small black, pyrite/clay rims.

Zeglingen Formation (MAR1-1-932.63)

MAR1-1-932.63, taken near the top of the «Dolomitzone» of the Zeglingen Formation, is a dolostone, composed of a stromatolitic layer (27 vol.-%; Tab. 3-1) and a fully dolomitised bed with echinoderms (5 vol.-%), bivalves (4 vol.-%), codiacean green algae (15 vol.-%), dolomitic micrite matrix (13 vol.-%) and dolomite rhombohedrons (36 vol.-%).

Schinznach Formation (MAR1-1-887.68, 875.65)

The bed of MAR1-1-887.68 seems to be, in a macroscopic point of view, a sandy dolostone. However, the thin section shows a different picture. It is a totally dolomitised pelmicrite, but without any quartz grain. We have a mosaic of various (0.01 – 0.05 mm), closely jointed, dolomite rhombohedrons (66 vol.-%, Tab. 3-1) with remains of pellets (13 vol.-%) and biogene components (7 vol.-%) as well as some dolomitic micrite matrix (10 vol.-%). The thin section also contains 4 vol.-% of porosity.

MAR1-1-875.65 is quite similar to MAR1-1-887.68, but now dolomitisation is finer crystalline and more pellets (23 vol.-%) are recognisable. Furthermore, beautifully formed bivalve leaching pores (11 vol.-%) have to be mentioned, indicated as porosity in Tab. 3-1.

Bänkerjoch Formation (MAR1-1-852.12, 836.29, 825.14, 811.65, 795.99)

Three of the five thin section samples were taken from the Bänkerjoch Formation to verify whether quartz sand is present, respectively how high the quartz content is. MAR1-1-852.12 and 825.14 are fine-layered anhydritic/dolomitic marls without quartz. They consist of anhydrite layers (52, resp. 18 vol.-%; Tab. 3-1) alternating with dolomitic marl layers, where dolomite rhombohedrons (37, resp. 56 vol.-%), pseudomorph after gypsum crystals, are floating in clay matrix (11, resp. 26 vol.-%). However, MAR1-1-811.65 is a fine-layered dolomitic siltstone with 44 vol.-%, silt-sized quartz with 34 vol.-% dolomitic matrix and 19 vol.-% anhydrite as cement within silty layers.

MAR1-1-836.29 was taken to check supposed ooids. But the thin section is again a fine-layered anhydritic/dolomitic marl, that means anhydrite layers are alternating with dolomite rhombohedrons bearing argillaceous layers.

The sample MAR1-1-795.99, taken from the interval 796.52 – 795.32 m which is described as an argillaceous sandstone (Dossier III), consists of 64 vol.-% dolomite rhombohedrons, pseudomorph after gypsum crystals, and clay matrix (36 vol.-%). Therefore, the sample seems to be a dolomitic marl, without any quartz or siliciclastic grains or rock fragments.

Klettgau Formation (MAR1-1-770.66, 766.92)

MAR1-1-770.66 is a pure dolomicrosparite, a dolostone (94 vol.-%) with few calcite (6 vol.-%) eyes of a fenestral fabric. But no grains or components are visible.

The Klettgau Formation seems to have ooids too, in a macroscopic point of view. However, MAR1-1-766.92, which was taken to check this determination, is a dolocrete with round dolomicritic components (22 vol.-%; Tab. 3-1, counted in the column of intraclasts) grown during pedogenesis (Fig. B-2).

Staffelegg Formation (MAR1-1-741.95, 739.08, 730.44, 720.00, 707.68, 705.66)

The sample MAR1-1-741.95 (Beggingen Member) is a hardground, consisting of limonitic, partly replaced by calcite, iron-ooids (22 vol.-%; Tab. 3-1), iron-stromatolite (22 vol.-%), biogene components (14 vol.-%), pyrite (6 vol.-%) and calcite cement/"stellate cement"/cone-in-cone calcite (21 vol.-%) as well as clay matrix (15 vol.-%).

MAR1-1-739.08 (Beggingen Member), a true "Spatkalk", is totally composed of biogenes, namely echinoderm elements (43 vol.-%) and bivalves (22 vol.-%), which are cemented by calcite (26 vol.-%) and few dolomite rhombohedrons (5 vol.-%). The pyrite/calcite/?coelestine vein, cutting the TS, was not counted in the context of the microfacies analysis.

Thin section MAR1-1-730.44 of the Frick Member is a claystone (silty, calcareous) with 14 vol.-% silt-sized quartz, small bivalve debris (5 vol.-%), somewhat calcite cement (6 vol.-%), dolomite (3 vol.-%), pyrite (5 vol.-%) and clay matrix (64 vol.-%) with micas (3 vol.-%).

The thin section, taken from the «Unterer Stein» from the Rietheim Member (MAR1-1-720.00), is a stromatolitic limestone (92 vol.-%) with few pyrite (8 vol.-%) (Fig. B-3).

With the two samples MAR1-1-707.68 and 705.66 we would like to check whether there is a difference between a normal, typical Gross Wolf nodular limestone layer (707.68) and a "not sharp limited" calcareous layer (705.66). Both have similar components – thin-shelled bivalves

(18 vol.-%, resp. 28 vol.-%). However, they differ significantly in matrix and cement. MAR1-1-705.66 has 47 vol.-% "stellate cement" of a "hiatus bed". MAR1-1-707.68, on the other hand, has only a micrite matrix (76 vol.-%).

Opalinus Clay (MAR1-1-700.13, 662.11, 629.24, 623.07, 614.75, 609.64, 609.27, 603.69, 602.01, 600.50, 594.13)

One half of the thin sections of the Opalinus Clay serve to analyse specific calcareous beds/layers, firmgrounds and hardgrounds. The others provide an insight into the microfacies of different lithologies, as clay-rich, shaly or sandy/silty facies.

MAR1-1-700.13 and 662.11 are representatives of a clay-rich fazies. Both are very similar: they differ only in the quartz and clay content. MAR1-1-700.13 is a claystone with 6 vol.-% quartz-silt (Tab. 3-1), 4 vol.-% thin-shelled bivalves, 3 vol.-% pyrite, 3 vol.-% Fe-dolomite, 2 vol.-% mica and 82 vol.-% clay matrix. MAR1-1-662.11 contains more quartz-grains (13 vol.-%): evenly spread silt-grains (0.05 mm) and sand-grains (0.07 mm) concentrated in small lenses, cemented by calcite and is therefore a claystone (sandy/silty).

The four thin sections MAR1-1-629.24, 609.64, 609.27 and 600.50 are taken from hardgrounds. The first hardground (MAR1-1-629.24; Fig. B-4) consists of micritic intraclasts (17 vol.-%; Tab. 3-1), relatively big echinoderms (16 vol.-%), bivalves (4 vol.-%), quartz (16 vol.-%), much pyrite (13 vol.-%), often replacing bivalves shells, calcite cement (11 vol.-%) around biogene components, and clay/marl matrix (21 vol.-%). The second hardground (MAR1-1-609.64) in contrast contains iron-ooids (10 vol.-%; Tab. 3-1), which are replaced by calcite (Fig. B-6), in addition intraclasts (4 vol.-%), quartz (12 vol.-%), biogene components (9 vol.-%), pyrite (3 vol.-%) and a sideritic (17 vol.-%) clay matrix (45 vol.-%). The third hardground (MAR1-1-609.27), is a nodular sideritic horizon with little iron-ooids (replaced by calcite, 3 vol.-%), biogene components, quartz, intraclasts, pyrite and siderite (75 vol.-%). The fourth hardground (MAR1-1-600.50; Fig. B-8) consists mostly of biogene components: 27 vol.-% echinoderms, 18 vol.-% bivalves and 3 vol.-% foraminifera and others. It also contains iron-ooids (3 vol.-%), intraclasts and pyrite. The grains are partly embedded in clay matrix (12 vol.-%), limonitic matrix (7 vol.-%), but also cemented by calcite (6 vol.-%) and "stellate cement" (12 vol.-%). Almost all iron-ooids of the Opalinus Clay have lost their original iron-mineral composition through partial or complete replacement by calcite or by leaching. If such calcitic iron-ooids have been noted in the "Fe-ooids" column in Tab. 3-1, they are additionally marked with an asterisk behind the number.

MAR1-1-623.07 and 614.75 were sampled from a silty/sandy facies between the calcareous beds. They look very similar: composed of closely joined small lenses of sand-sized grains of quartz and bioclasts. Quartz (34, resp. 32 vol.-%, Tab. 3-1), echinoderms (12, resp. 8 vol.-%) and bivalves (9, resp. 6 vol.-%) are the main components (Fig. B-5). They are cemented by calcite (14, resp. 13 vol.-%); clay matrix lies between the sand lenses.

The thin section MAR1-1-603.69 shows a bioclastic layer (arenitic) of echinoderm skeletal elements (24 vol.-%; Tab. 3-1), bivalves (6 vol.-%), quartz-silt (6 vol.-%) some intraclasts (6 vol.-%) and pyrite (4 vol.-%). The composition of the matrix is not very clear: it seems to be a mixture between fine-crystalline siderite (25 vol.-%) and clay (27 vol.-%).

MAR1-1-602.01 consists of quartz-silt lenses (Fig. B-7) whereof most have been bioturbated and mixed with the clay matrix. The thin section overall contains 32 vol.-% quartz (Tab. 3-1), 8 vol.-% biogene components, few small pyrite cubes (6 vol.-%) and calcite cement (11 vol.-%) as well as 40 vol.-% clay matrix.

MAR1-1-594.13 (Fig. B-9) represents a clay-rich facies at the top of the Opalinus Clay: It contains 18 vol.-% quartz-silt (Tab. 3-1), some small echinoderm and bivalve detritus (12 vol.-%), pyrite (2 vol.-%) and clay matrix (66 vol.-%) with mica (2 vol.-%).

«Murchisonae-Oolith Formation» (MAR1-1-590.32, 589.23)

The lower thin section of the «Murchisonae-Oolith Formation» (MAR1-1-590.32) is an iron-oolite (calcareous, biodetritic) with 35 vol.-% iron-ooids (Tab. 3-1), 23 vol.-% bivalves and echinoderms, whereof some are limonitic, 7 vol.-% different intraclasts, few quartz grains (5 vol.-%), pyrite (4 vol.-%) with a limonitic micrite matrix (26 vol.-%). The bed is interpreted to be a hardground.

The upper thin section (MAR1-1-589.23) is a limestone (iron-oolitic, biodetritic). It contains 21 vol.-% iron-ooids (Tab. 3-1, also marked with an asterisk). Some of the iron-ooids have a strange appearance: a "banana-shaped" core and a calcitic rim (Fig. B-10). Then 24 vol.-% bioclasts, 8 vol.-% intraclasts and 7 vol.-% quartz grains are also present in a micrite matrix (40 vol.-%).

Wedelsandstein Formation (MAR1-1-583.88, 582.17, 574.66, 571.98, 569.18, 567.82, 565.73, 561.96, 558.47, 556.84)

The Wedelsandstein Formation consists of silty to sandy marls, calcareous marls and claystones (calcareous) with more or less bioclasts and more or less quartz sand. This marly formation contains some interstratified calcareous/quartz-rich beds, which have usually more calcite. To record the microfazies of the different lithologies 10 thin sections were sampled.

MAR1-1-583.88, 571.98 and 558.47 (Fig. B-14) are sandy marls to claystone (sandy, calcareous, biodetritic): They have 10 – 24 vol.-% bioclasts (Tab. 3-1), 32 – 42 vol.-% quartz sand, a bit calcite cement/"stellate cement" (0 – 8 vol.-%) and 30 – 45 vol.-% clay matrix. Thin section MAR1-1-558.47 (Fig. B-14) contains the highest calcite content (32 vol.-%) of these three samples.

MAR1-1-574.66 was taken from a calcareous nodule: the totally 28 vol.-% biogene components are very well cemented by calcite (9 vol.-%) and "stellate cement" (22 vol.-%).

The samples MAR1-1-567.82, 561.96 and 556.84 have been chosen for analysing the biogene content: MAR1-1-561.96 is a biodetritic limestone, an "echinoderm arenite" bed with 47 vol.-% echinoderm skeletal elements (Tab. 3-1), 10 vol.-% bivalves, 6 vol.-% bryozoan, some quartz sand (9 vol.-%), 16 vol.-% calcite cement and 12 vol.-% micrite matrix. MAR1-1-567.82 contains more quartz (42 vol.-%) than biogene components (totally 22 vol.-%), whereof many are serpulids (12 vol.-%). Whereas MAR1-1-556.84 consists of 40 vol.-% biogene components (echinoderms, bivalves, brachiopodes) and 16 vol.-% quartz with marly matrix and calcite cement.

MAR1-1-582.17 (Fig. B-11), 569.18 (Fig. B-12) and 565.73 (Fig. B-13) are well-cemented, calcareous- and quartz-rich beds, intercalated in the marly and clayey succession of the Wedelsandstein Formation. They differ in their content (14 – 31 vol.-%; Tab. 3-1) and composition of biogene components (echinoderms, bivalves, serpulids, sponge spicules and others) and in their quartz content (15 – 34 vol.-%). But the most important factor is the strong cementation of the beds: MAR1-1-582.17 shows a microsparitic mosaic of calcite (Fig. B-11). That means a neomorphic change during diagenesis of micrite matrix to a somewhat microsparitic cement. There

it is difficult to distiguish what are really biogene components (probably more than the counted 14 vol.-%) and what is cement. MAR1-1-569.18 shows 12 vol.-% (Tab. 3-1) "normal" calcite cement (grown in the original pore space) and 19 vol.-% "stellate cement" of a hiatus bed (Fig. B-12). MAR1-1-565.73 has 22 vol.-% (Tab. 3-1) "normal" calcite cement (Fig. B-13).

«Humphriesioolith Formation» (MAR1-1-555.12, 550.47, 547.75, 546.90, 546.02)

The thin section analyses concern one sample MAR1-1-555.12 from the lower iron-oolitic interval and four (550.47, 547.75, 546.90, 546.02) from the upper iron-oolitic interval.

MAR1-1-555.12 was taken from a complex hardground (Fig. B-15) with an iron-stromatolitic crust (8 vol.-%; Tab. 3-1), iron-stromatolitic intraclasts (5 vol.-%), few iron-ooids (5 vol.-%) and many biogene components (47 vol.-%), whereof many serpulids (17 vol.-%) and few of them are limonitic. The components have been sedimented with micrite matrix (24 vol.-%), whereof a part got limonitised during diagenesis.

MAR1-1-550.47 comes from a limonitic calcareous marl (iron-oolitic, biodetritic). The thin section consists of small (grain-size average of 0.2 mm), round and angular limonitic components (Fig. B-16). They have been counted (25 vol.-%, Tab. 3-1) as iron-ooids, although most of them show no concentric structure. 15 vol.-% limonitic bivalves + echinoderms, 10 vol.-% bivalves, 6 vol.-% echinoderms and 7 vol.-% other biogenes are present in a marly matrix (20 vol.-%) with some calcite cement (7 vol.-%) and "stellate cement" (5 vol.-%).

MAR1-1-547.75 is a limestone (iron-oolitic, biodetritic), consisting of 28 vol.-% (Tab. 3-1) chamositic and limonitic iron-ooids (Fig. B-17), as well as 28 vol.-% biogene components and 40 vol.-% micrite matrix.

The sample with the most iron-ooids is MAR1-1-546.90: an iron-oolite with 60 vol.-% iron-ooids (Tab. 3-1, Fig. B-18). They are lying in a strange limonitic matrix (20 vol.-%) with very small (limonitic) dolomite rhombohedrons, which have limonitic cores (Fig. B-19).

The sample MAR1-1-546.02 is an iron-oolite too, with 45 vol.-% iron-ooids (Tab. 3-1), which have a limonitic composition and an average size of 1.2 mm. The iron-ooids have small calcite cement rims within the limonitic micrite matrix (47 vol.-%). In addition, 8 vol.-% biogene components are present.

«Parkinsoni-Württembergica-Schichten» (MAR1-1-544.48, 526.04)

A further iron-oolitic bed is developped close to the base of the «Parkinsoni-Württembergica-Schichten» which may represent the «Parkinsoni-Oolith». The thin section MAR1-1-544.48 contains only few (8 vol.-%; Tab. 3-1) limonitic/calcitic iron-ooids (Fig. B-20), which are widespread in a microsparitic limestone (62 vol.-%), together with some biogene components (8 vol.-%), quartz-silt (8 vol.-%), pyrite (5 vol.-%) and some "stellate cement" (9 vol.-%).

The sample MAR1-1-526.04 serves to anlyse one of the calcareous/quartz-rich beds of the «Parkinsoni-Württembergica-Schichten». The bed is a biodetritic, silty limestone (Fig. B-21), consisting of small thin-shelled bivalves (14 vol.-%; Tab. 3-1), echinoderms (11 vol.-%), foraminifera (3 vol.-%), quartz-silt (18 vol.-%) and microsparitic matrix (20 vol.-%) with "normal" calcite cement (9 vol.-%) and "stellate cement" (23 vol.-%).

Variansmergel Formation (MAR1-1-505.85)

Sample MAR1-1-505.85 represents a reddish, limonitic calcareous marl containing many biodetritic components (totally 40 vol.-%; Tab. 3-1), amongst others limonitic echinoderms and bivalves (7 vol.-%), brachiopodes (6 vol.-%, column "other biogenes") and sponge spicules (4 vol.-%). They have been sedimented in a marly matrix (25 vol.-%), where a part (13 vol.-%) is limonitic. Then during diagenesis Fe-dolomite (15 vol.-%) and calcite cement (8 vol.-%) have grown.

Wutach Formation (MAR1-1-503.60, 502.81, 502.33)

The thin sections MAR1-1-503.60 and 502.81 have been taken, among other things, to test if these beds also contain glauconite and not only iron-ooids. The microfacies analysis showed that they contain no glauconite. MAR1-1-503.60 is composed of a limestone (biodetritic, iron-oolitic) and a marl (iron-oolitic). The iron-ooids (totally 18 vol.-%; Tab. 3-1, Fig. B-22) are round, up to 1.2 mm in diameter in the limestone part but flattened in the marly part. Then 31 vol.-% biogene components are present, as well as few quartz- silt grains (5 vol.-%) and iron-dolomite (5 vol.-%) in micritic, partly limonitic and marly matrix.

MAR1-1-502.81 and 502.33 (Fig. B-23) are marly iron-oolites with 52, respectively 45 vol.-% iron-ooids (Tab. 3-1). Furthermore, the latter contains 14 vol.-% iron-oolitic intraclasts. Most of the iron-ooids have been replaced by calcite. The marly matrix (27, resp. 15 vol.-%) contains Fe-dolomite rhombohedrons (13, resp. 18 vol.-%).

Wildegg Formation (MAR1-1-501.62, 501.51)

The samples MAR1-1-501.62 and 501.51 have been taken to verfy the lithological composition of the subunits «Glaukonitsandmergel Bed» and «Mumienkalk Bed», both *sensu* Gygi (1977, 2000, 2012).

MAR1-1-501.62 contains beautiful, greenish and brownish grains of glauconite (18 vol.-%, Tab. 3-1) with sizes of 0.1 – 0.5 mm, as well as iron-ooids (12 vol.-%) and quartz sand (17 vol.-%). The grains are embedded in a marly (15 vol.-%) and limonitic (30 vol.-%) matrix.

MAR1-1-501.51 (Fig. B-24) contains also glauconite grains (14 vol.-%), which are laying together with some coated grains, oncoids (11 vol.-%), quartz (11 vol.-%), echinoderms (7 vol.-%), bivalves (4 vol.-%) and foraminifera (2 vol.-%, other biogenes) and pyrite (2 vol.-%) are further components in a marly matrix (49 vol.-%).

Villigen Formation (MAR1-1-483.04)

Thin section MAR1-1-483.04 shows a nodular calcareous marl, consisting of little micritic nodules of sponge origin, a big (few cm) sponge nodule, where the original sponge structure is still visible (sponges totally 34 vol.-%; Tab. 3-1), together with echinoderms (5 vol.-%), bivalves (3 vol.-%), pellets (6 vol.-%), quartz (4 vol.-%) and glauconite grains (1 vol.-%) as well as marly matrix (47 vol.-%).

Tab. 3-1: Microfacies analysis from MAR1-1 (1'036.39 – 483.04 m); numbers in vol.-%

Microfacies analysis MAR1-1 (1'036.39 - 483.04 m)	components (and biohermal organisms)																			cements, diagenesis												
				calcitic biogenes									allochems																				
	clay matrix, micrite, microsparite	dolomitic matrix	limonitic matrix	echinoderms	bivalves	limonitic echinod. + bivalves	serpulids	corals	sponges, spicules	other biogenes	Fe-stromatolite + stromatolitic clasts	pellets, peloids	ooids	oncoids	Fe-ooids	intraclasts	detritial quartz + silic. rock fragm.	quartz grainsize (mm)	calcite cement	"stellate cement" (s) cone-in-cone calcite (c)	(Fe)-dolomite	dedolomite	anhydrite, gypsum	quartz cement	pyrite	limonite, Fe-min. nodules	siderite	glauconite	mica	porosity
483.04m: calc. marl with sponge nod. *Villigen Fm.*	47			5	3				34			6					4											1		
501.51m: calcareous marl, sandy *Wildegg Fm. («Mumienkalk Bed»)*	49			7	4					2				11			11	0.10							2			14		
501.62m: calc. marl (sandy, limonitic) *Wildegg Fm. («Glaukonitsandmergel Bed»)*	15		30	5						3					12		17	0.08										18		
502.33m: iron-oolite, marly *Wutach Fm.*	15			2	4										45	14			2		18									
502.81m: iron-oolite, marly *Wutach Fm.*	27			3	5										52						13									
503.60m: limestone (biodet., iron-ool.) *Wutach Fm.*	24		17	18	6				4	3					18		5	0.05			5									
505.85m: calcareous marl (biodetritic) *Variansmergel Fm.*	12		13	16	7	7			4	6							8	0.05	8		15				4					
526.04m: limestone (biodetritic, silty) *«Parkinsoni-Württembergica-Sch.»*	20			11	14					3							18	0.05	9	23					2					
544.48m: limestone (biodet., iron-ool.) *«Parkinsoni-Württembergica-Sch.»*	62			3	5										8		8	0.05		9					5					
546.02m: iron-oolite, calcareous *«Humphriesioolith Fm.»*			47	3	4					1					45															
546.90m: iron-oolite, calcareous *«Humphriesioolith Fm.»*			20	3	2										60		4	0.07	3		8									
547.75m: limestone (iron-ool., biodet.) *«Humphriesioolith Fm.»*	40			12	6	5			2	3					28				4											
550.47m: calc. marl (iron-ool., biodet.) *«Humphriesioolith Fm.»*	20			6	10	15				7					25		5	0.06	7	5										
555.12m: hardground, stromat., biod. *«Humphriesioolith Fm.»*	11		13	12	7	8	17			3	8				5	5	6	0.05								5				
556.84m: calc. marl (biodet., silty) *Wedelsandstein Fm.*	34			18	5		4			13							16	0.05	4						4			2		
558.47m: sandy marl (biodetritic) *Wedelsandstein Fm.*	30			16	5					3							32	0.10	8		4							2		
561.96m: biodet. limestone (packst.) *Wedelsandstein Fm.*	12			47	10					6							9	0.07	16											
565.73m: sandy limestone (biodetritic) *Wedelsandstein Fm.*	12			17	13												34	0.08	22									2		
567.82m: calc. sandstone (argill.) *Wedelsandstein Fm.*	25			4	6		12										42	0.08	8									3		
569.18m: limestone (sandy, biodet.) *Wedelsandstein Fm.*	20			6	7		9		9								15	0.07	12	19								3		
571.98m: sandy claystone (calc.) *Wedelsandstein Fm.*	45			4	6												42	0.08										3		
574.66m: limestone (sandy, biodet.) *Wedelsandstein Fm.*	27			6	18				2	2							14	0.07	9	22										
582.17m: limestone (sandy, biodet.) *Wedelsandstein Fm.*	48			4	8					2							17	0.06	9	10								2		
583.88m: sandy marl (biodetritic) *Wedelsandstein Fm.*	38			8	10					2							36	0.07		4								2		
589.23m: limestone (iron-ool., biodet.) *«Murchisonae-Oolith Fm.»*	40			7	9	4				4					21*	8	7	0.10												
590.32m: iron-oolite, calc., biodetritic *«Murchisonae-Oolith Fm.»*			26	11	7	5									35	7	5	0.07							4					
594.13m: claystone (silty) *Opalinus Clay*	66			4	8												18	0.05							2			2		
600.50m: hardground, calc., biodetr. *Opalinus Clay*	12		7	27	18					3					3	2	6	0.06	6	12					4					
602.01m: silty claystone (calcareous) *Opalinus Clay*	40			3	5												32	0.05	11						6			3		
603.69m: calc. marl (biodet., sideritic) *Opalinus Clay*	27			24	6											6	6	0.04							4		25	2		
609.27m: hardground, sideritic, nod. *Opalinus Clay*				3	2					1					3*	1	6	0.06			5				4		75			
609.64m: hardground, iron-ool., sid. *Opalinus Clay*	45			4	5										10*	4	12	0.06							3		17			
614.75m: sandy marl (biodetritic) *Opalinus Clay*	36			8	6												32	0.07	13						2			3		
623.07m: sandy marl (biodetritic) *Opalinus Clay*	27			12	9												34	0.08	14						2			2		
629.24m: hardground, biodet., intracl. *Opalinus Clay*	21			16	4											17	16	0.07	11						13			2		
662.11m: claystone (sandy/silty) *Opalinus Clay*	75				3												13	0.05	4						3			2		
700.13m: claystone *Opalinus Clay*	82				4												6	0.05			3				3			2		
705.66m: biodet. limestone (packst.) *Staffelegg Fm. (Gross Wolf Mb.)*	17			3	28											3				47					2					
707.68m: limestone (biodet., wackest.) *Staffelegg Fm. (Gross Wolf Mb.)*	76			2	18					2															2					
720.00m: limestone, stromatolite *Staffelegg Fm. (Rietheim Mb.)*											92														8					
730.44m: claystone (silty, calcareous) *Staffelegg Fm. (Frick Mb.)*	64				5												14	0.04	6		3				5			3		
739.08m: biodetritic limstone (grainst.) *Staffelegg Fm. (Beggingen Mb.)*				43	22					4									26		5									
741.95m: hardground, Fe-ool.,-strom. *Staffelegg Fm. (Beggingen Mb.)*	15			3	8					3	22				22				7	14					6					
766.92m: dolostone, nod. (dolocrete) *Klettgau Fm. (Seebi Mb.)*		78														22														
770.66m: dolostone *Klettgau Fm. (Seebi Mb.)*		94																	6											
795.99m: dolomitic marl *Bänkerjoch Fm.*	36																				64									
811.65m: dolomitic siltst. (anhydritic) *Bänkerjoch Fm.*		34															44	0.05					19					3		
825.14m: dolomitic marl (anhydritic) *Bänkerjoch Fm.*	26																				56		18							
836.29m: anhydrite/dol. marl (layered) *Bänkerjoch Fm.*	31																				14		55							
852.12m: dolo. marl + anhydite layers *Bänkerjoch Fm.*	11																				37		52							
875.65m: dolostone (dol. pelmicrite) *Schinznach Fm. (Stamberg Mb.)*	18				6							23									42									11
887.68m: dolostone (dol. pelmicrite) *Schinznach Fm. (Stamberg Mb.)*		10		3	4							13									66									4
932.63m: dolost. (dol.biomic.,stroma.) *Zeglingen Fm.*		13		5	4					15	27										36									
1'023.15m: biodetritic limestone (sandy) *Kaiseraugst Fm.*	40			17	15												17	0.60	5		6									
1'028.34m: dol. sandst. + stromatolite *Kaiseraugst Fm.*											18						59	0.20			23									
1'030.14m: sandstone (argillaceous) *Dinkelberg Fm.*	24																74	0.40	2											
1'036.39m: sandst.+calc.+chalced. nod. *Dinkelberg Fm.*	5																20	0.30	45					30						

3.2 Ammonite stratigraphy

From the recovered ammonites (list in Appendix A2), only one specimen (depth 707.74 m) could not be extracted because there was no separation between the rock matrix and the fossil, and the rock matrix did not react to potassium hydroxide. Several ammonites were unfortunately so damaged by coring or sampling that the genus or species could not be determined.

Typically, the ammonites are distributed differently over the individual time periods cored by the borehole. They are relatively common in the Toarcian and Early Aalenian, where ammonite fragments and cross sections are locally very common in the range from 710 m to 705 m and 698 m to 695 m. In the Late Aalenian and Early Bajocian, ammonites are very rare, with the exception of the Humphriesianum Zone. Only in the Late Bajocian they could be found more frequently again. Ammonites are rarer in the Bathonian and Callovian and often too small to be identified. Also, in the Oxfordian, ammonites were rare. Due to the generally small sample size and the poor, often incomplete preservation of the ammonites, a more-or-less large uncertainty in the age determinations must be expected, which can have an effect on the biostratigraphic classification.

We documented a selection of ammonites with photographs, and these are shown on four plates (Plates I – IV) in Appendix C. In addition to ammonites, other conspicuous fossils were identified to the extent possible (Appendix A3), even when they were not subsequently, or only occasionally, recovered.

In general, the more ammonites are present in a specific profile section, the more precisely we can determine the biostratigraphic classification of that section (Tab. 3-2). Furthermore, it must be considered that not all ammonites have the same index value and that the state of preservation of the objects also plays an important role in the biostratigraphic determination. In this respect, a certain error must always be expected. This error is in the range of about one ammonite Subzone (SZ) but can be as high as one ammonite Zone (Z), when the available data is insufficient.

Staffelegg Formation

723.40 m: *Amaltheus* ex gr. *margaritatus* (de Montfort, 1808). The ammonite is a compressed steinkern and rather poorly preserved. Age: Late Pliensbachian, Margaritatus Zone. Lithology: slightly argillaceous biodetritic limestone with belemnites. The ammonite is illustrated on Plate I, Fig. 1 (Appendix C, for all figures in this section).

710.20 m: *Grammoceras* sp. A truncated steinkern, partly encrusted with pyrite. Age: Thouarsense Zone. Lithology: splintery grey biodetritic limestone with occasional belemnites. The ammonite fragment is illustrated on Plate I, Fig. 2.

708.90 m: *Pseudogrammoceras* ex gr. *fallaciosum* (Bayle, 1878). Two flattened steinkerns with sulfidic inner whorls. Age: very common in the Thouarsense Zone, probably Fallaciosum Subzone. Lithology: grey calcareous marl with some biodetritus. Other fossils are belemnite rostra. The ammonites are illustrated on Plate I, Fig. 3.

708.23 m: *Dumortieria* sp. Three incomplete, crushed steinkerns. Age: Levesquei Zone. Lithology: grey biodetritic marl. The biodetritus consists mainly of echinoderm skeletal elements. The ammonites are illustrated on Plate I, Fig. 4.

707.74 m: Not preparable, mineralised steinkern. Age: Late Toarcian. Lithology: light-brown calcareous concretion in dark grey biodetritic marl (echinoderms). Not illustrated.

705.78 m: *Pleydellia* ex gr. *buckmani* (Maubeuge, 1947). One flattened, somewhat indistinct imprint. Age: Aalensis Zone, Torulosum Subzone. Lithology: grey biodetritic marl. The ammonite is illustrated on Plate I, Fig. 5.

Opalinus Clay

705.04 m: *Leioceras* ex gr. *subglabrum* (Buckman, 1902). Age: lowermost part of the Opalinum Zone, Opalinum Subzone. Lithology: dark grey claystone with biodetritus (fragments of *Bositra buchi*? (Roemer, 1836)). The ammonite is illustrated on Plate I, Fig. 6.

696.13 m: *Leioceras opalinum* (Reinecke, 1818) Microconch. Two flattened specimens with recrystallised calcitic shell preservation. Age: Opalinum Zone, Opalinum Subzone. Lithology: dark-grey claystone. Other fossils: two indeterminable ammonites and numerous ammonite fragments, also, some sulfidic burrows with diameters up to 3 mm. The ammonites are illustrated on Plate II, Fig. 1.

597.85 m: *Leioceras* sp., truncated cast. Age: Opalinum Zone, probably Bifidatum Subzone (previously «Comptum» Subzone, Dietze et al. 2021). Lithology: dark-grey silty claystone with mica. The ammonite is illustrated on Plate II, Fig. 2.

«Murchisonae-Oolith Formation»

589.19 m: *Staufenia* ex gr. *staufensis* (Oppel, 1858). One truncated specimen with partly recrystallised shell preservation. Age: Bradfordensis Zone, Bradfordensis Subzone. Lithology: grey limestone (iron-oolitic, sligthly argillaceous) with intraclasts, overlain with dark-grey, sligthly silty marl containing light intraclasts. The iron-ooids in the limestone measure up to 0.5 mm in diameter and are of complex structure. Other fossils: shells and a small ammonite. In the marly parts there are also shells (*Chlamys textoria* [Schlotheim, 1820] and others) and a belemnite. This ammonite is illustrated on Plate II, Figs. 3a and 3b.

«Humphriesioolith Formation»

555.03 m: *Emileia* sp. Truncated ammonite with recrystallised shell preservation and mineralised phragmocone. Age: Sauzei Zone?. Lithology: brown-grey biodetritic arenite with limonitised components. Biodetritus: bivalves and echinoderms. The ammonite is illustrated on Plate II, Figs. 4a and 4b.

548.21 m: *Chondroceras* ex gr. *gervillii* (Sowerby, 1818), several specimens. Age: Humphriesianum Zone, Humphriesianum Subzone, *gervillii-cycloides* faunal horizon. Lithology: biodetritic limestone (components include echinoderm ossicles) with limonitised components. Other fossils include numerous bivalves and a gastropod. The ammonite is illustrated on Plate III, Figs. 1a and 1b.

547.66 m: *Stephanoceras* sp. Age: Humphriesianum Zone, Humphriesianum Subzone. Lithology: reddish grey limestone (iron-oolitic, sligthly argillaceous). Diameters of the iron-ooids range up to 1 mm. Other fossils: few bivalve fragments and small ammonites. The ammonite is illustrated on Plate III, Figs. 2a and 2b.

546.40 m: Truncated ammonite in steinkern preservation. Age: due to the form of the venter, the ammonite probably originates from the Late Bajocian. Lithology: grey-brown limestone (iron-oolitic, sligthly argillaceous). The iron ooids are goethitic/limonitic and reach diameters up to 0.9 mm. Other fossils are bivalves. The ammonite is not illustrated.

«Parkinsoni Württembergica-Schichten»

544.39 m: *Parkinsonia* ex gr. *subarietis-rarecostata* Microconch. Two truncated ammonites in steinkern preservation. Age: Parkinsoni Zone, Acris Subzone. Lithology: dark-grey marl (iron-oolitic). The iron-ooids are cloud-like distributed in the rock. The ammonites are in small, light-brown, iron-ooid-containing concretions. Diameters of the ooids in the clay matrix are ca. 0.5 mm. The shape of the iron-ooids is round to oval in cross section. Other fossils are belemnites. One of those ammonites is illustrated on Plate III, Figs. 3a and 3b.

544.28 m: *Parkinsonia* sp. Macroconch, flattened steinkern. Age: Parkinsoni Zone. Lithology: dark-grey marl (iron-oolitic). The iron-ooids are cloud-like distributed with diameters up to 0.8 mm. The shape of the iron-ooids is round to oval in cross section. Other fossils are belemnites. The ammonite is illustrated on Plate III, Fig. 4.

543.61 m: *Parkinsonia* sp. Macroconch. Truncated, flattened steinkern. Age: Parkinsoni Zone. Lithology: dark-grey marl with chamositic iron-ooids. Other fossils are belemnites and sulfide-containing burrows. The ammonite is illustrated on Plate III, Fig. 5.

537.10 m: *Parkinsonia* ex gr. *schloenbachi* (Schlippe, 1888)?. Truncated ammonite, partly in pyrite steinkern preservation. Age: Parkinsoni Zone, Bomfordi Subzone?. Lithology: grey silty marl. Other fossils: numerous burrows, partly pyritised. The ammonite is illustrated on Plate III, Fig. 6.

530.20 m: Not preparable and therefore unidentifiable ammonite preserved as a pyrite steinkern. Lithology: mica-bearing grey marl. This ammonite is not illustrated.

518.36 m: *Oecotraustes* ex gr. *decipiens* (de Grossouvre, 1919). Flattened steinkern. Age: Early Bathonian. Lithology: mica-bearing grey marl with another ammonite fragment. The ammonite is illustrated on Plate IV, Fig. 1.

Variansmergel Formation

511.91 m: Ammonite indet., flattened steinkern. Lithology: mica-bearing grey calcareous marl. Other fossil: an ammonite fragment. The ammonite is not illustrated.

Wutach Formation

502.87 m: *Macrocephalites* sp. Truncated specimen in steinkern preservation. Age: Late Bathonian to Early Middle Callovian, probably Early Callovian. Lithology: red limestone (iron-oolitic, argillaceous). The iron-ooids are dark and up to 0.5 mm in diameter. They are of goethitic to limonitic composition. The ammonite is illustrated on Plate IV, Figs. 2a and 2b.

Wildegg Formation

501.52 m *Ochetoceras* ex gr. *canaliculatum* (von Buch, 1831). Truncated specimen with partial preservation of the shell. The ammonite is in an intraclast (thus the name "mummy"). Age: probably Transversarium Zone. Lithology: dark-grey glauconite-bearing marl with iron-ooid bearing light clasts and partly limonite-encrusted glauconite-bearing intraclasts with some biodetritus (echinoderms). Other fossils are belemnites. The ammonite is illustrated on Plate IV, Fig. 3.

494.27 m: *Euaspidoceras* ex gr. *oegir* (Oppel, 1863). Truncated specimen in steinkern preservation. Age: Transversarium Zone to Early Bifurcatus Zone. Lithology: grey, bioturbated limestone (argillaceous) with some biodetritus (echinoderms). Other Fossils are a small ammonite and belemnites. The ammonite is illustrated on Plate IV, Fig. 4.

Tab. 3-2: Ammonite and other macrofossil determination from MAR1-1

Depth [m MD]	**Identification**	**Ammonite Zone (Subzone) or Age**
494.27	*Euaspidoceras* ex gr. *oegir*	Transversarium Z to Early Bifurcatus Z
501.52	*Ochetoceras* ex gr. *canaliculatum*	Transversarium Zone?
502.87	*Macrocephalites* sp.	(Late Bathonian to Early Middle Callovian. Probably Early Callovian)
511.91	Ammonite (not preparable)	
518.36	*Oecotraustes* ex gr. *decipiens*	(Early Bathonian)
530.20	Ammonite fragment (not preparable)	
537.10	*Parkinsonia* ex gr. *schloenbachi*	Parkinsoni-Zone (Bomfordi Subzone?)
543.61	*Parkinsonia* sp.	Parkinsoni Zone
544.28	*Parkinsonia* sp.	Parkinsoni Zone
544.39	*Parkinsonia* ex gr. *subarietis-rarecostata*	Parkinsoni Zone (Acris Subzone)
546.40	Ammonite in steinkern preservation	(Late Bajocian)
547.66	*Stephanoceras* sp.	Humphriesianum Z (Humphriesianum SZ)
548.21	*Chondroceras* ex gr. *gervillii*	Humphriesianum Z (Humphriesianum SZ, *gervillii-cycloides* faunal horizon)
555.03	*Emileia* sp.	Sauzei Zone?
589.19	*Staufenia* ex gr. *staufensis*	Bradfordensis Zone (Bradfordensis SZ)
597.85	*Leioceras* sp.	Opalinum Zone (Bifidatum Subzone?)
696.13	*Leioceras opalinum*	Opalinum Zone (Opalinum Subzone)
705.04	*Leioceras* ex gr. *subglabrum*	Opalinum Zone (Opalinum Subzone)
705.78	*Pleydellia* ex gr. *buckmani*	Aalensis Zone (Torulosum Subzone)
707.74	Ammonite steinkern (not preparable)	
708.23	*Dumortieria* sp.	Levesquei Zone
708.90	*Pseudogrammoceras* ex gr. *fallaciosum*	Thouarsense Zone (Fallaciosum Subzone?)
710.20	*Grammoceras* sp.	Thouarsense Zone
723.40	*Amaltheus* ex gr. *margaritatus*	Margaritatus Zone

System		Stage		Zone	Subzone
Jurassic	Late	Oxfordian	Late	Bifurcatus ?	Grossouvrei
					Stenocycloides
			Middle	Transversarium ?	Rotoides
					Schilli
					Luciaeformis
					Parandieri
				Plicatilis	Antecedens
					Vertebrale
			Early	Cordatum	Cordatum
					Costicardia
					Bukowski
				Mariae	Praecordatum
					Scarburgense
	Middle	Callovian	Late	Lamberti	Lamberti
					Henrici
				Athleta	Spinosum
					Proniae
					Phaeinum
			Middle	Coronatum	Grossouvrei
					Obductum
				Jason	Jason
					Medea
			Early	Calloviense	Enodatum
					Calloviense
				Koenigi	Galilaeii
					Curtilobus
					Gowerianus
				Herveyi	Kamptus
					Terebratus
					Keppleri
		Bathonian	Late	Discus	Discus
					Hollandi
				Orbis	Hannoveranus
					Blanazense
				Hodsoni	
			Middle	Morrisi	
				Subcontractus	
				Progracilis	
			Early	Zigzag	Tenuiplicatus
					Yeovilensis
					Macrescens
					Convergens
		Bajocian	Late	Parkinsoni	Bomfordi ?
					Truellei
					Acris
				Garantiana	Tetragona
					Garantiana
					Dichotoma
				Niortense	Baculata
					Polygyralis
					Banksii
			Early	Humphriesianum	Blagdeni
					Humphriesianum
					Romani
					Pinguis
				Sauzei ?	Macrum
					Kumaterum
				Laeviuscula	Laeviuscula
					Trigonalis
				Ovale	
				Discites	
		Aalenian	Late	Concavum	Formosum
					Concavum
			Middle	Bradfordensis	Gigantea
					Bradfordensis
				Murchisonae	Murchisonae
					Haugi
			Early	Opalinum	Bifidatum * ?
					Opalinum

System		Stage		Zone	Subzone
Jurassic	Early	Toarcian	Late	Aalensis	Torulosum
					Aalensis
				Levesquei	Moorei
					Levesquei
				Insigne	Dispansum
					Insigne
				Thouarsense	Fallaciosum ?
					Thouarsense
				Variabilis	
			Early	Bifrons	Crassum
					Fibulatum
					Commune
				Falcifer	Falcifer
					Elegans
					Exaratum
					Elegantulum
				Tenuicostatum	Semicelatum
					Clevelandicum
					Paltum
		Pliensbachian	Late	Spinatum	Hawskerense
					Apyrenum
				Margaritatus	Gibbosus
					Subnodosus
					Stokesi
			Early	Davoei	Figulinum
					Capricornus
					Maculatum
				Ibex	Luridum
					Valdani
					Masseanum
				Jamesoni	Jamesoni
					Brevispina
					Polymorphus
					Taylori
		Sinemurian	Late	Raricostatum	Aplanatum
					Macdonnelli
					Raricostatum
					Densinodulum
				Oxynotum	Oxynotum
					Simpsoni
				Obtusum	Denotatus
					Stellare
					Obtusum
			Early	Turneri	Turneri
				Semicostatum	Sauzeanum
					Scipionanum
					Charlesi
				Bucklandi	Bucklandi
					Rotiforme
					Conybeari
		Hettangian		Angulata	Complanata
					Extranodosa
				Liasicus	Laquaeus
					Portlocki
				Planorbis	Johnstoni
					Planorbis

MAR1-1

Grey highlighted zones and subzones are documented in the drill core with ammonites. Fields with additional interrogation points are not surely proven with ammonites.

Biostratigraphy modified after Cariou & Hanzpergue (1997)
* after Dietze et al. (2021), former «Comptum» Subzone

Fig. 3-1: Zones and subzones which are documented by ammonites in MAR1-1

3.3 Palynostratigraphy

The studied samples mostly yielded a good palynological residue with rich and diverse palynofloras. Preservation is good. The palynomorph assemblages are composed of mainly dinoflagellate cysts and pollen and spores. Minor components are prasinophytes, acritarchs, fungal remains, foraminiferal test linings and green algae (e.g. *Botryococcus*). A total of 177 dinoflagellate cyst taxa, 20 other aquatic palynomorphs and 51 pollen and spore taxa are recorded.

Some reworked sporomorphs (*Densosporites* spp., *Ovalipollis* spp., *Rhaetipollis germanicus, Ricciisporites tuberculatus*) indicate erosion of Triassic sediments in the source area. Other reworking is indicated by the occurrence of a few single specimens of the dinoflagellate cyst *Luehndea spinosa*, a typical Early Jurassic species with a main distribution in the Late Pliensbachian and earliest Toarcian.

The studied samples from the Marthalen-1-1 core are dated to span the interval from the Aalenian to the Oxfordian. Seven palynological samples were taken from six ammonite samples (marked in grey in Appendix A4; from ammonite at 555.03 m two palynological samples were taken: 555.00 m and 555.06 m). There are 16 sample intervals differentiated and, where possible, assigned to ammonite biostratigraphy. A list of the analysed samples and the age dating of each sample is given in Tab. 3-3. The indicated ages, zones (Z) and subzones (SZ) for each sample are the result of the palynostratigraphical analysis and interpretation. The results of the quantitative analysis are illustrated in a range chart (Appendix D1). A Depth/Age plot is illustrated in Appendix D2.

Sample interval 705.78 – 600.02 m (8 samples): Early Aalenian, Opalinum Zone, Opalinum Subzone

Dinoflagellate cyst assemblages of this sample interval are rich and diverse. They are composed of common to abundant *Evansia*? cf. *granochagrinata*, diverse Phallocystaceae (*Andreedinium elongatum*, *Andreedinium* sp. 2, *Andreedinium* spp., *Dodekovia bullula, D. knertensis, D. pseudochytroeides, Dodekovia* spp., *D. syzygia, Ovalicysta hiata, Parvocysta bjaerkei, P.*? *tricornuta, Phallocysta*? *frommernensis, Reutlingia nasuta, R. cardobarbata, Susadinium scrofoides*) and Valvaeodiniaceae (*Comparodinium punctatum, Valvaeodinium cavum, V. sphaerechinatum, V. spongiosum, Valvaeodinium* spp., *V. vermipellitum*), species of *Nannoceratopsis* (*N. dictyambonis, N. gracilis* s.l. and s.s., questionable *N. plegas*, *Nannoceratopsis* sp. 1. *Nannoceratopsis* spp., *N. triangulata, N. triceras*) and *Scriniocassis* (*S. limbicavatus, S. priscus, S. weberi*), as well as *Hystrichodinium*? sp., *Kallosphaeridium praussii*, *Mancodinium semitabulatum* and *Wallodinium laganum*. The species *Evansia*? cf. *granochagrinata* is very abundant in the two samples at the base of the interval (705.78 m, 705.04 m). Its abundance decreases up section but is still high. The species *Phallocysta*? *frommernensis* shows an acme from 685.09 m to 600.69 m.

The interval is defined by the first occurrence of *Phallocysta*? *frommernensis* to the last occurrence of unquestionable *Nannoceratopsis triangulata*, *Scriniocassis weberi* and *Wallodinium laganum*.

According to Feist-Burkhardt & Pross (2010) there are four marker species for the Early Aalenian Opalinuston Formation (German stratigraphy): *Kallosphaeridium praussii, Phallocysta*? *frommernensis*, *Nannoceratopsis triangulata* and *Wallodinium laganum*. All four marker species occur in this interval. Very high abundance or dominance of *Evansia*? cf. *granochagrinata* is typical for an age of the samples straddling the Toarcian/Aalenian boundary, Aalensis Zone/

Opalinum Subzone and defines the palynostratigraphical unit A of Feist-Burkhardt & Pross (2010). The acme of *Phallocysta*? *frommernensis* defines the palynostratigraphical unit B of Feist-Burkhardt & Pross (2010) of the Opalinuston Formation.

The sample interval is dated as Early Aalenian Opalinum Zone, Opalinum Subzone. The high abundance of *Evansia*? cf. *granochagrinata* in the basal two samples indicates an age close to the Aalenian/Toarcian boundary at the base of the sample interval.

The occurrence of *Luehndea spinosa* in the uppermost sample (600.02 m) indicates reworking of Early Jurassic Late Pliensbachian to earliest Toarcian sediments in the source area.

Sample interval 590.38 – 590.21 m (2 samples): Early Aalenian, Opalinum Zone to Middle Aalenian, lower Bradfordensis Zone

Assemblages in this interval are reduced in the diversity of phallocystacean dinoflagellate cysts. At the base of the interval occur the first questionable *Nannoceratopsis plegas plegas* and *N. plegas brevicorna*, and questionable *Batiacasphaera* spp. *Kallospharidium praussii* is common to abundant in the two samples. *Evansia*? cf. *granochagrinata* last occurs at the top of the interval.

The interval is defined as from the last occurrence of unquestionable *Nannoceratopsis triangulata, Scriniocassis weberi* and *Wallodinium laganum* in the interval below, and the first occurrence of questionable *Batiacasphaera* spp. and diverse subspecies of *Nannoceratopsis plegas* to the first occurrence of *Dissiliodinium lichenoides* in the interval above.

Batiacasphaera spp. has its FAD in the upper part of Opalinum Zone. The FAD of *Dissiliodinium lichenoides* is within Bradfordensis Zone.

The interval is interpreted Opalinum Zone to lower Bradfordensis Zone.

The occurrence of *Luehndea spinosa* (sample 590.21 m) indicates reworking of Early Jurassic Late Pliensbachian to earliest Toarcian sediments in the source area.

Sample 589.23 m (1 sample): Middle Aalenian, Bradfordensis Zone

The sample is characterised by the first occurrence of *Dissiliodinium lichenoides* and *Dissiliodinium* spp. Last occurring in this sample are *Nannoceratopsis plegas dictyornata, N. plegas plegas, N. triceras* and species of *Scriniocassis* (*Scriniocassis priscus, Scriniocassis* spp.).

The interval is defined as from the first occurrence of *Dissiliodinium lichenoides* to the last occurrence of *Scriniocassis* spp.

The FAD of *Dissiliodinium* spp. and *Dissiliodinium lichenoides* is within the Bradfordensis Zone. The LAD of *Scriniocassis* spp. and *Scriniocasssis priscus* is also in the Bradfordensis Zone.

The sample is dated Bradfordensis Zone.

The occurrence of *Luehndea spinosa* indicates reworking of Early Jurassic Late Pliensbachian to earliest Toarcian sediments in the source area.

Sample 588.95 m (1 sample): inconclusive (contaminated sample)

The palynological preparation yielded a mixture of palynofloras of different ages, suspected to be due to contamination that may have happened in the processing laboratory or while sampling the core. Therefore, the core was sampled again at the same depth and a new sample was processed from scratch. The new preparation yielded a clean palynoflora that is discussed in the next sample interval.

Sample interval 588.95 – 578.01 m (4 samples): Early Bajocian, Ovale Zone

The dinoflagellate cyst assemblages in this interval differ a lot from the samples below. Representatives of the genus *Dissiliodinium* are abundant. The following species have their first occurrence at the base of the interval: *Dissiliodinium* aff. *giganteum*, *Dissiliodinium giganteum, Dissiliodinium* sp. B, *Evansia*? *eschachensis, Evansia*? *spongogranulata, Gongylodinium erymnoteichon* and *Pareodinia* spp., in the next sample up there is also *Durotrigia daveyi*. Last occurring in the interval are *Andreedinium elongatum* and, at the top, *Nannoceratopsis dictyambonis*.

The interval is defined as from the first occurrence of *Dissiliodinium giganteum* to the first occurrence of *Cavatodissiliodinium hansgochtii* in the interval above.

The FAD of *Dissiliodinium giganteum* is Ovale Zone. The FAD of *Cavatodissiliodinium hansgochtii* is Laeviuscula Zone.

The interval is dated Ovale Zone.

Sample interval 571.98 – 563.00 m (2 samples): Early Bajocian, Ovale to Laeviuscula Zone

In addition to species known from below, the sample at the base of this interval shows the first occurrence of *Cavatodissiliodinium hansgochtii*. In the sample at the top of the interval *Cavatodissiliodinium hansgochtii* becomes common, the first questionable specimen of *Batiacasphaera laevigata* occurs and *Evansia*? *eschachensis* occurs for the last lime.

The interval is defined by the first occurrence of *Cavatodissiliodinium hansgochtii* to the first occurrence of questionable *Batiacasphaera laevigata* and the last occurrence of *Evansia*? *eschachensis*.

The LAD of *Evansia*? *eschachensis* is in Ovale Zone. The FAD of *Cavatodissiliodinium hansgochtii* and *Batiacasphaera laevigata* is in Laeviuscula Zone.

The sample interval is dated Ovale to Laeviuscula Zone.

Sample 555.54 m (1 sample): Early Bajocian, Laeviuscula Zone

The dinoflagellate cyst assemblage is similar to the interval below but without *Evansia*? *eschachensis*. *Dissiliodinium giganteum* is common and shows its acme top. *Cavatodissiliodinium hansgochtii* is less abundant. The species *Batiacasphaera laevigata* has its first unquestionable occurrence in this sample.

The interval is defined as from the first unquestionable occurrence of *Batiacasphaera laevigata* to the first occurrence of *Kallosphaeridium hypornatum* in the interval above.

The FAD of *Batiacasphaera laevigata* is Laeviuscula Zone. The FAD of *Kallosphaeridium hypornatum* is Sauzei Zone.

The interval is dated Laeviuscula Zone.

Sample interval 555.06 – 553.85 m (3 samples): Early Bajocian, Sauzei Zone

Assemblages in this interval still resemble those from below. *Kallosphaeridium hypornatum* has its first occurrence at the base of the interval. Last occurrences at the top of the interval are those of *Cavatodissiliodinium hansgochtii, Dissiliodinium giganteum*, and questionable *Evansia*? *spongogranulata*.

The interval is defined as from the first occurrence of *Kallosphaeridium hypornatum* to the last occurrence of *Dissiliodinium giganteum* and questionable *Evansia*? *spongogranulata*.

The FAD of *Kallosphaeridium hypornatum* is in Sauzei Zone. The LADs of *Dissiliodinium giganteum* and *Evansia*? *spongogranulata* are in Sauzei Zone.

The interval is dated Sauzei Zone.

Sample interval 550.87 – 548.21 m (3 samples): Early Bajocian, Humphriesianum Zone, Romani to Humphriesianum Subzone

The sample interval is characterised by a succession of several new first occurrences. From bottom to top of the interval the following taxa show first occurrences. First, *Durotrigia filapicata, Phallocysta thomasii* and *Wanaea* sp. 1, then *Acanthaulax crispa, Cavatodissiliodinium* sp. 1 and questionable "*Hypolytodinium*" sp., and last *Aldorfia aldorfensis, Cavatodissiliodinium* sp. 2 and sp. 3 and *Valensiella/Ellipsoidictyum* spp. Last occurring in the interval are "*Hypolytodinium*" sp. (questionable) and *Phallocysta thomasii*.

The interval is defined as from the first occurrence of *Durotrigia filapicata* and *Phallocysta thomasii* to the last occurrence of questionable "*Hypolytodinium*" sp.

All species mentioned have FADs within early Humphriesianum Zone. The ranges of "*Hypolytodinium*" sp. and *Phallocysta thomasii* are considered to be restricted to the Romani and Humphriesianum Subzones of the Humphriesianum Zone.

The samples are dated Romani to Humphriesianum Subzones of the Humphriesianum Zone.

Sample interval 547.66 – 546.90 m (2 samples): Late Bajocian, Niortense Zone

Samples in this interval are characterised by numerous first occurrences. These are, inter alia, *Atopodinium polygonale, Atopodinium* sp. 1, *Batiacasphaera* sp. 1, *Bradleyella adela, Carpathodinium predae, Carpathodinium* sp. 1, *Chytroeisphaeridia chytroeides* (questionable), *Endoscrinium asymmetricum* (questionable), *Gonyaulacysta pectinigera* (questionable), *Meiourogonyaulax valensii, Nannoceratopsis spiculata, Pareodinia* sp. 2, *Pareodinia* sp. 3, *Reutlingia gochtii, Rhynchodiniopsis*? *regalis, Rhynchodiniopsis*? sp. 1, *Rosswangia simplex, Valvaeodinium spinosum, Wanaea indotata* and *Willeidinium baiocassinum*. Last occurring at the top of the interval is *Nannoceratopsis gracilis* s.l.

The interval is defined as from the first occurrence of *Atopodinium polygonale, Carpathodinium predae Gonyaulacysta pectinigera, Rosswangia simplex* and *Valvaeodinium spinosum* and to the last occurrence of *Nannoceratopsis gracilis* s.l.

The FADs of *Atopodinium polygonale, Carpathodinium predae Gonyaulacysta pectinigera, Rosswangia simplex* and *Valvaeodinium spinosum* are Niortense Zone. The LAD of *Nannoceratopsis gracilis* s.l. is Niortense Zone.

The interval is dated Niortense Zone.

Sample interval 546.02 – 545.65 m (2 samples): Late Bajocian, Garantiana Zone

There are again several first occurrences. These are, inter alia, *Ctenidodinium continuum, Ctenidodinium sellwoodii* group, *Ctenidodinium* spp., *Endoscrinium asymmetricum* (consistent), *Gongylodinium hocneratum, Korystocysta gochtii* s.l., *Microdinium* sp. of Feist-Burkhardt & Wille (1992) and *Protobatioladinium mercieri*. The rare species *Microdinium* sp. of Feist-Burkhardt & Wille (1992) occurs only in the sample at the base of the interval. *Durotrigia daveyi* occurs in the interval and up to the base of the interval above.

The interval is defined as from the first occurrence of *Microdinium* sp. of Feist-Burkhardt & Wille (1992) and *Ctenidodinium sellwoodii* group to the first occurrence of *Valvaeodinium vermicylindratum* in the interval above.

The FADs of *Endoscrinium asymmetricum* and *Gongylodinium hocneratum* are in the higher Niortense Zone, those of *Ctenidodinium sellwoodii* group and *Microdinium* sp. of Feist-Burkhardt & Wille (1992) are in Garantiana Zone. The top of consistent *Durotrigia daveyi* is considered to be top Humphriesianum Zone, but the species may reach up to Garantiana Zone. The FAD of *Valvaeodinium vermicylindratum* is in Parkinsoni Zone.

The sample interval is interpreted as Garantiana Zone.

Sample interval 544.80 – 543.41 m (3 samples): Late Bajocian, Parkinsoni Zone

Dinoflagellate cyst assemblages are quite similar to below, with *Acanthaulax crispa* consistently occurring up to the top of the interval and commonly occurring representatives of *Ctenidodinium* including *Ct. continuum* and *Ct. sellwoodii* group. *Ctenidodinium combazii* does not yet occur but is recorded at the base of the interval above. First occurring in this interval are, inter alia, *Durotrigia omentifera, Lithodinia* spp., *Orobodinium automobile* (questionable), *Orobodinium rete* (questionable), *Sirmiodiniopsis* sp. of Feist-Burkhardt & Wille (1992) and *Valvaeodinium vermicylindratum*.

The interval is defined as from the first occurrence of *Valvaeodinium vermicylindratum*, questionable *Orobodinium automobile* and *Sirmiodiniopsis* sp. to the last occurrence of *Acanthaulax crispa*.

The FADs of *Valvaeodinium vermicylindratum, Orobodinium automobile* and *Sirmiodiniopsis* sp. are Parkinsoni Zone. The LAD of *Acanthaulax crispa* is in the Parkinsoni Zone.

The interval is dated Parkinsoni Zone.

Sample interval 534.10 – 523.67 m (2 samples): Early Bathonian, Zigzag Zone

The assemblages are characterised by the common and diverse occurrence of species of the genus *Ctenidodinium*, with *Ctenidodinium* spp., *Ct. combazii, Ct. continuum, Ct. ornatum* and *Ct. sellwoodii* group. Taxa first occurring at the base of the interval are, inter alia, *Cleistosphaeridium* sp. 1, *Dissiliodinium minimum, Gonyaulacysta eisenackii. Kalyptea stegasta, Lithodinia* sp. 1 (questionable) and *Meiourogonyaulax* sp. 1. The species *Meiourogonyaulax valensii* last occurs at the top of the interval.

The sample interval is defined as from the first occurrence of *Ctenidodinium combazii* to the last occurrence of *Meiourogonyaulax valensii*.

The FAD of *Ctenidodinium combazii* is within the uppermost part of Parkinsoni Zone, close to the base of the Zigzag Zone. The LAD of *Meiourogonyaulax valensii* is in the Zigzag Zone.

The high diversity and abundance of *Ctenidodinium* species and the presence of *Ctenidodinium combazii* are typical for the Bathonian and earliest Callovian.

The sample interval is interpreted Zigzag Zone.

Sample interval 517.85 – 504.94 m (5 samples): Early Bathonian, Zigzag Zone, Tenuiplicatus Subzone to Late Bathonian, Discus Zone

The assemblages are quite similar to those from below with abundant and diverse representatives of the genus *Ctenidodinium*. Abundance of *Ctenidodinium* increases towards the top of the interval. At the base of the interval *Tubotuberella dangeardii* occurs for the first time. There is a succession of first occurrences within the interval including the first chorate dinoflagellate cysts, such as *Adnatosphaeridium caulleryi* and specimens close to *Cleistosphaeridium ehrenbergii* s.l. which are here recorded within *Cleistosphaeridium* spp. Other first occurrences in the interval are *Ambonosphaera* spp., *Atopodinium prostatum*, *Gonyaulacysta jurassica, Nannoceratopsis pellucida* and *Pareodinia prolongata* (questionable). Last occurring within this interval are *Carpathodinium predae*, *Gongylodinium hocneratum, Rhynchodiniopsis*? *regalis*, *Valvaeodinium spinosum,* and at the top, *Ctenidodinium combazii* and *Gongylodinium erymnoteichon*. The species *Meiourogonyaulax valensii* is last recorded in the interval below.

The interval is defined as from the first occurrence of *Tubotuberella dangeardii* and the last occurrence of *Meiourogonyaulax valensii* in the interval below to the last occurrence of *Ctenidodinium combazii* and *Gongylodinium erymnoteichon*.

The FAD of *Tubotuberella dangeardii* is Zigzag Zone, that of *Cleistosphaeridium ehrenbergii* s.l. is in the Tenuiplicatus Subzone of the Zigzag Zone. The LAD of *Meiourogonyaulax valensii* is just below Tenuiplicatus Subzone of Zigzag Zone. The LAD of *Gongylodinium erymnoteichon*

was previously considered to be in the Hodsoni Zone, but the species has recently been observed to occur up to the Discus Zone (S. Feist-Burkhardt, pers. obs. 2020). The LAD of *Ctenidodinium combazii* is Herveyi Zone.

The sample interval is interpreted Tenuiplicatus Subzone of Zigzag Zone to Discus Zone.

Sample 502.81 m (1 sample): Early Callovian, Herveyi to Calloviense Zone

Composition of the dinoflagellate cyst assemblage in this sample is different to below. Abundance of representatives of the genus *Ctenidodinium* has strongly decreased. *Ctenidodinium combazii* is not recorded anymore. Chorate dinoflagellate cysts are common. There are several first occurrences, inter alia, *Korystocysta pachyderma, Lithodinia caytonensis, Mendicodinium groenlandicum, Sentusidinium? varispinosum, Sirmiodinium grossii* and *Stephanelytron scarburghense.* Last occurring in this sample is *Valvaeodinium vermicylindratum.* Several specimens of unquestionable *Atopodinium polygonale* are recorded.

There are species with FADs in the Herveyi Zone (*Lithodinia caytonensis, Sentusidinium*? *varispinosum, Sirmiodinium grossii, Stephanelytron scarburghense*), and in the Koenigi Zone (*Korystocysta pachyderma, Mendicodinium groenlandicum*). The LADs of *Atopodinium polygonale* and *Ctenidodinium combazii* are Herveyi Zone, that of *Valvaeodinium vermicylindratum* is Calloviense Zone.

The sample is interpreted Herveyi to Calloviense Zone. If the record of *Atopodinium polygonale* were regarded as reworked, age interpretation ought to be Koenigi to Calloviense Zone.

Sample 502.33 m (1 sample): Early Callovian, Herveyi Zone to Middle Callovian, Coronatum Zone

Composition of the dinoflagellate cyst assemblage is similar to below. In addition, there are, inter alia, *Compositosphaeridium polonicum, Mosaicodinium mosaicum, Rhynchodiniopsis cladophora, Rigaudella aemula* and *Stephanelytron redcliffense*. Last occurring in this sample are *Aldorfia aldorfensis*, *Atopodinium polygonale, Gonyaulacysta pectinigera, Lithodinia caytonensis, Mendicodinium groenlandicum, Mosaicodinium mosaicum, Nannoceratopsis spiculata, Sentusidinium? varispinosum* and *Wanaea indotata*. The species *Ctenidodinium combazii* is not recorded.

There are species with FADs in the Herveyi Zone (*Rhynchodiniopsis cladophora*), in the Koenigi Zone (*Mendicodinium groenlandicum*), in the Jason Zone (*Compositosphaeridium polonicum, Stephanelytron redcliffense*) and in the Coronatum Zone (*Rigaudella aemula*). There are species with LADs in the Herveyi Zone (*Atopodinium polygonale, Gonyaulacysta pectinigera*), in the Calloviense Zone (*Aldorfia aldorfensis, Sentusidinium*? *varispinosum),* in the Jason Zone (*Nannoceratopsis spiculata*), and in the Coronatum Zone (*Lithodinia caytonensis*).

Occurrence of all these species in the one sample indicates that there is a mixture of palynofloras of different age. The sample is interpreted Herveyi to Coronatum Zone. If the records of *Atopodinium polygonale* and *Gonyaulacysta pectinigera* were regarded as reworked, age interpretation ought to be Koenigi to Coronatum Zone.

Sample interval 501.62 – 501.30 m (2 samples): Middle Oxfordian, Transversarium Zone to Late Oxfordian, Bifurcatus Zone

Composition of the dinoflagellate cyst assemblages in this sample interval is different to below. Chorate dinoflagellate cysts are abundant, as well as *Rhynchodiniopsis cladophora* and *Sentusidinium rioultii*. There are numerous first occurrences, inter alia, *Acanthaulax* spp., *Amphorula dodekovae, Belodinium asaphum, Dingodinium tuberosum, Endoscrinium galeritum, Glossodinium dimorphum, Leptodinium arcuatum, Omatidium amphiacanthum, Polygonifera* spp., *Scriniodinium crystallinum, Systematophora areolata, Systematophora* spp. and *Taeniophora iunctispina* (questionable). Other important taxa present in the sample interval are *Compositosphaeridium polonicum, Ctenidodinium ornatum, Gonyaulacysta eisenackii, Nannoceratopsis pellucida, Rigaudella aemula, Rigaudella filamentosa* and *Sirmiodiniopsis orbis*.

There are species with their FAD in the Plicatilis Zone (*Glossodinium dimorphum, Leptodinium arcuatum, Systematophora areolata*), in the Transversarium Zone (*Taeniophora iunctispina*) and in the Bifurcatus Zone (*Amphorula dodekovae, Dingodinium tuberosum*). There are species with their LAD considered to be Plicatilis Zone (*Scriniodinium crystallinum*) and Transversarium Zone (*Compositosphaeridium polonicum, Ctenidodinium ornatum, Endoscrinium galeritum, Gonyaulacysta eisenackii, Nannoceratopsis pellucida, Sirmiodiniopsis orbis*).

The oldest possible age is Plicatilis Zone. There are a few single specimens of *Scriniodinium crystallinum*, a species that is considered to have an LAD in the Plicatilis Zone, but these are single specimens that may have been reworked. Most dinoflagellate cysts present have an LAD of Transversarium Zone. Unusual is the co-occurrence of these species with several good specimens of unambiguous *Amphorula dodekovae* and *Dingodinium tuberosum*, both being considered to have an FAD of Bifurcatus Zone.

The co-occurrence of these taxa is interpreted to correspond most likely to an age at the transition between Transversarium Zone and Bifurcatus Zone.

N.B.: The sample at the base of the interval (at 501.62 m) has been contaminated with older material. It shows several records of distinctly older taxa interpreted as not in situ. In the range-chart these taxa are indicated as "reworked" ("Rw").

Tab. 3-3: List of analysed palynology samples from MAR1-1

The indicated ages, zones and subzones for each sample are the result of the palynostratigraphical analysis and interpretation.

Depth [m MD]	**Age**	**Zone & Subzone**
501.30	Late – Middle Oxfordian	Bifurcatus – Transversarium Zone
501.62	Late – Middle Oxfordian	Bifurcatus – Transversarium Zone
502.33	Middle – Early Callovian	Coronatum – Herveyi Zone
502.81	Early Callovian	Calloviense – Herveyi Zone
504.94	Late – Early Bathonian	Discus – Zigzag Zone (Tenuiplicatus SZ)
505.85	Late – Early Bathonian	Discus – Zigzag Zone (Tenuiplicatus SZ)
506.48	Late – Early Bathonian	Discus – Zigzag Zone (Tenuiplicatus SZ)
509.33	Late – Early Bathonian	Discus – Zigzag Zone (Tenuiplicatus SZ)
517.85	Late – Early Bathonian	Discus – Zigzag Zone (Tenuiplicatus SZ)
523.67	Early Bathonian	Zigzag Zone
534.10	Early Bathonian	Zigzag Zone
543.41	Late Bajocian	Parkinsoni Zone
544.39	Late Bajocian	Parkinsoni Zone
544.80	Late Bajocian	Parkinsoni Zone
545.65	Late Bajocian	Garantiana Zone
546.02	Late Bajocian	Garantiana Zone
546.90	Late Bajocian	Niortense Zone
547.66	Late Bajocian	Niortense Zone
548.21	Early Bajocian	Humphriesianum Z (Humphriesianum SZ – Romani SZ)
549.41	Early Bajocian	Humphriesianum Z (Humphriesianum SZ – Romani SZ)
550.87	Early Bajocian	Humphriesianum Z (Humphriesianum SZ – Romani SZ)
553.85	Early Bajocian	Sauzei Zone
555.00	Early Bajocian	Sauzei Zone
555.06	Early Bajocian	Sauzei Zone
555.54	Early Bajocian	Laeviuscula Zone
563.00	Early Bajocian	Laeviuscula – Ovale Zone
571.98	Early Bajocian	Laeviuscula – Ovale Zone
578.01	Early Bajocian	Ovale Zone
583.88	Early Bajocian	Ovale Zone
586.94	Early Bajocian	Ovale Zone
588.95 new prep.	Early Bajocian	Ovale Zone
588.95	Inconclusive (contaminated sample)	
589.23	Middle Aalenian	Bradfordensis Zone
590.21	Middle – Early Aalenian	lower Bradfordensis – Opalinum Zone
590.38	Middle – Early Aalenian	lower Bradfordensis – Opalinum Zone
600.02	Early Aalenian	Opalinum Zone (Opalinum SZ)
600.69	Early Aalenian	Opalinum Zone (Opalinum SZ)
626.09	Early Aalenian	Opalinum Zone (Opalinum SZ)
645.23	Early Aalenian	Opalinum Zone (Opalinum SZ)
664.62	Early Aalenian	Opalinum Zone (Opalinum SZ)
685.09	Early Aalenian	Opalinum Zone (Opalinum SZ)
705.04	Early Aalenian	Opalinum Zone (Opalinum SZ)
705.78	Early Aalenian	Opalinum Zone (Opalinum SZ)

3.4 Chemostratigraphy

The sampling of the MAR1-1 cores focused primarily on the Lias Group (Figs. 3-2 and 3-3) and Dogger Group (Figs. 3-4 to 3-7) and, therefore inter alia, on clay mineral-rich layers of the Opalinus Clay. The summary Figs. 3-8 and 3-9 illustrate the fully analysed interval from the middle of the Staffelegg Formation up to the Wildegg Formation (721.94 – 494.00 m). The data presented here (applies for all subsequent figures in this section) are shown in comparison to other data collected during the drilling campaign: Stratigraphic profile after Dossier III, Dry Clay (values in wt.-% with vertical axis in m MD log depth; *cf.* Dossier X), XRD measurements (horizontal bars; calcite: blue, dolomite and ankerite: green, siderite: red; *cf.* Dossier VIII) and C(org) measurements in blue (*cf.* Dossier VIII). In addition, formation boundaries were highlighted with black lines and other formal or informal subintervals with grey lines. The following stratigraphic abbreviations were used in Figs. 3-2 to 3-9: G = Grünschholz Member; B + R = Breitenmatt Member and Rickenbach Member; OPA = Opalinus Clay; G. Wolf = Gross Wolf Member; «M.O.» = «Murchisonae-Oolith Formation»; «Humphriesio.» or «Hum.» = «Humphriesioolith Formation»; Bi. = Birmenstorf Member; Ef. = Effingen Member.

In addition to the continuous samples (roughly in metre resolution), some specific samples were taken (Appendix E1) to complete the information about the calcareous beds and macrofossils. Some of the hardground samples were drilled directly from the remaining thin section blocks to correlate the bulk geochemical data with the microfacies analysis. All these data points are distinguished in different colours on Figs. 3-2, 3-4 and 3-6 (in light blue: calcareous samples (firm- and hardgrounds, "hiatus beds", "hiatus concretions", calcareous concretions); in violet: septarian nodules; in green: macrofossils) but may not be shown on the individual plots because of the data ranges (see Appendix E1 for data).

The data will be discussed in three intervals: Lias Group, the lower part of the Dogger Group – mainly Opalinus Clay and the upper part of the Dogger Group. Not all data are discussed to the same extent as for example the $\delta^{18}O_{carb}$ and $\delta^{15}N_{org}$ data. The oxygen isotopes are strongly influenced by diagenesis. This can be exemplarily shown with the measured belemnites (Appendix E1) in the Lias Group (green points in Fig. 3-2). These are 3 to 4‰ more positive than the marlier bulk rock and therefore much less diagenetically overprinted. The nitrogen isotopes may not be as meaningful in some cases, because the combined $\delta^{13}C_{org}$ and $\delta^{15}N_{org}$ measurements showed a too low concentration of N in most of the measurements.

Although the calculated carbonate content (TCarb) is only a semi-quantitative method, the values presented here correspond quite good to the XRD values measured at the University of Bern (*cf.* Dossier VIII). The XRD data are illustrated in the following Figs. 3-2, 3-4 and 3-6 to provide a visual comparison between the data presented here and those from Dossier VIII. As discussed in Wohlwend et al. (2019b) based on measurements from the BDB-1 borehole at the Mont Terri Rock Laboratory, the values calculated here follow nicely the calcite and dolomite wt.-% with an additional mixed signal from the other carbonates (mainly siderite). Because during the reaction time of 60 min at 72 °C, a complete reaction for example for siderite does not take place, the TCarb values are slightly too low in siderite-rich successions (red bars in the XRD data), which is for example often the case in the «Mixed clay-silt-carbonate sub-unit» (688.88 – 642.77 m; Fig. 3-4).

In contrast to the carbonate measurements (bulk samples), the organic measurements were not always measured in metre resolution, depending on the variability of the expected isotope data. If no major isotope changes occur over longer stratigraphic successions, as can be expected in the middle part of the Opalinus Clay as well as in the «Parkinsoni-Württembergica-Schichten» and the Variansmergel Formation (e.g. Wohlwend et al. 2021b), only every second sample (2 m interval) was analysed for the MAR1-1 cores.

Lias Group

Starting from the bottom up (Fig. 3-2), the oldest sediments measured belong to the Early Jurassic (probably Late Pliensbachian to Early Toarcian). The lowermost measurements (721.94 – 721.58 m) are coming from the uppermost combined Breitenmatt Member and Rickenbach Member. The following measurements between 721.45 m and 705.50 m represent the upper two members of the Staffelegg Formation. They show, especially in the carbonate content, larger variations in their individual data, which can be explained by the overall higher sampling resolution in the Lias Group (some intervals in the Rietheim Member with around 10 cm spacing) as well as by the nodular calcareous lithology of the Gross Wolf Member.

The semi-quantitative carbonate content (TCarb) values represent the lithological variations in the Rietheim Member and the hanging Gross Wolf Member. In the Rietheim Member the TCarb values show a decreasing trend from almost 50 wt.-% to values around 20 wt.-% just below the «Unterer Stein» (720.02 – 719.77 m). From here upwards, the TCarb values are around 40 to 50 wt.-%. The interval is clearly interrupted by higher values measured from the four calcareous interbeds. The three lower beds («Unterer Stein»: 720.02 – 719.77 m, «Homogene Kalkbänke»: 719.27 – 719.10 m and «Oberer Stein»: 718.33 – 718.10 m; nomenclature *sensu* Kuhn & Etter 1994) show a stepwise lower TCarb content with the highest value of 99.1 wt.-% measured from the lowest one, 94.1 wt.-% from the middle to 81.8 wt.-% from the upper bed. The uppermost calcareous bed, with a value up to 90.3 wt.-%, represents probably the «Monotisbank» (713.19 – 713.07 m) *sensu* Kuhn & Etter 1994.

The $\delta^{13}C_{carb}$ values are rather stable around 0.5‰ in the lowermost 0.6 m of the Rietheim Member followed by a prominent negative excursion with the most negative value (-6.3‰) measured from the sample from the «Unterer Stein» (719.85 m). The negative trend is subsequently followed by a rapid increase to positive values close to 2.5‰. The values stabilise thereafter to the top of the Rietheim Member and decrease afterwards slightly to around 0.5‰. Only the uppermost two samples (705.66 m and 705.50 m) show distinct more negative values (-0.7‰). The discussed negative excursion below the «Unterer Stein» represents one of the major Mesozoic negative carbon-isotope excursions (CIE) – the Toarcian-Oceanic Anoxic Event (T-OAE). When looking in detail, the data points, which belong to the four calcareous beds (see discussion above) show more negative values then the marlier sediment. The calcareous beds are clearly diagenetically altered and therefore the most negative value from the «Unterer Stein» does not represent the most negative part of the T-OAE (e.g. Röhl & Schmid-Röhl 2005, Montero-Serrano et al. 2015). This can be tested with the $\delta^{13}C_{org}$ values (Fig. 3-3), where the most negative one, with a value of -32.5‰, was measured just below the marker bed (at 720.20 m). The following rapid positive shift is also clearly documented in the organic matter, where the most positive value (-26.9‰) was measured from the sample just below the «Oberer Stein». The $\delta^{13}C_{org}$ curve shows great similarity with the data documented from the Aubach section in the Wutach area (Hougård et al. 2021). The following $\delta^{13}C_{org}$ trend to more negative values ends with a very prominent shift or jump at the Rietheim / Gross Wolf Member boundary. This prominent "shift" correlates nicely with the semi-quantitative organic carbon (TOC) content as well as with the C/N ratio. The $\delta^{13}C_{org}$ signal is influenced by different sources of the organic matter during the time of the Rietheim Member to Gross Wolf Member and therefore represents also nicely the lithological boundary between the bituminous – Type I-II kerogene (e.g. Suan et al. 2015, Hougård et al. 2021) – Rietheim Member and the overlying more calcareous Gross Wolf Member.

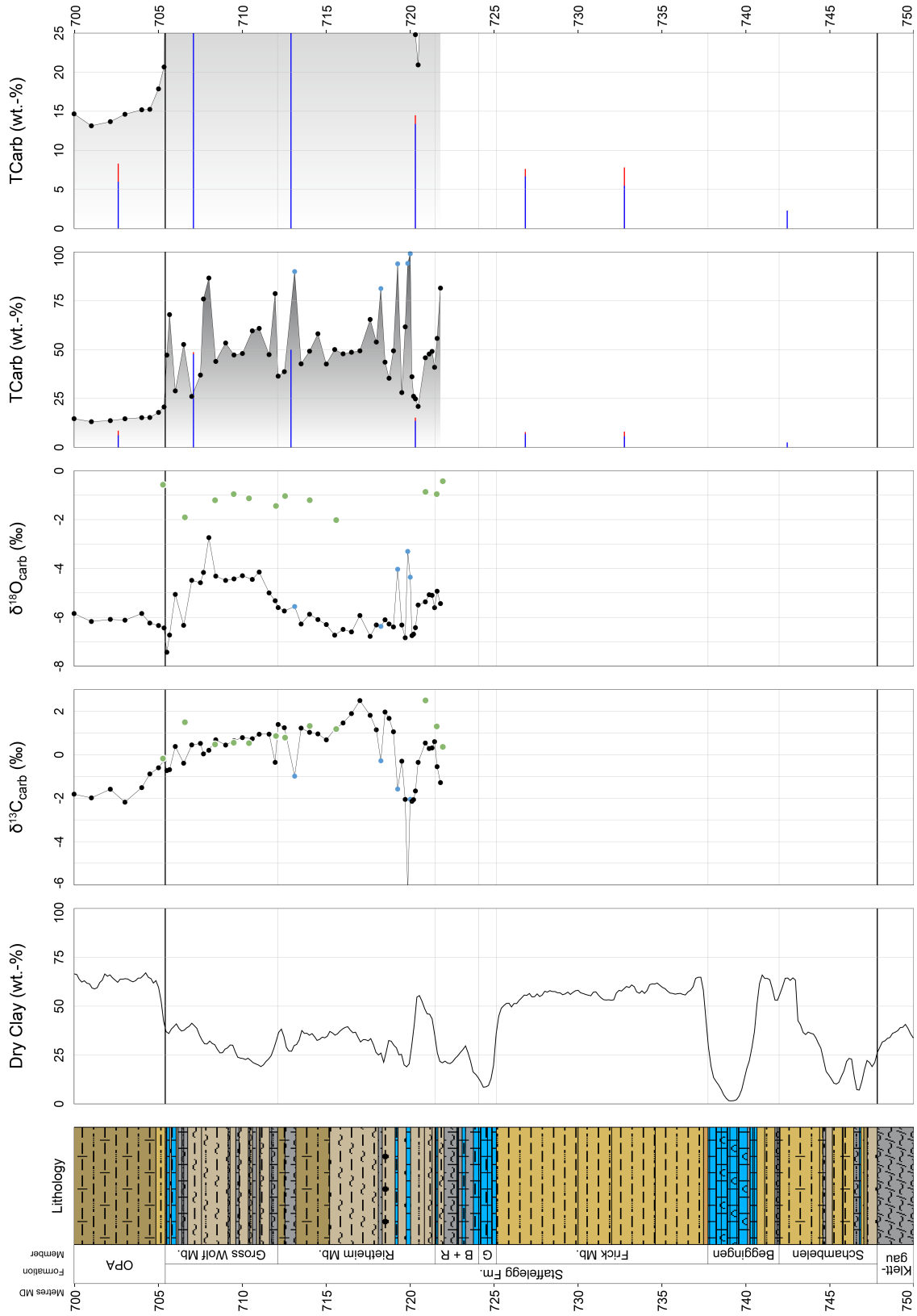

Fig. 3-2: Bulk rock (carbonate) isotopic data from the Lias Group

Geochemical data from 721.94 – 701.00 m, additional explanations and references see text at the beginning of Section 3.4.

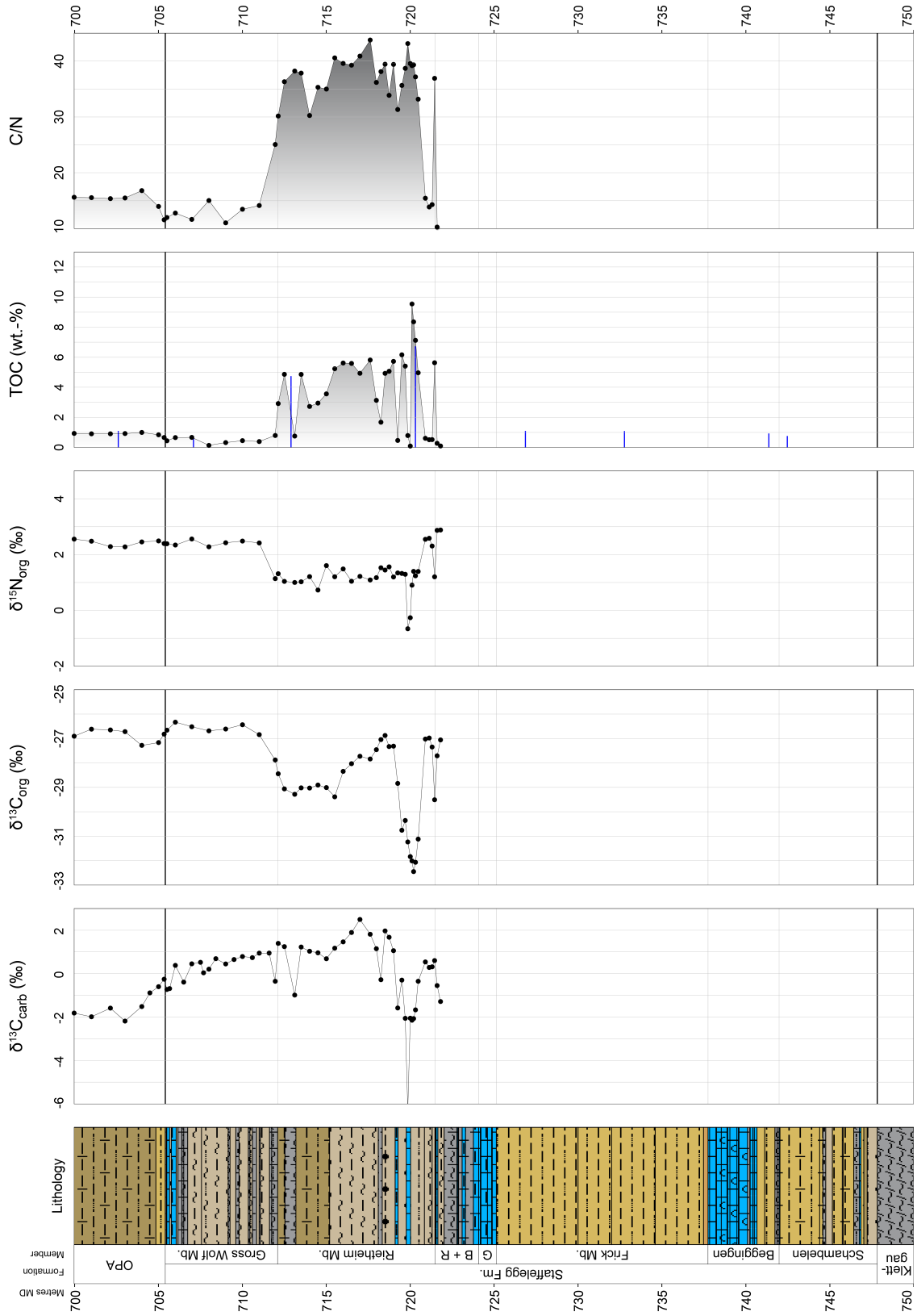

Fig. 3-3: Organic isotopic data from the Lias Group

Geochemical data from 721.94 – 701.00 m, additional explanations and references see text at the beginning of Section 3.4.

As already mentioned, above the Rietheim Member is very bituminous. The member itself was defined at the base of the lowermost cm-thick seam of bituminous shale which can be found between 721.48 m and 721.45 m (*cf.* Dossier III). This thin bed, with a semi-quantitative TOC content of 5.6 wt.-% clearly stands out when comparing the samples below and above (Fig. 3-3). Together with the negative CIE of the T-OAE, very high values occur, with maximum values around 8.4 to 9.6 wt.-% contemporaneous with the most negative $\delta^{13}C_{org}$ value between 720.20 and 720.10 m. The lower and middle Rietheim Member have an average TOC content of around 5 – 6 wt.-%, which is higher than the content in the upper part with values around 3 – 5 wt.-%. The hanging Gross Wolf Member has an obvious different lithological composition which is nicely documented by the very stable but much lower TOC content, which is around 0.5 wt.-%.

The C/N ratios somehow show the same trends as the TOC, with the highest ratios measured contemporaneous with the more bituminous lower and middle part of the Rietheim Member (35 – 44). The overlying Gross Wolf Member shows again a striking different C/N ratio, which is much lower (10 – 15). Such high C/N ratios, measured in the Rietheim Member, are very unusual for marine organic matter, which usually has values between 5 and 8 (e.g. Emerson & Hedges 1988, Meyers 1997) and would therefore pretend that the organic material would be of terrigenous source. However, such high C/N ratios were also reported from mid-Pleistocene sapropels from the Tyrrhenian Basin (Meyers & Bernasconi 2005) which are also clearly produced by marine organic matter. Van Mooy et al. (2002) proposed a model for these very unusual C/N ratios in which they determined from sediment trap studies that suboxic microbial degradation via denitrification preferentially utilises nitrogen-rich amino acids and hence leaves a larger proportion of the nitrogen-poor organic matter components intact than under oxic conditions. C/N values of the surviving organic matter necessarily rise.

Lower part of the Dogger Group – mainly Opalinus Clay

The interval described in the following section, the lower part of the Dogger Group (the Opalinus Clay, «Murchisonae-Oolith Formation» and the transition into the lower part of the Wedelsandstein Formation), is also the interval at the main focus of these investigations (Figs. 3-4 and 3-5).

The semi-quantitative carbonate content (TCarb) values from the more homogeneous clay mineral-dominated lithologies compared to those from the underlying Staffelegg Formation (Fig. 3-4) are rather low and very stable. From the base of the Opalinus Clay to around 694.50 m the average TCarb is around 15 wt.-%. In the above following succession up to 684.00 m the TCarb shows slightly lower values around 10 wt.-%. Between the samples 684.00 m and 683.00 m an obvious shift to even less carbonate rich sediments with values around 5 to 7 wt.-% is documented. The values increase slightly in the «Mixed clay-silt-carbonate sub-unit» and the «Upper silty sub-unit» (642.77 – 626.41 m) reaching values around 10 wt.-%. The uppermost informal sub-unit («Sub-unit with silty calcareous beds»: 626.41 – 590.35 m) shows again similar average values between 5 – 10 wt.-% as in the lower part of the Opalinus Clay. In the uppermost 5 to 7 m of the Oplainus Clay a clear trend to almost carbonate free claystone (values around 1.4 wt.-%) is documented. In the thin «Murchisonae-Oolith Formation» and in the lower part of the hanging Wedelsandstein Formation the TCarb increases.

The above-mentioned uppermost informal unit in the Opalinus Clay («Sub-unit with silty calcareous beds») comprises several calcareous beds (see Appendix E1 for data). They and also additional ones from the lower part of the Opalinus Clay are illustrated in Fig. 3-4 by thicker light blue lines ending with blue dots marking the TCarb values. Some of them are classified as measurements from calcareous or sideritic concretions. In addition, also the bulk sediment from a septarian nodule and the calcite cement from its crack were measured, illustrated in violet. The

calcareous beds (mainly hardground) are located in the uppermost «Sub-unit with silty calcareous beds». Most of them comprise semi-quantitative carbonate contents that are typical for calcareous marl to limestone. The lowermost calcareous concretions at 695.22 m and 695.13 m, belong to a level in the «Clay-rich sub-unit» (705.40 – 688.88 m), which seems to be correlatable over several boreholes (e.g. TRU1-1; Wohlwend et al. 2021b).

The $\delta^{13}C_{carb}$ data show two negative excursions or intervals (Fig. 3-4): a lower one in the lowermost «Clay-rich sub-unit» and an upper one in the uppermost «Sub-unit with silty calcareous beds». The last mentioned is less developed compared to the lower one. The succession in between shows more positive values fluctuating around 0 to 1‰ with a few measurements reaching $\delta^{13}C_{carb}$ values up to 1.7‰ and one extrem positive value of 3.2‰ at 620.00 m. The lower negative excursion is represented by clearly decreasing and increasing trends, reaches the most negative values (-3.9‰ at 694.50 m) just above the lower calcareous concretions mentioned above at 695.22 and 695.13 m. The upper negative excursion, with a clear decreasing and following increasing trend, reaches the lowest value of -2.0‰ at 601.00 m just beneath a thin calcareous, biodetric, slightly iron-oolitic hardground from 600.62 – 600.52 m. The negative excursion ends below another calcareous bed at 597.33 m, which is slightly less visible in the cores. From 596.50 m to the top of Opalinus Clay the values show a decreasing trend with the most negative value (-2.2‰) just beneath the top at 590.99 m.

The $\delta^{13}C_{carb}$ data from the calcareous beds or intraclasts document possibly an early diagenetic signal (e.g. Wetzel & Allia 2000). The calcareous concretions or "hiatus concretions" are the only macroscopic features with very negative $\delta^{13}C_{carb}$ values (-16.9 to -27.3‰, Appendix E1). Very fine authigenic calcite was probably precipitated in the very fine original porosity of the Opalinus Clay, which led to the more negative $\delta^{13}C_{carb}$ values in the lower and upper negative excursions (see also Wohlwend et al. 2016.). Also remarkable is the scatter of the individual measurements (metre resolution) in the lower part of the «Mixed clay-silt-carbonate sub-unit» (~ 685 – ~ 662 m) and in the «Upper silty sub-unit» (~ 641 – ~ 623 m). The succession comprises silt lenses, some of them up to several centimetre thick, some of them very thin. It was therefore not always possible to sample only the clay mineral-rich sediment. The scatter can be explained by varying amounts of silt, which probably comprises very thin calcite pore fillings in the primary porosity of these lenses.

The $\delta^{13}C_{carb}$ data from the «Murchisonae-Oolith Formation» show again more positive values (around 0 – 0.5‰) compared to the ones just beneath in the uppermost Opalinus Clay. The positive trend can also be seen into the lower part of the Wedelsandstein Formation with values up to 1‰.

The $\delta^{13}C_{org}$ data (Fig. 3-5) show a different picture compared to the $\delta^{13}C_{carb}$ values. The curve is relatively stable and shows only a slight increasing trend in the central part (from 689.00 m upwards to 623.00 m). The organic carbon isotopes indicate variations only at the base of the Opalinus Clay («Clay-rich sub-unit») and at the top (upper part of the «Sub-unit with silty calcareous beds»). At the base, three to four individual negative trends or peaks can be recognised (704.00 m: -27.3‰; 698.97 m: -27.3‰; 694.50 m: -28.1‰; 693.00 m: -27.9‰). The upper two may can be combined to form a larger excursion with a short positive peak. The amplitude of the three to four variations increases upwards and reaches the maximum in the third with 1.7‰ between the most negative and the most positive ones. The values above these variations stabilise around -27.0‰. In the «Mixed clay-silt-carbonate sub-unit» and «Upper silty sub-unit», there is an overall trend towards +0.5‰ heavier values visible, reaching values around -26.7‰ at 635.00 m to 623.00 m.

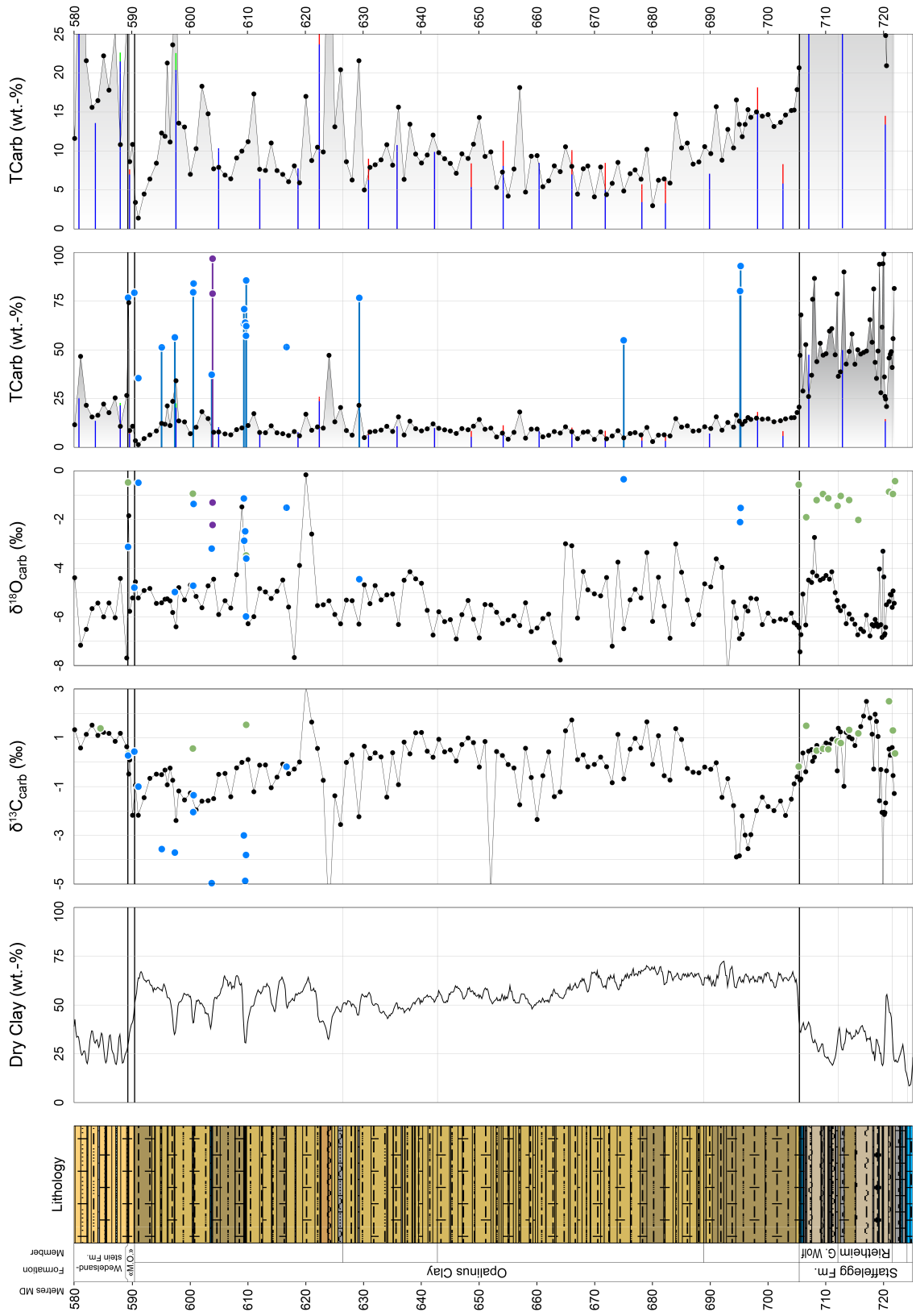

Fig. 3-4: Bulk rock (carb.) isotopic data from the lower Dogger Group – mainly Opalinus Clay

Geochemical data from 721.94 – 581.01 m, additional explanations and references see text at the beginning of Section 3.4.

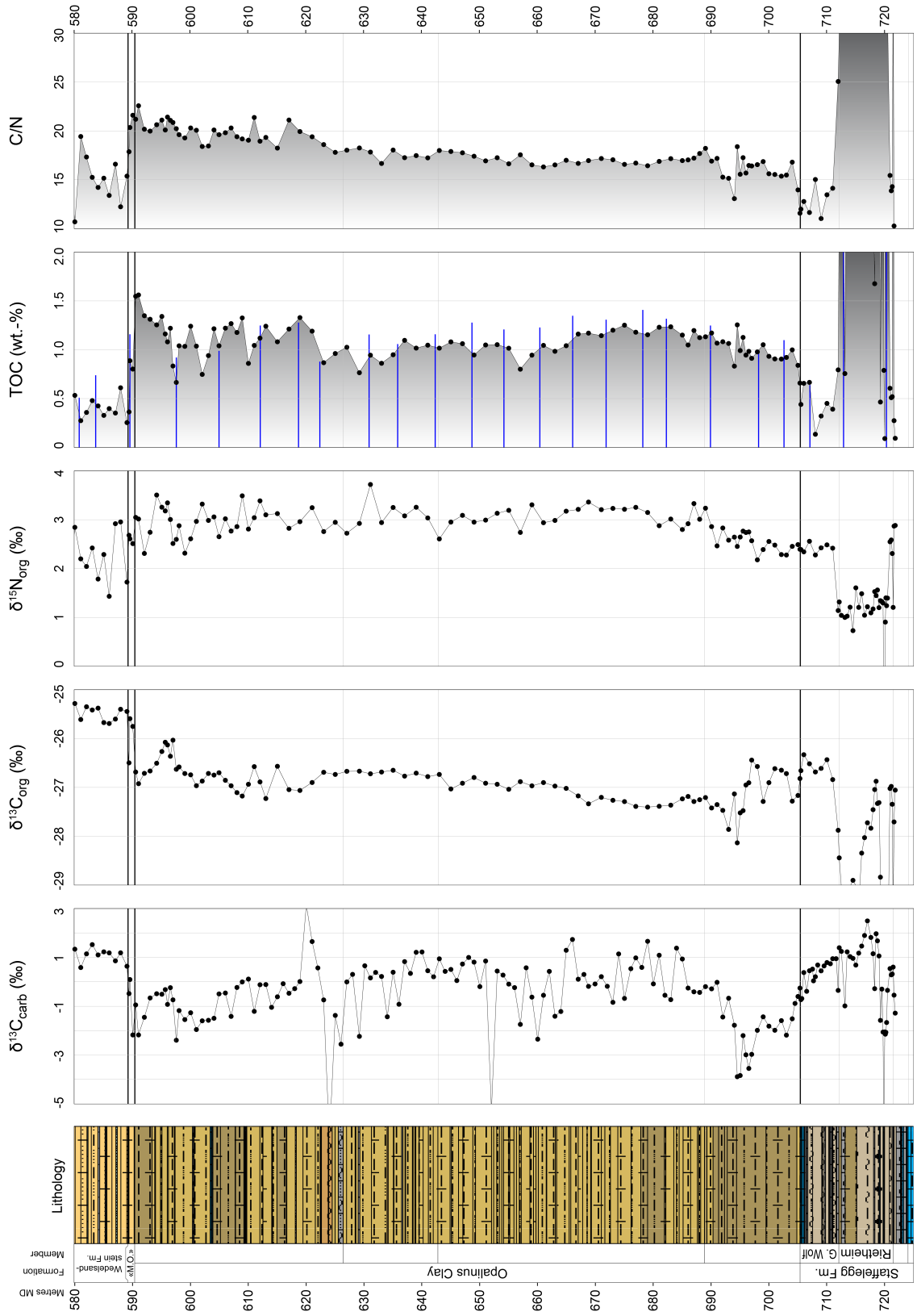

Fig. 3-5: Organic isotopic data from the lower Dogger Group – mainly Opalinus Clay

Geochemical data from 721.94 – 581.01 m, additional explanations and references see text at the beginning of Section 3.4.

The upper part of the Opalinus Clay («Sub-unit with silty calcareous beds») shows slight variations in the $\delta^{13}C_{org}$ data with a first 0.5‰ more negative shift before the $\delta^{13}C_{org}$ values increase to an overall positive peak in the Opalinus Clay at 596.95 m with -26.0‰. This more positive $\delta^{13}C_{org}$ excursion is measured in the sample just above the uppermost calcareous beds, similar to the positive shift in the $\delta^{13}C_{carb}$ data.

The two first measurements (590.00 m and 589.50 m) from the argillaceous siltstone from the «Murchisonae-Oolith Formation» document a clear positive shift in the $\delta^{13}C_{org}$ data (1‰ more positive) to values around -25.6‰. These positive values lead over into the lower part of the Wedelsandstein Formation.

The C/N ratios show a minor variation in the «Clay-rich sub-unit» and afterwards a stable interval in the «Mixed clay-silt-carbonate sub-unit» with a ratio around 17 to 18. In the uppermost sub-unit the C/N ratio increases to almost 23 at the top of the Opalinus Clay. The very thin «Murchisonae-Oolith Formation» documents the beginning of a decreasing trend into the lowermost part of the Wedelsandstein Formation (12 at 587.90 m).

Upper part of the Dogger Group

The following described interval, the upper Dogger Group («Murchisonae-Oolith Formation», Wedelsandstein Formation, «Humphriesioolith Formation», «Parkinsoni-Württembergica-Schichten», Variansmergel Formation, Wutach Formation and Wildegg Formation), covers in time the whole Middle Aalenian to Middle Oxfordian substages (Figs. 3-8 and 3-9).

The semi-quantitative TCarb (Fig. 3-6) represents the alternation of silty claystones, argillaceous to calcareous marls and limestones in the upper part of the Dogger Group. However, the TCarb contents are somehow underestimated because of the sampling strategy of not sampling every single limestone bed (focus on the bulk, clay mineral-rich sediments). Nevertheless, the carbonate content curve reflects in general the inverse wet clay content curve (*cf.* Dossier X). The Wedelsandstein Formation can be divided into two subintervals, representing two different lithologies: The lower one (base to around sample at 561.96 m, lithological boundary in the profile at 561.85 m) includes several calcareous marl to limestone beds in an argillaceous to argillaceous marly sediment with a TCarb content mostly slightly beyond 25 wt.-%. The upper subinterval (up to the top of the formation) certainly contains less carbonate, interrupted by two higher values at 558.00 m and 557.00 m. The argillaceous to argillaceous marly succession is than overlain by the distinct more calcareous «Humphriesioolith Formation». The lower and upper boundary is clearly represented by a shift in the carbonate content, which therefore goes hand in hand with the occurrence of iron-ooids, defining this formation. Upward the succession only changes again noticeably with the Wutach Formation and Wildegg Formation, both representing a calcareous marl or limestone with a variable content of iron-ooids in the Wutach Formation and at the very base of the Wildegg Formation.

As already mentioned above, the $\delta^{13}C_{carb}$ data show an overall positive trend from the uppermost Opalinus Clay up section. The C-isotope stabilise between +1.0 and +1.7‰ throughout the Wedelsandstein Formation. The most positive value of 2.8‰ was measured at 555.12 m already in the lower iron-oolitic succession of the «Humphriesioolith Formation». In the marlier interval to the top of the «Humphriesioolith Formation», the $\delta^{13}C_{carb}$ data documents a clear trend to more negative values (554.00 – 546.02 m). Just above, in the «Parkinsoni-Württembergica-Schichten» the clear negative value with -4.3‰ at 544.48 m may be correlated with the «Parkinsoni-Oolith» (544.52 – 543.73 m; *cf.* Dossier III). The $\delta^{13}C_{carb}$ values in the «Parkinsoni-Württembergica-Schichten» and Variansmergel Formation vary between 0.2 and 1.2‰ and are rather stable until the Wutach Formation. The striking positive shift of almost two per mil to values around +2.6‰

with a maximum of +3.1‰ at 501.04 m is typical for the Callovian/Oxfordian boundary and was already documented by Rais et al. (2007) in other locations and in the Weiach borehole as well as in the Bülach-1-1 borehole (Wohlwend et al. 2021a). The most positive $\delta^{13}C_{carb}$ values were documented by Rais et al. (2007) in the Middle Oxfordian (Transversarium Zone).

The $\delta^{13}C_{org}$ data (Fig. 3-7) show a somehow similar overall increasing trend through the Wedelsandstein Formation as discussed above. Although the values first slightly decrease in the middle part (579.00 – 565.97 m) to around -26.0‰, before the $\delta^{13}C_{org}$ values increase to a maximum value of -24.8‰ just below the top of the Wedelsandstein Formation at 556.00 m. The two more negative values (around -28.0‰) in the lowermost part of the «Parkinsoni-Württembergica-Schichten» (544.00 m and 543.00) mark a turnaround to again more positive values into the Variansmergel Formation. Similar to the $\delta^{13}C_{carb}$ data, the $\delta^{13}C_{org}$ data also document the striking positive shift to a peak value of -23.2‰ at 501.62 m close to the Callovian/Oxfordian boundary.

The semi-quantitative TOC content is usually around 0.5 wt.-%. However, the Wedelsandstein Formation and the «Humphriesioolith Formation» have a distinct lower TOC than the «Parkinsoni-Württembergica-Schichten». C/N ratio varies throughout the upper part of the Dogger Group between 15 and 25 with higher peak values measured from individual calcareous beds. The «Parkinsoni-Württembergica-Schichten» clearly show more stable C/N ratios between 15 and 20.

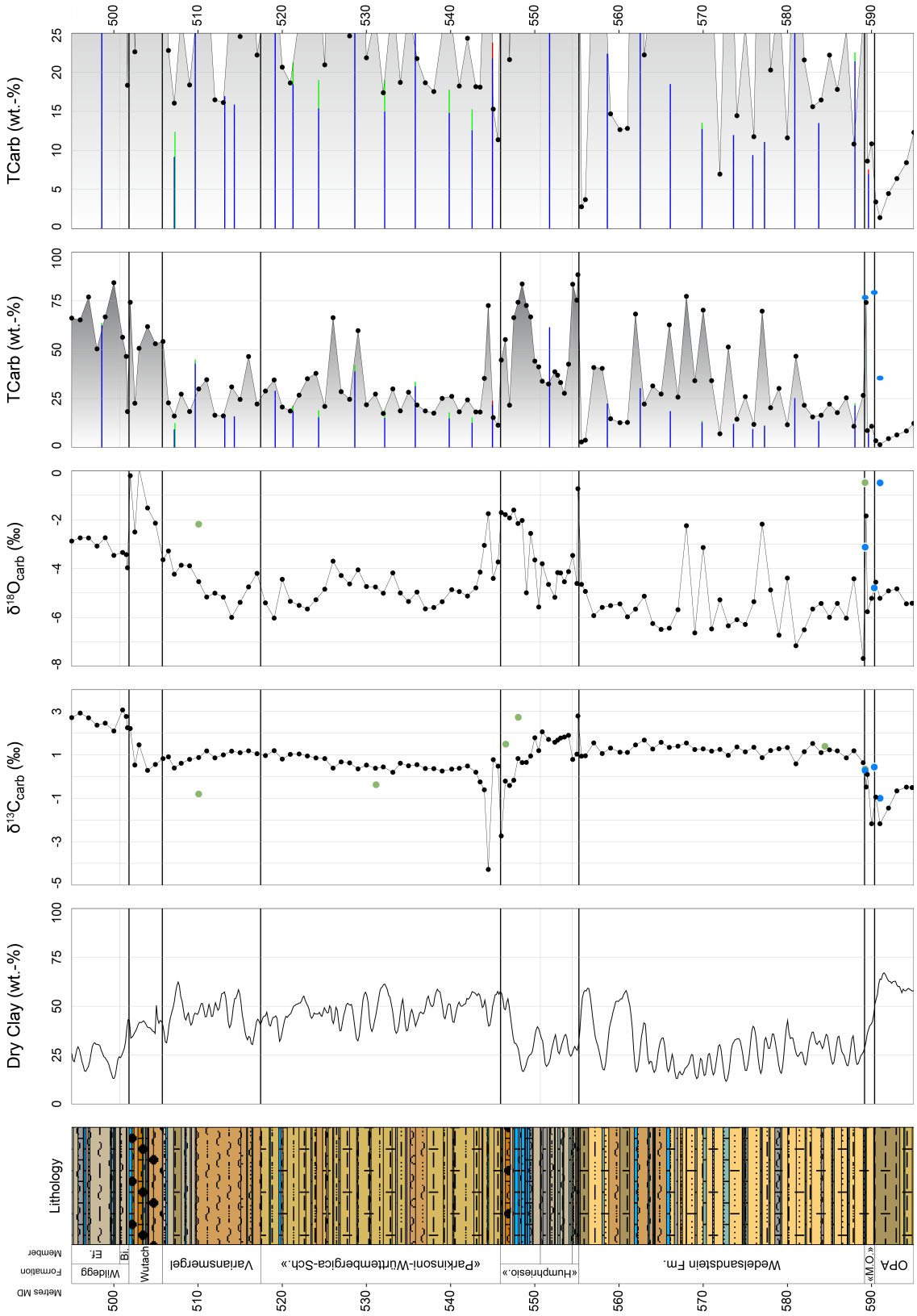

Fig. 3-6: Bulk rock (carbonate) isotopic data from the upper part of the Dogger Group

Geochemical data from 594.13 – 495.00 m, additional explanations and references see text at the beginning of Section 3.4.

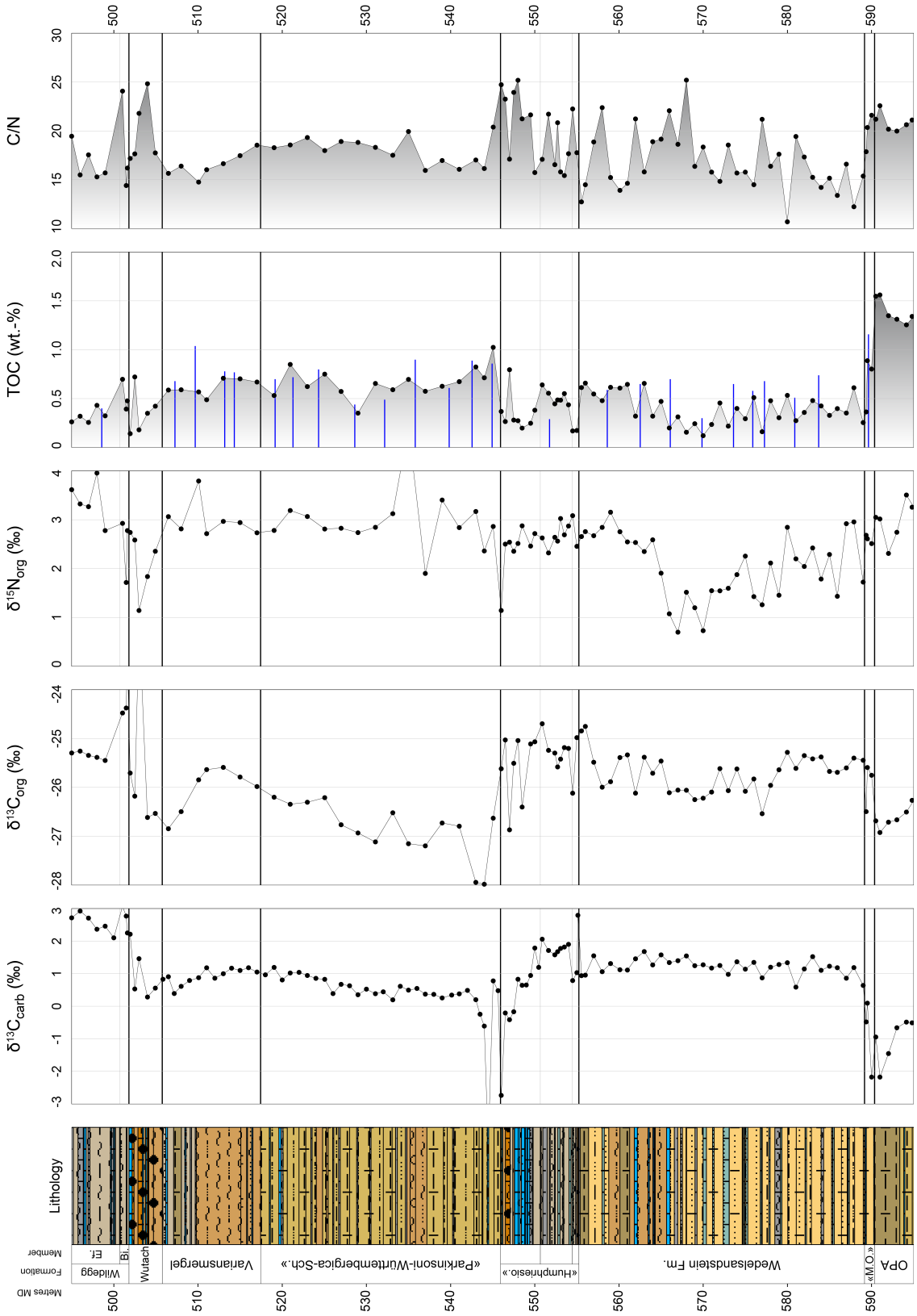

Fig. 3-7: Organic isotopic data from the upper part of the Dogger Group

Geochemical data from 594.1 – 495.00 m, additional explanations and references see text at the beginning of Section 3.4.

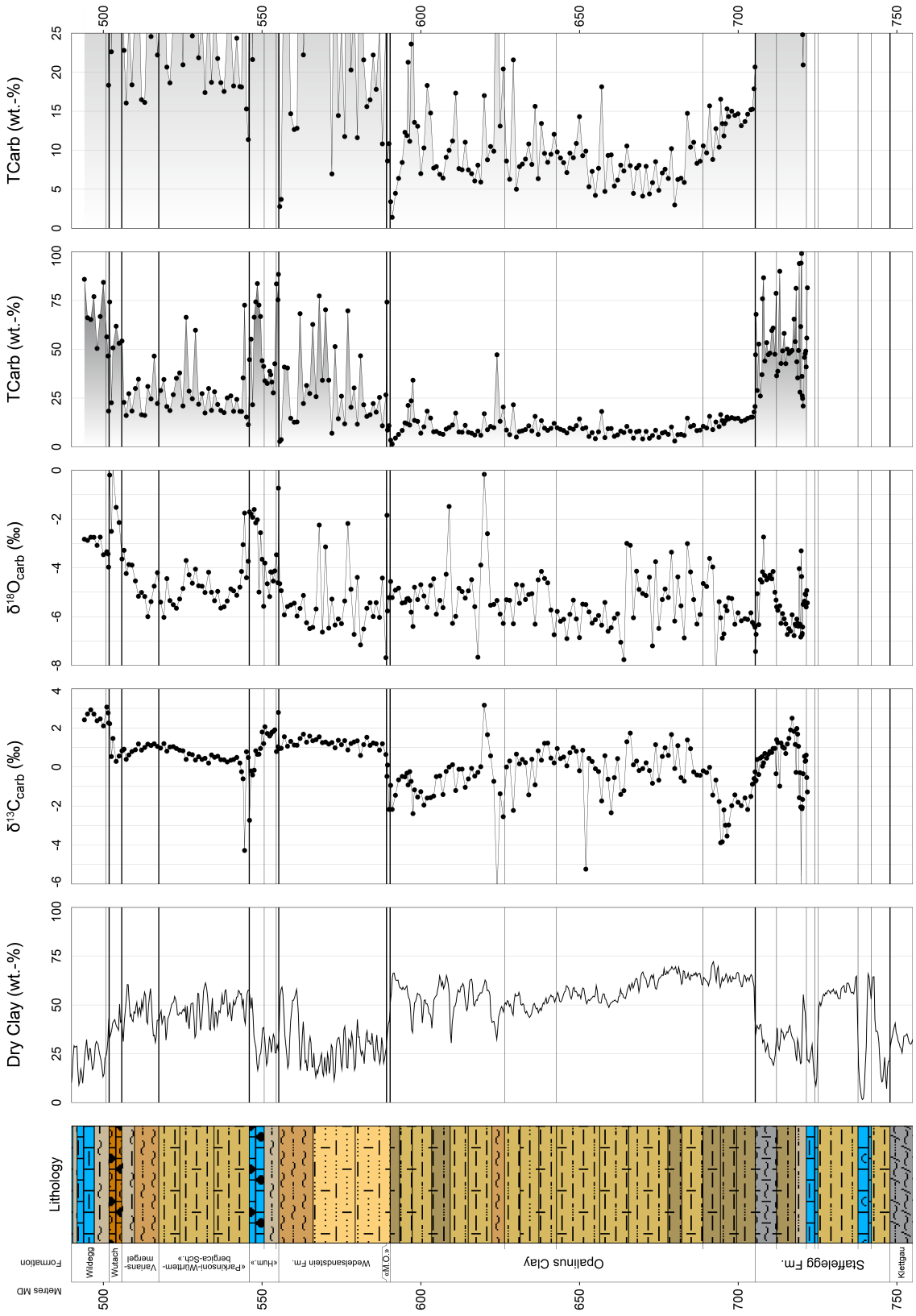

Fig. 3-8: Whole bulk rock (carbonate) isotopic data from MAR1-1

Geochemical data from 721.94 to 494.00 m, additional explanations and references see text at the beginning of Section 3.4.

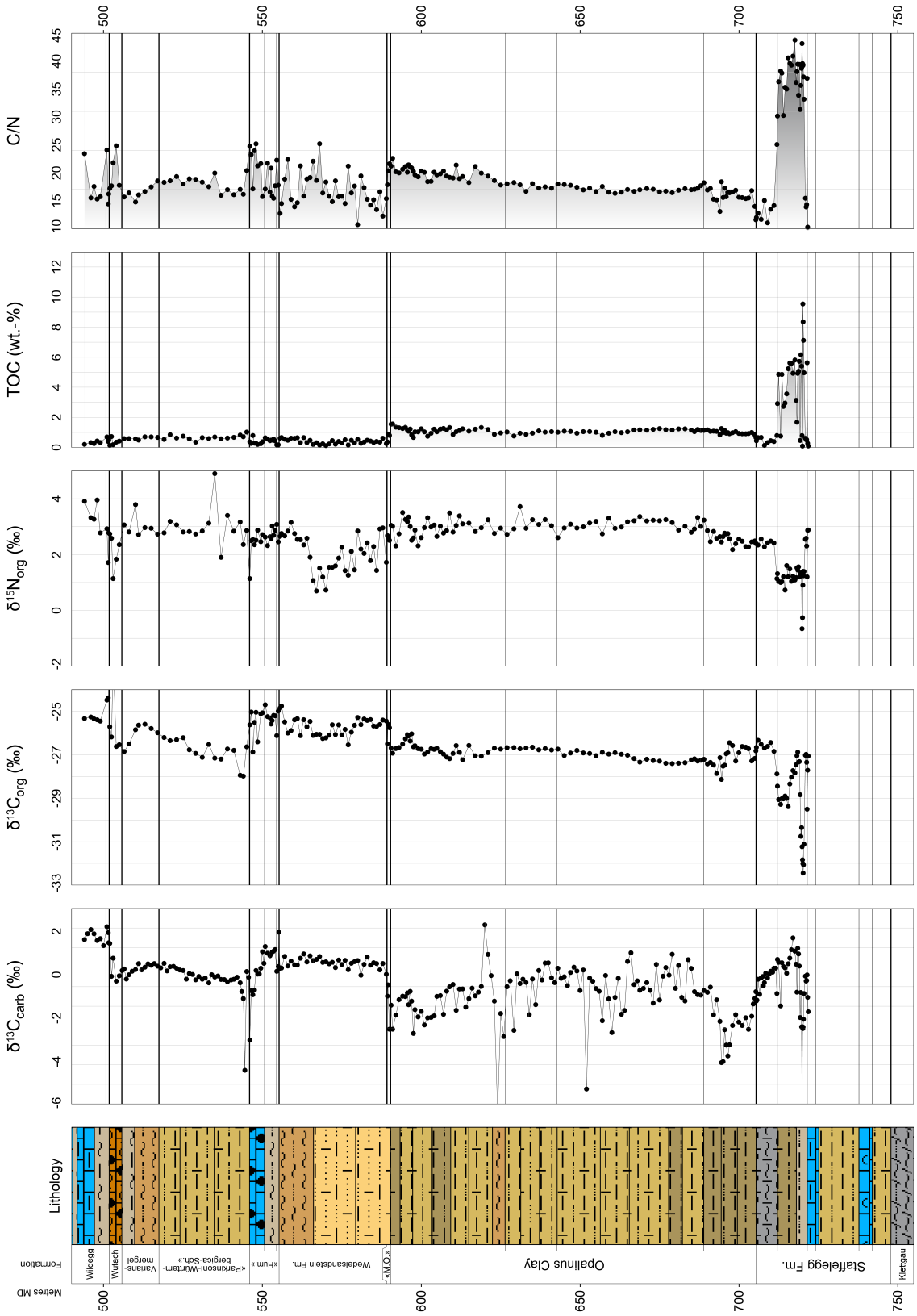

Fig. 3-9: Whole organic isotopic data from MAR1-1

Geochemical data from 721.94 to 494.00 m, additional explanations and references see text at the beginning of Section 3.4.

4 Definition of specific lithostratigraphic boundaries

The boundaries between stratigraphical units, as also shown in the stratigraphical logs of the lithostratigraphy report (Dossier III), were mostly defined by using lithological criteria. According to the guidelines on stratigraphical nomenclature of Remane et al. (2005), the definition of lithostratigraphical units should be based, both vertically and horizontally, on lithological variations regardless of their age. In fact, the formation boundaries, as used by Nagra for the ongoing borehole campaign of Stage 3 of the Sectoral Plan for Geological Repositories (Jordan & Deplazes 2019), were not always obvious in the borehole, and definitions were difficult to apply, either because of the small core diameter or because of differences in facies. The exact location of some of the formation boundaries caused discussions during core description and the process of quality control. Most of the important data for questionable boundaries were already present before the data-freeze (14.09.2020) and were used for the log descriptions and drawings. In the following paragraphs, the underlying considerations are explained for providing a better understanding of how boundaries were demarcated. We are aware of the fact that several boundaries are no longer based on lithological criteria alone and that chronostratigraphic criteria (ammonite, palyno- and chemostratigraphy) are included in the definitions.

Opalinus Clay (705.40 – 590.35 m)

The *lower boundary* of the Opalinus Clay is set at 705.40 m at the uppermost surface of a fossiliferous calcareous marl from the underlaying Staffelegg Formation (*cf.* Dossier III). The lithological boundary is therefore evident above all in the carbonate content (TCarb). The values decrease from 68 wt.-% and 47 wt.%, measured from the uppermost two samples (705.66 m and 705.50 m) of the Gross Wolf Member, to values from 10 – 20 wt.-% in the basal Opalinus Clay (Fig. 3-2). The lithological change between the Gross Wolf Member and the Opalinus Clay is also visible in the slight increase in TOC from values around 0.5 wt.-% to values around 1 wt.-% in the Opalinus Clay (Fig. 3-5).

The *upper boundary* of the Opalinus Clay is set at 590.35 m at the base of the overlying limestone (iron-oolitic) bed (590.35 – 590.26 m) (*cf.* Dossier III). Placing the boundary at this level was not based on lithological reasons alone. Although, the carbonate content (TCarb) and the TOC document a change in the lithology to clearly less TOC-rich and more calcareous in the hanging part (Figs. 3-4 and 3-5). The argillaceous siltstone from 590.26 m to 589.38 m, which directly overlays the hardground, cannot clearly be distinguished from intervals from the upper part of the Opalinus Clay. However, the hanging succession is probably slightly siltier and slightly more calcareous, which is reinforced by the marked decrease in the TCarb in the uppermost 5 m of the Opalinus Clay. The boundary was also placed at this level by comparison with the newly established stratigraphy in the Benken borehole (Bläsi et al. 2013), where the palynological sample, taken directly from the hardground, has given already an age from the Bradfordensis Zone. This finding is identical to the palynological sample from 590.38 m at MAR1-1, directly overlaying the Opalinus Clay, which was dated to lower Bradfordensis to Opalinum Zone, which indeed is also similar to the palynological sample 816.03 m in TRU1-1 (Wohlwend et al. 2021b). The positive chemostratigraphic shift or even jump with an amplitude of around +1‰ in the $\delta^{13}C_{org}$ values to average values above -26.0‰ (*cf.* Wohlwend et al. 2021a) occurs in that interval too (590.50 m = -26.7‰ and at 590.00 m = -25.8‰; Fig. 3-5). Therefore, the hardground as well as the argillaceous siltstone are almost certainly the same in lithology and age.

«Murchisonae-Oolith Formation» (590.35 – 589.17 m)

The *lower boundary* of the «Murchisonae-Oolith Formation» is set at 590.35 m at the base of the limestone (iron-oolitic) bed (590.35 – 590.26 m) (*cf.* Dossier III). The iron-oolitic hardground consists of several calcareous concretions, which are also encrusted and bored and iron-ooid-rich. The thin section from that hardground (590.32 m) documents an iron-oolite (35 vol.-% iron-ooids) with a limonitic micritic matrix. The palynological sample from that hardground (590.38 m) yields an age of lower Bradfordensis to Opalinum Zone. Detailed discussion about the boundary can be found above at the upper boundary of the Opalinus Clay.

The *upper boundary* of the «Murchisonae-Oolith Formation» is set at 589.17 m at the top of the fossiliferous interval (589.24 – 589.17 m) with reworked iron-ooid-bearing calcareous intraclasts in an argillaceous siltstone (*cf.* Dossier III). Placing the boundary at the top of the hardground is supported by the biostratigraphic findings. The ammonite which lies directly on the hardground (average depth 589.19 m: *Staufenia* ex gr. *staufensis*) belongs clearly to the Bradfordensis Subzone of the Bradfordensis Zone. This age is also confirmed by the palynological sample at 589.23 m (Bradfordensis Zone). Therefore, the hardground was dated as Bradfordensis Zone. The palynological sample above the hardground (588.95 m) already yields Ovale Zone. The lithological comparison with the Benken borehole and the newly established stratigraphy therein (Bläsi et al. 2013) shows the same expression. In both boreholes similar bored iron-oolitic intraclasts are present in the discussed bed. In TRU1-1, due to the lack of biostratigraphic ages, the boundary was drawn at the base of the hardground (Wohlwend et al. 2021b), which is in agreement with the definition of the boundary to the hanging Wedelsandstein Formation, which per definition is located at the subface of the «Sowerbyi-Oolith» (deposited during the Discites Zone; German Stratigraphic Scheme; Bloos et al. 2005). Findings in Benken and the new borehole MAR1-1 document a hardground building during the Bardfordensis Zone and probably a gap or at most a very reduced sedimentation during the Concavum to Discites Zone. The onset of the sedimentation of the hanging Wedelsandstein Formation starts in the Ovale Zone.

Wedelsandstein Formation (589.17 – 555.23 m)

The *lower boundary* of the Wedelsandstein Formation is set at 589.17 m, just above the hardground (589.24 – 589.17 m) with reworked intraclasts of limestone (iron-oolitic) (*cf.* Dossier III). The onset of the sedimentation of the Wedelsandstein Formation starts in the Ovale Zone (palynological sample at 588.95 m). Detailed discussion about the boundary and a comparison with TRU1-1 can be found above at the upper boundary of the «Murchisonae-Oolith Formation».

The *upper boundary* of the Wedelsandstein Formation is set at 555.23 m at the base of the overlying dark reddish-brown iron-oolite of the «Humphriesioolith Formation» (*cf.* Dossier III). Below, a medium grey calcareous marl (silty) and claystones (slightly silty, calcareous) occur. The occurrence of iron-oolitic or limonitic sediments in the hanging succession was used as lithological criteria to define the upper boundary to the overlying «Humphriesioolith Formation» (Bläsi et al. 2013). The resulting age of the purely lithologically defined upper boundary lays close to the Laeviuscula to Sauzei Zone boundary. The uppermost palynological sample from the Wedelsandstein Formation at 555.54 m still belongs to the Laeviuscula Zone, the sample above (555.06 m) from the hanging «Humphriesioolith Formation» already yields Sauzei Zone which is also supported by the ammonite *Emileia* sp. at 555.03 m probably belonging to the Sauzei Zone.

«Humphriesioolith Formation» (555.23 – 545.93 m)

The *lower boundary* of the «Humphriesioolith Formation» is set at 555.23 m at the base of the dark reddish-brown iron-oolite and therefore with the onset of iron-ooids (*cf.* Dossier III). The age of the base was dated by a palynological sample (555.06 m) to Sauzei Zone and by an ammonite *Emileia* sp. (555.03 m) to probably Sauzei Zone. A short discussion about the lower boundary and its age can be found above at the upper boundary of the Wedelsandstein Formation.

The *upper boundary* of the «Humphriesioolith Formation» is set at 545.93 m at the uppermost occurrence of an iron-oolitic hardground (*cf.* Dossier III). The few iron-ooids found above this hardground are suggested to be reworked from the «Humphriesioolith Formation» during the onset of the hanging «Parkinsoni Württembergica-Schichten». The occurrence of iron-oolitic or limonitic sediments in the succession were used as lithological criteria to define the upper (as well as lower) boundary of the «Humphriesioolith Formation» (Bläsi et al. 2013). The resulting age of the purely lithologically defined upper boundary lays in the Garantiana Zone. The uppermost palynological sample (546.02 m) from the «Humphriesioolith Formation» as well as the lowermost sample (545.65 m) of the «Parkinsoni-Württembergica-Schichten» yield Garantiana Zone.

5 Conclusion

The present study documents data on microfacies analysis, ammonite stratigraphy and palyno-stratigraphy as well as detailed geochemical analyses (C, O and N isotopes). With this data collection, it was possible to predict the delimitation of the Mesozoic strata more accurately. Most of the important data for the boundaries in question were already present at the data-freeze (14.09.2020). Therefore, the present report complements the lithostratigraphic report of Dossier III for the deep borehole Marthalen-1-1. The lithological boundaries, and therefore the stratigraphic profile, were mostly defined by lithological criteria. Nevertheless, the customary formal and informal formation boundaries were not always obvious in the drill cores, either because of the small core diameter or changing facies conditions. The exact location of specific formation boundaries led to discussions requiring additional data to determine the exact profile description and illustration. We are aware that certain boundaries are thus no longer based solely on lithological criteria, and that the definitions therefore also include chronostratigraphic criteria (ammonite stratigraphy, palyno- and chemostratigraphy).

6 References

Bayle, E. (1878): Fossiles principaux des terrains de la France. Explication de la carte géologique de la France 4/1, Paris.

Bläsi, H.R., Deplazes, G., Schnellmann, M. & Traber, D. (2013): Sedimentologie und Stratigraphie des 'Braunen Doggers' und seiner westlichen Äquivalente. Nagra Arbeitsbericht NAB 12-51.

Bloos, G., Dietl, G. & Schweigert, G. (2005): Der Jura Süddeutschlands in der Stratigraphischen Tabelle von Deutschland 2002. Newsletters on Stratigraphy 41, 263-277.

Buch, C.L. von (1831): Recueil de Planches de Pétrifications Remarquables. Berlin, p. 136-155 (4 pls).

Buckman, S.S. (1887 – 1907): A Monograph of the ammonites of the Inferior Oolite Series. Palaeontographical Society Monographs, London, The Palaeontographical Society, 456 pp.

Cariou, E. & Hantzpergue, P. (eds.) (1997): Biostratigraphie du Jurassique ouest-européen et méditerranéen: zonations parallèles et distribution des invertébrés et microfossiles. Bull. Centre Rech. Elf Explor. Prod.

Dickson, J.A. (1965): Modified staining technique for carbonates in thin section. Nature 205, 587.

Dietze, V., Gräbenstein, S., Franz, M., Schweigert, G. & Wetzel, A. (2021): The Middle Jurassic Opalinuston Formation (Aalenian, Opalinus Zone) at its type locality near Bad Boll and adjacent outcrops (Swabian Alb, SW Germany). Palaeodiversity 14/1, 15-113.

Emerson, S. & Hedges, J.I. (1988): Processes controlling the organic carbon content of open ocean sediments. Paleoceanography 3, 621-634.

Feist-Burkhardt, S. & Monteil, E. (1997): Dinoflagellate cysts from the Bajocian stratotype (Calvados, Normandy, Western France). Bulletin du Centre de Recherches Elf Exploration Production [1997] 21/1, 31-105.

Feist-Burkhardt, S. & Pross, J. (2010): Dinoflagellate cyst biostratigraphy of the Opalinuston Formation (Middle Jurassic) in the Aalenian type area in southwest Germany and north Switzerland. Lethaia 43, 10-31.

Feist-Burkhardt, S. & Wille, W. (1992): Jurassic palynology in southwest Germany - state of the art. Cahiers de Micropaléontologie 7(1/2), 141-164.

Fernandez, A., van Dijk, J., Müller, I.A. & Bernasconi, S.M. (2016): Siderite acid fractionation factors for sealed and open vessel digestions at 70°C and 100°C. Chemical Geology 444, 180-186.

Gocht, H. (1964): Planktonische Kleinformen aus dem Lias/Dogger-Grenzbereich Nord- und Süddeutschlands. N. Jb. Geol. Paläont., Abh., 119(2), 113-133.

Grossouvre, A. de (1919): Bajocien-Bathonien dans la Nièvre. Bull. Soc. Géol. France 4/18, 337-459.

Gygi, R.A. (1977): Revision der Ammonitengattung Gregoryceras (Aspidoceratidae) aus dem Oxfordian (Oberer Jura) der Nordschweiz und von Süddeutschland. Taxonomie. Phylogenie. Stratigraphie. Eclogae geol. Helv. 70/2, 435- 542.

Gygi, R.A. (2000): Annotated index of lithostratigraphic units currently used in the Upper Jurassic of northern Switzerland. Eclogae geol. Helv. 93/1, 125-146.

Gygi, R.A. (2012): Quantitative geology of late Jurassic epicontinental sediments in the Jura Mountains of Switzerland. Springer, Basel, Heidelberg etc. p. 216.

Hougård, I.W., Bojesen-Koefoed, J.A., Vickers, M.L., Ullmann, C.V., Bjerrum, C.J., Rizzi, M. & Korte, C. (2021): Redox element record shows that environmental perturbations associated with the T-OAE were of longer duration than the carbon isotope record suggests – the Aubach section, SW Germany. Newsletters on Stratigraphy 54/2, 229-246.

Isler, A., Pasquier, F. & Huber, M. (1984): Geologische Karte der zentralen Nordschweiz 1:100'000. Herausgegeben von der Nagra und der Schweiz. Geol. Komm.

Jordan, P. & Deplazes, G. (2019): Lithostratigraphy of consolidated rocks expected in the Jura Ost, Nördlich Lägern and Zürich Nordost regions. Nagra Arbeitsbericht NAB 19-14.

Kuhn, O. & Etter, W. (1994): Der Posidonienschiefer der Nordschweiz: Lithostratigraphie, Biostratigraphie und Fazies. Eclogae geol. Helv. 87/1, 113-138.

Kukal, Z. (1971): Geology of recent sediments. Academie Press, New York, 490 pp.

Maubeuge, P.L. (1947): Sur quelques ammonites de l'Aalénien ferrugineux du Luxembourg et sur l'échelle stratigraphique de la Formation Ferrifère Franco–Belgo–Luxembourgeoise. Archives de l'Institut Grand–Ducal de Luxembourg, Section des Sciences naturelles, physique et mathématique, Nouvelle Série 17, 73-87.

Meyers, P.A. (1997): Organic geochemical proxies of paleoceanographic, paleolimnologic, and paleoclimatic processes. Org. Geochem. 27, 213-250.

Meyers, P.A. & Bernasconi, S.M. (2005): Carbon and nitrogen isotope excursions in mid-Pleistocene sapropels from the Tyrrhenian Basin: Evidence for climate-induced increases in microbial primary production. Marine Geology 220, 41-58.

Montfort, P.D. de (1808): Conchyliologie systématique, et classification méthodique des coquilles: offrant leurs figures, leur arrangement générique, leurs descriptions caractéristiques, leurs noms; ainsi que leur synonymie en plusieurs langues; ouvrage destiné à faciliter l'étude des coquilles, ainsi que leur disposition dans les cabinets d'histoire naturelle. Coquilles univalves, cloisonnées. – Tomes premier et second, Paris. Schoell.

Montero-Serrano, J.C., Föllmi, K.B., Adatte, T., Spangenberg, J.E., Tribovillard, N., Fantasia, A. & Suan, G. (2015): Continental weathering and redox conditions during the early Toarcian Oceanic Anoxic Event in the northwestern Tethys: Insight from the Posidonia Shale section in the Swiss Jura Mountains. Palaeogeography, Palaeoclimatology, Palaeoecology 429, 83-99.

Nagra (2014): SGT Etappe 2: Vorschlag weiter zu untersuchender geologischer Standortgebiete mit zugehörigen Standortarealen für die Oberflächenanlage. Geologische Grundlagen. Dossier II: Sedimentologische und tektonische Verhältnisse. Nagra Technischer Bericht NTB 14-02.

Ogg, J.G., Ogg, G. & Gradstein, F.M. (2016): The Concise Geologic Time Scale. Cambridge University Press. 184 pp.

Oppel, A. (1856 – 1858): Die Juraformation Englands, Frankreichs, und des südwestlichen Deutschlands. Ebner & Seubert, Stuttgart, und Württ. Naturwiss. Jh 12-14 ,857 pp.

Oppel, A. (1862 – 1883): Über jurassische Cephalopoden. Paläont. Mitt. Mus. königl. bayer. Staat 3, 127-266.

Parsons, T.R. (1975): Particulate organic carbon in the sea. *In:* Riey, J.P. & Skirrow, G. (eds.): Chemical oceanography. Academie Press, London, 338-425.

Pietsch, J. & Jordan, P. (2014): Digitales Höhenmodell Basis Quartär der Nordschweiz – Version 2013 (SGT E2) und ausgewählte Auswertungen. Nagra Arbeitsbericht NAB 14-02.

Rais, P., Louis-Schmid, B., Bernasconi, S.M. & Weissert, H. (2007). Palaeoceanographic and palaeoclimatic reorganization around the Middle–Late Jurassic transition. Palaeogeography, Palaeoclimatology, Palaeoecology 251/3-4, 527-546.

Reinecke, J.C.M. (1818): Maris protogaei Nautilos et Argonautae vulga Cornua Ammonis in Agro Coburgico et vicinio reperiundos; descripsit et delineavit, simul Observationes de Fossilum Protypis. L.C.A. Ahlii imp., Coburg, 90 pp.

Remane, J., Adatte, T., Berger, J.P., Burkhalter, R., Dall'Agnolo, S., Decrouez, D., Fischer, H., Funk, H., Furrer, H., Graf, H.R., Gouffon, Y., Heckendorn, W. & Winkler, W. (2005): Richtlinien zur stratigraphischen Nomenklatur. Eclogae geol. Helv. 98/3, 385-405.

Roemer, F.A. (1836): Die Versteinerungen des norddeutschen Oolithengebirges: Nebst Nachtr. (Vol. 1). Hahn.

Röhl, H.J. & Schmid-Röhl, A. (2005): Lower Toarcian (Upper Liassic) black shales of the Central European epicontinental basin: a sequence stratigraphic case study from the SW German Posidonia Shale. *In:* Harris, N.B. (ed.): The Deposition of Organic-Carbon-Rich Sediments: Models, Mechanisms, and Consequences. SEPM Special Publication 82, 165-189.

Scheffer, F. & Schachtschnabel, P. (1984): Lehrbuch der Bodenkunde. Enke Verlag, Stuttgart.

Schlippe, A.O. (1888): Die Fauna des Bathonien im oberrheinischen Tiefland. Abh. Geol. Spez.-Karte-Lothr. 4/4, 1-166.

Schlotheim, E.F. (1820 – 1823): Die Petrefactenkunde auf ihrem jetzigen Standpunkte durch die Beschreibung seiner Sammlung versteinerter und fossiler Überreste des Thier und Pflanzenreichs der Vorwelt erläutert. Gotha, 437 pp.

Sowerby, J. (1812 – 1846): The Mineral Conchology of Great Britain. Meridith, London, Vol. 1-7.

Stratabugs, version 2.1 (June 2016). StrataData Ltd., UK. http://www.stratadata.co.uk.

Suan, G., Van De Schootbrugge, B., Adatte, T., Fiebig, J. & Oschmann, W. (2015): Calibrating the magnitude of the Toarcian carbon cycle perturbation. Paleoceanography 30/5, 495-509.

Timescale Creator, version 7.0 (30. July 2016). Geologic TimeScale Foundation. https://engineering.purdue.edu/Stratigraphy/tscreator/.

Van Mooy, B.A.S., Keil, R.G., Devol, A.H. (2002): Impact of suboxia on sinking particulate organic carbon: enhanced carbon flux and preferential degradation of amino acids via denitrification. Geochim. Cosmochim. Acta 66, 457-465.

Voigt, E. (1968): Über Hiatus-Konkretionen (dargestellt an Beispielen aus dem Lias). Geologische Rundschau 58, 281-296.

Wetzel, A. & Allia, V. (2000): The significance of hiatus beds in shallow-water mudstones: an example from the Middle Jurassic of Switzerland. Journal of sedimentary research 70/1, 170-180.

Wohlwend, S., Hart, M. & Weissert, H. (2016): Chemostratigraphy of the Upper Albian to mid-Turonian Natih Formation (Oman) – How authigenic carbonate changes a global pattern. The Depositional Record 2/1, 97-117.

Wohlwend, S., Bläsi, H.R., Feist-Burkhardt, S., Hostettler, B., Menkveld-Gfeller, U., Dietze, V. & Deplazes, G. (2019a): Die Passwang-Formation im östlichen Falten- und Tafeljura: Fasiswald (SO) – Unt. Hauenstein (SO) – Wasserflue (AG) – Thalheim (AG) – Frickberg (AG) – Cheisacher (AG) – Böttstein (AG) – Tegerfelden (AG) – Acheberg (AG). Nagra Arbeitsbericht, NAB 18-11.

Wohlwend, S., Bernasconi, S.M., Deplazes, G. & Jaeggi, D. (2019b): SO Experiment: Chemostratigraphic study of Late Aalenian to Early Bajocian. Mont Terri Technical Report TR 19-05. Mont Terri Project, Switzerland.

Wohlwend, S., Bläsi, H.R., Feist-Burkhardt, S., Hostettler, B., Menkveld-Gfeller, U., Dietze, V. & Deplazes, G. (2021a): TBO Bülach-1-1: Data Report – Dossier IV: Microfacies, Bio- and Chemostratigraphic Analysis. Nagra Arbeitsbericht NAB 20-08.

Wohlwend, S., Bläsi, H.R., Feist-Burkhardt, S., Hostettler, B., Menkveld-Gfeller, U., Dietze, V. & Deplazes, G. (2021b): TBO Trüllikon-1-1: Data Report – Dossier IV: Microfacies, Bio- and Chemostratigraphic Analysis. Nagra Arbeitsbericht NAB 20-09.

Wood, G.D., Gabriel, A.M. & Lawson, J.C. (1996): Palynological techniques – processing and microscopy. In: Jansonius, J. & McGregor, D.C. (eds): Palynology, principles and applications. American Association of Stratigraphic Palynologists Foundation 2, 29-50.

Appendix A: List of all samples

Appendix A1: List of all thin sections from MAR1-1 (1'036.39 – 483.04 m)

For the description and indivual counting of the thin sections see Section 3.1; selected photos can be found in Appendix B.

Top [m]	**Bottom** [m]	**Avg. depth** [m]	**Formation**	**Retrieval date** [dd.mm.yyyy]	**Sample ID**
483.02	483.06	483.04	Villigen Fm.	17.05.2020	MAR1-1-483.04-TS
501.49	501.53	501.51	Wildegg Fm.	17.05.2020	MAR1-1-501.51-TS
501.60	501.64	501.62	Wildegg Fm.	17.05.2020	MAR1-1-501.62-TS
502.31	502.35	502.33	Wutach Fm.	17.05.2020	MAR1-1-502.33-TS
502.79	502.83	502.81	Wutach Fm.	17.05.2020	MAR1-1-502.81-TS
503.58	503.62	503.60	Wutach Fm.	17.05.2020	MAR1-1-503.60-TS
505.83	505.87	505.85	Variansmergel Fm.	17.05.2020	MAR1-1-505.85-TS
526.02	526.06	526.04	«Parkinsoni-Württ.-Sch.»	17.05.2020	MAR1-1-526.04-TS
544.46	544.50	544.48	«Parkinsoni-Württ.-Sch.»	17.05.2020	MAR1-1-544.48-TS
546.00	546.04	546.02	«Humphriesioolith Fm.»	17.05.2020	MAR1-1-546.02-TS
546.88	546.92	546.90	«Humphriesioolith Fm.»	17.05.2020	MAR1-1-546.90-TS
547.73	547.77	547.75	«Humphriesioolith Fm.»	17.05.2020	MAR1-1-547.75-TS
550.45	550.49	550.47	«Humphriesioolith Fm.»	17.05.2020	MAR1-1-550.47-TS
555.10	555.14	555.12	«Humphriesioolith Fm.»	17.05.2020	MAR1-1-555.12-TS
556.82	556.86	556.84	Wedelsandstein Fm.	17.05.2020	MAR1-1-556.84-TS
558.45	558.49	558.47	Wedelsandstein Fm.	17.05.2020	MAR1-1-558.47-TS
561.94	561.98	561.96	Wedelsandstein Fm.	17.05.2020	MAR1-1-561.96-TS
565.71	565.75	565.73	Wedelsandstein Fm.	17.05.2020	MAR1-1-565.73-TS
567.80	567.84	567.82	Wedelsandstein Fm.	26.05.2020	MAR1-1-567.82-TS
569.16	569.20	569.18	Wedelsandstein Fm.	17.05.2020	MAR1-1-569.18-TS
571.96	572.00	571.98	Wedelsandstein Fm.	17.05.2020	MAR1-1-571.98-TS
574.64	574.68	574.66	Wedelsandstein Fm.	17.05.2020	MAR1-1-574.66-TS
582.15	582.19	582.17	Wedelsandstein Fm.	17.05.2020	MAR1-1-582.17-TS
583.86	583.90	583.88	Wedelsandstein Fm.	17.05.2020	MAR1-1-583.88-TS
589.21	589.25	589.23	«Murchisonae-Oolith Fm.»	26.05.2020	MAR1-1-589.23-TS
590.30	590.34	590.32	«Murchisonae-Oolith Fm.»	26.05.2020	MAR1-1-590.32-TS
594.11	594.15	594.13	Opalinus Clay	26.05.2020	MAR1-1-594.13-TS
600.48	600.52	600.50	Opalinus Clay	26.05.2020	MAR1-1-600.50-TS
601.99	602.03	602.01	Opalinus Clay	26.05.2020	MAR1-1-602.01-TS
603.67	603.71	603.69	Opalinus Clay	26.05.2020	MAR1-1-603.69-TS
609.25	609.29	609.27	Opalinus Clay	26.05.2020	MAR1-1-609.27-TS
609.62	609.66	609.64	Opalinus Clay	26.05.2020	MAR1-1-609.64-TS
614.73	614.77	614.75	Opalinus Clay	26.05.2020	MAR1-1-614.75-TS
623.05	623.09	623.07	Opalinus Clay	01.07.2020	MAR1-1-623.07-TS
629.22	629.26	629.24	Opalinus Clay	26.05.2020	MAR1-1-629.24-TS
662.09	662.13	662.11	Opalinus Clay	26.05.2020	MAR1-1-662.11-TS
700.11	700.15	700.13	Opalinus Clay	26.05.2020	MAR1-1-700.13-TS
705.64	705.68	705.66	Staffelegg Fm.	26.05.2020	MAR1-1-705.66-TS
707.66	707.70	707.68	Staffelegg Fm.	26.05.2020	MAR1-1-707.68-TS
719.98	720.02	720.00	Staffelegg Fm.	26.05.2020	MAR1-1-720.00-TS
730.42	730.46	730.44	Staffelegg Fm.	26.05.2020	MAR1-1-730.44-TS
739.06	739.10	739.08	Staffelegg Fm.	26.05.2020	MAR1-1-739.08-TS
741.93	741.97	741.95	Staffelegg Fm.	26.05.2020	MAR1-1-741.95-TS
766.90	766.94	766.92	Klettgau Fm.	08.08.2020	MAR1-1-766.92-TS
770.64	770.68	770.66	Klettgau Fm.	08.08.2020	MAR1-1-770.66-TS
795.97	796.00	795.99	Bänkerjoch Fm.	08.08.2020	MAR1-1-795.99-TS
811.63	811.67	811.65	Bänkerjoch Fm.	08.08.2020	MAR1-1-811.65-TS
825.12	825.15	825.14	Bänkerjoch Fm.	08.08.2020	MAR1-1-825.14-TS
836.27	836.30	836.29	Bänkerjoch Fm.	08.08.2020	MAR1-1-836.29-TS
852.10	852.13	852.12	Bänkerjoch Fm.	08.08.2020	MAR1-1-852.12-TS
875.63	875.67	875.65	Schinznach Fm.	08.08.2020	MAR1-1-875.65-TS
887.66	887.70	887.68	Schinznach Fm.	15.09.2020	MAR1-1-887.68-TS
932.61	932.65	932.63	Zeglingen Fm.	15.09.2020	MAR1-1-932.63-TS
1'023.13	1'023.17	1'023.15	Kaiseraugst Fm.	15.09.2020	MAR1-1-1023.15-TS
1'028.32	1'028.36	1'028.34	Kaiseraugst Fm.	15.09.2020	MAR1-1-1028.34-TS
1'030.13	1'030.16	1'030.15	Dinkelberg Fm.	15.09.2020	MAR1-1-1030.15-TS
1'036.37	1'036.41	1'036.39	Dinkelberg Fm.	15.09.2020	MAR1-1-1036.39-TS

Appendix A2: List of all sampled macrofossils from MAR1-1 (723.40 – 494.27 m)

For the definitive determination of the individual macrofossils see Section 3.2 (Tab. 3-2).

Top [m]	**Bottom** [m]	**Sample depth** [m]	**Formation**	**Retrieval date** [dd.mm.yyyy]	**Sample ID**
494.24	494.30	**494.27**	Wildegg Fm.	17.05.2020	MAR1-1-494.27-BS(MF)
501.48	501.55	**501.52**	Wildegg Fm.	17.05.2020	MAR1-1-501.52-BS(MF)
502.83	502.90	**502.87**	Wutach Fm.	17.05.2020	MAR1-1-502.87-BS(MF)
511.90	511.92	**511.91**	Wutach Fm.	17.05.2020	MAR1-1-511.91-BS(MF)
518.35	518.37	**518.36**	«Parkinsoni-Württ.-Sch.»	17.05.2020	MAR1-1-518.36-BS(MF)
530.19	530.21	**530.20**	«Parkinsoni-Württ.-Sch.»	17.05.2020	MAR1-1-530.20-BS(MF)
537.09	537.11	**537.10**	«Parkinsoni-Württ.-Sch.»	17.05.2020	MAR1-1-537.10-BS(MF)
543.59	543.63	**543.61**	«Parkinsoni-Württ.-Sch.»	17.05.2020	MAR1-1-543.61-BS(MF)
544.27	544.30	**544.28**	«Parkinsoni-Württ.-Sch.»	17.05.2020	MAR1-1-544.28-BS(MF)
544.36	544.42	**544.39**	«Parkinsoni-Württ.-Sch.»	17.05.2020	MAR1-1-544.39-BS(MF)
546.38	546.42	**546.40**	«Humphriesioolith Fm.»	17.05.2020	MAR1-1-546.40-BS(MF)
547.63	547.68	**547.66**	«Humphriesioolith Fm.»	17.05.2020	MAR1-1-547.66-BS(MF)
548.18	548.23	**548.21**	«Humphriesioolith Fm.»	17.05.2020	MAR1-1-548.21-BS(MF)
555.00	555.06	**555.03**	«Humphriesioolith Fm.»	17.05.2020	MAR1-1-555.03-BS(MF)
589.16	589.21	**589.19**	«Murchisonae-Oolith Fm.»	26.05.2020	MAR1-1-589.19-BS(MF)
597.83	597.86	**597.85**	Opalinus Clay	26.05.2020	MAR1-1-597.85-BS(MF)
696.12	696.15	**696.13**	Opalinus Clay	26.05.2020	MAR1-1-696.13-BS(MF)
705.03	705.05	**705.04**	Opalinus Clay	26.05.2020	MAR1-1-705.04-BS(MF)
705.76	705.79	**705.78**	Staffelegg Fm.	26.05.2020	MAR1-1-705.78-BS(MF)
707.72	707.75	**707.74**	Staffelegg Fm.	26.05.2020	MAR1-1-707.74-BS(MF)
708.22	708.24	**708.23**	Staffelegg Fm.	26.05.2020	MAR1-1-708.23-BS(MF)
708.88	708.91	**708.90**	Staffelegg Fm.	26.05.2020	MAR1-1-708.90-BS(MF)
710.18	710.22	**710.20**	Staffelegg Fm.	26.05.2020	MAR1-1-710.20-BS(MF)
723.38	723.42	**723.40**	Staffelegg Fm.	26.05.2020	MAR1-1-723.40-BS(MF)

Appendix A3: List of other provisionally determined conspicuous macrofossils from MAR1-1 (720.45 – 494.00 m)

Top [m]	**Bottom** [m]	**Fossil**	**Determination (provisional)**
494.00	494.20	Ammonite	
501.50	501.55	Ammonite	Cardioceras ??
501.60		Belemnite	*Hibolites* (Semihastatus) *rotundus*
502.27		2 Ammonites	Perisphinctide
503.18	503.195	Ammonite	Perisphinctide indet.
504.03		Ammonite	Oppelidae indet.
512.835		Bivalve	*Goniomya literata*
517.86		Bivalve	*Grammatodon* sp.
518.78		Fossile wood	
522.275		Bivalves	Pleuromya?
536.80		Bivalve	Pleuromya
561.27		Ammonite	
598.09		Ammonite	*Leioceras* sp.
603.08		Ammonite	*Leioceras* sp.
606.89		Crab fragment	
609.34		Ammonite fragment	*Leioceras* ??
695.58	698.02	Numerous ammonites	*Leioceras* sp.
708.02		Ammonite	Dumortieria
719.43		Driftwood	
720.45		Ammonite	Dactylioceras??

Appendix A4: List of all palynological samples from MAR1-1 (705.78 – 501.30 m)

Palynological samples in grey are taken from ammonite samples retrieved at specific depths. Sampling was always as close as possible to the ammonite.

Top [m]	**Bottom** [m]	**Avg. Depth** [m]	**Formation**	**Retrieval date** [dd.mm.yyyy]	**Sample ID**
501.29	501.31	501.30	Wildegg Fm.	25.05.2020	MAR1-1-501.30-BS(Pa)
501.60	501.64	501.62	Wildegg Fm.	25.05.2020	MAR1-1-501.62-BS(Pa)
502.31	502.35	502.33	Wutach Fm.	25.05.2020	MAR1-1-502.33-BS(Pa)
502.79	502.83	502.81	Wutach Fm.	25.05.2020	MAR1-1-502.81-BS(Pa)
504.93	504.95	504.94	Wutach Fm.	25.05.2020	MAR1-1-504.94-BS(Pa)
505.83	505.87	505.85	Variansmergel Fm.	25.05.2020	MAR1-1-505.85-BS(Pa)
506.47	506.49	506.48	Variansmergel Fm.	25.05.2020	MAR1-1-506.48-BS(Pa)
509.32	509.34	509.33	Variansmergel Fm.	25.05.2020	MAR1-1-509.33-BS(Pa)
517.84	517.86	517.85	«Parkinsoni-Württ.-Sch.»	25.05.2020	MAR1-1-517.85-BS(Pa)
523.66	523.68	523.67	«Parkinsoni-Württ.-Sch.»	25.05.2020	MAR1-1-523.67-BS(Pa)
534.09	534.11	534.10	«Parkinsoni-Württ.-Sch.»	25.05.2020	MAR1-1-534.10-BS(Pa)
543.40	543.42	543.41	«Parkinsoni-Württ.-Sch.»	25.05.2020	MAR1-1-543.41-BS(Pa)
544.36	544.42	544.39	«Parkinsoni-Württ.-Sch.»	17.05.2020	MAR1-1-544.39-BS(Pa)
544.79	544.81	544.80	«Parkinsoni-Württ.-Sch.»	25.05.2020	MAR1-1-544.80-BS(Pa)
545.64	545.66	545.65	«Parkinsoni-Württ.-Sch.»	25.05.2020	MAR1-1-545.65-BS(Pa)
546.00	546.04	546.02	«Humphriesioolith Fm.»	25.05.2020	MAR1-1-546.02-BS(Pa)
546.88	546.92	546.90	«Humphriesioolith Fm.»	25.05.2020	MAR1-1-546.90-BS(Pa)
547.63	547.68	547.66	«Humphriesioolith Fm.»	17.05.2020	MAR1-1-547.66-BS(Pa)
548.18	548.23	548.21	«Humphriesioolith Fm.»	17.05.2020	MAR1-1-548.21-BS(Pa)
549.40	549.42	549.41	«Humphriesioolith Fm.»	26.05.2020	MAR1-1-549.41-BS(Pa)
550.86	550.88	550.87	«Humphriesioolith Fm.»	26.05.2020	MAR1-1-550.87-BS(Pa)
553.84	553.86	553.85	«Humphriesioolith Fm.»	26.05.2020	MAR1-1-553.85-BS(Pa)
555.00	555.01	555.00	«Humphriesioolith Fm.»	17.05.2020	MAR1-1-555.00-BS(Pa)
555.05	555.06	555.06	«Humphriesioolith Fm.»	17.05.2020	MAR1-1-555.06-BS(Pa)
555.53	555.55	555.54	Wedelsandstein Fm.	26.05.2020	MAR1-1-555.54-BS(Pa)
562.99	563.01	563.00	Wedelsandstein Fm.	26.05.2020	MAR1-1-563.00-BS(Pa)
571.96	572.00	571.98	Wedelsandstein Fm.	26.05.2020	MAR1-1-571.98-BS(Pa)
578.00	578.02	578.01	Wedelsandstein Fm.	26.05.2020	MAR1-1-578.01-BS(Pa)
583.86	583.90	583.88	Wedelsandstein Fm.	26.05.2020	MAR1-1-583.88-BS(Pa)
586.93	586.95	586.94	Wedelsandstein Fm.	24.09.2020	MAR1-1-586.94-BS(Pa)
588.94	588.96	588.95	Wedelsandstein Fm.	26.05.2020	MAR1-1-588.95-BS(Pa)
588.94	588.96	588.95	Wedelsandstein Fm.	24.09.2020	MAR1-1-588.95-BS(Pa)
589.21	589.25	589.23	«Murchisonae-Oolith Fm.»	26.05.2020	MAR1-1-589.23-BS(Pa)
590.20	590.22	590.21	«Murchisonae-Oolith Fm.»	26.05.2020	MAR1-1-590.21-BS(Pa)
590.37	590.39	590.38	Opalinus Clay	26.05.2020	MAR1-1-590.38-BS(Pa)
600.01	600.03	600.02	Opalinus Clay	26.05.2020	MAR1-1-600.02-BS(Pa)
600.68	600.70	600.69	Opalinus Clay	26.05.2020	MAR1-1-600.69-BS(Pa)
626.08	626.10	626.09	Opalinus Clay	26.05.2020	MAR1-1-626.09-BS(Pa)
645.22	645.24	645.23	Opalinus Clay	26.05.2020	MAR1-1-645.23-BS(Pa)
664.61	664.63	664.62	Opalinus Clay	26.05.2020	MAR1-1-664.62-BS(Pa)
685.08	685.10	685.09	Opalinus Clay	26.05.2020	MAR1-1-685.09-BS(Pa)
705.03	705.05	705.04	Opalinus Clay	26.05.2020	MAR1-1-705.04-BS(Pa)
705.76	705.79	705.78	Staffelegg Fm.	26.05.2020	MAR1-1-705.78-BS(Pa)

Appendix B: Photos microfacies

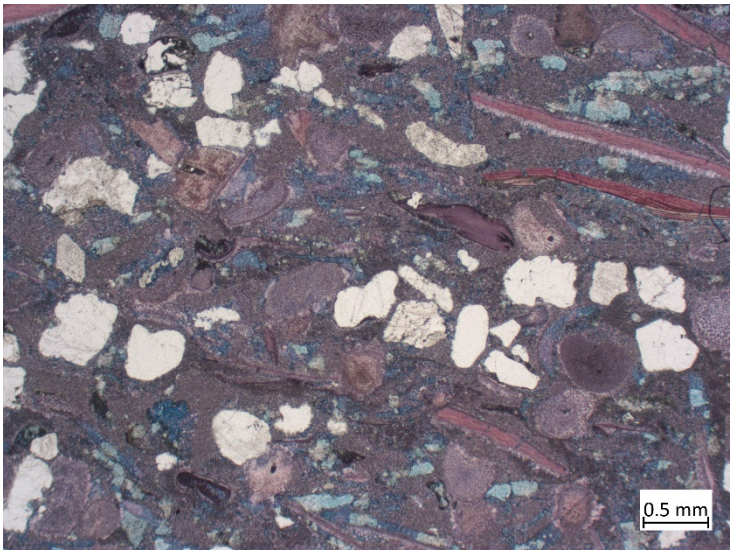

Fig. B-1:

Biodetritic limestone (sandy):
echinoderm skeletal elements (lila), bivalves (red) and quartz grains (white) with iron-dolomite (pale blue).

Thin section photo,
TS stained for calcite = red

MAR1-1-1023.15
Kaiseraugst Fm.

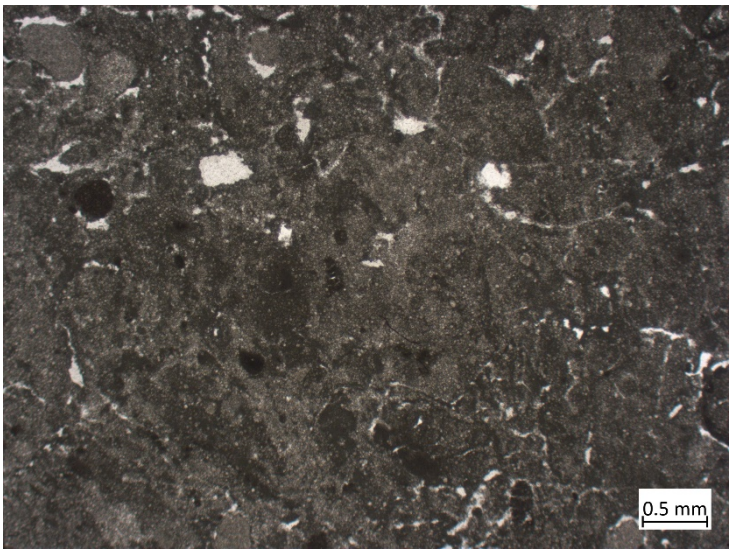

Fig. B-2:

Dolostone, nodular (dolocrete):
dolomite nodules, grown during pedogenesis within a dolomitic soil

Thin section photo

MAR1-1-766.92
Klettgau Fm. (Seebi Mb.)

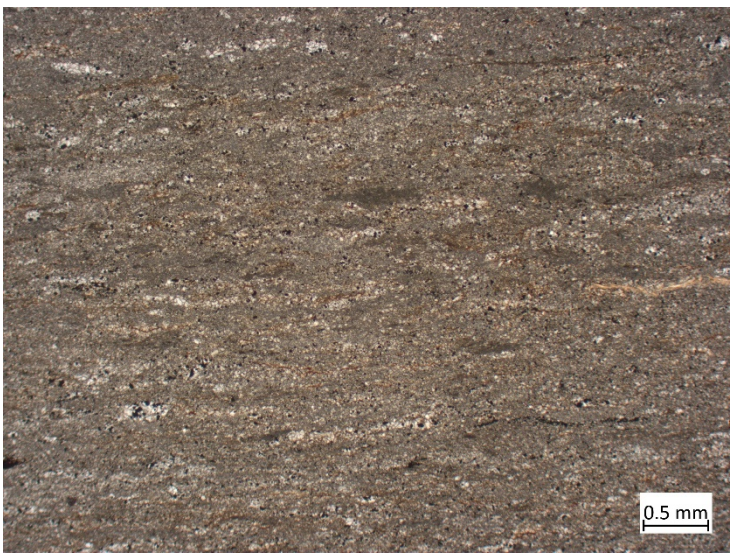

Fig. B-3:

Stromatolite:
limestone, formed by laminated microbial mats

Thin section photo

MAR1-1-720.00
Staffelegg Fm. (Rietheim Mb.: «Unterer Stein»)

Selected photos of microfacies from Kaiseraugst Fm., Klettgau Fm. and Staffelegg Fm.

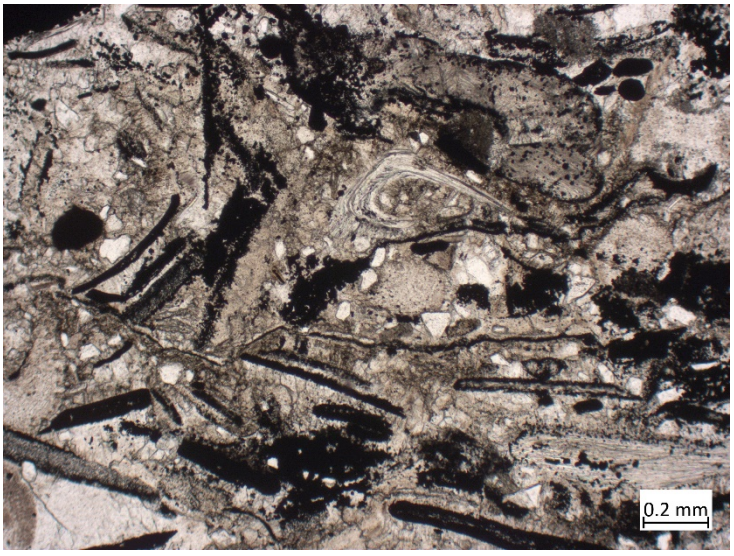

Fig. B-4:

Hardground:
pyritic bivalves (black), echinoderm skeletal elements and quartz grains, sedimented with micrite matrix

Thin section photo

MAR1-1-629.24
Opalinus Clay

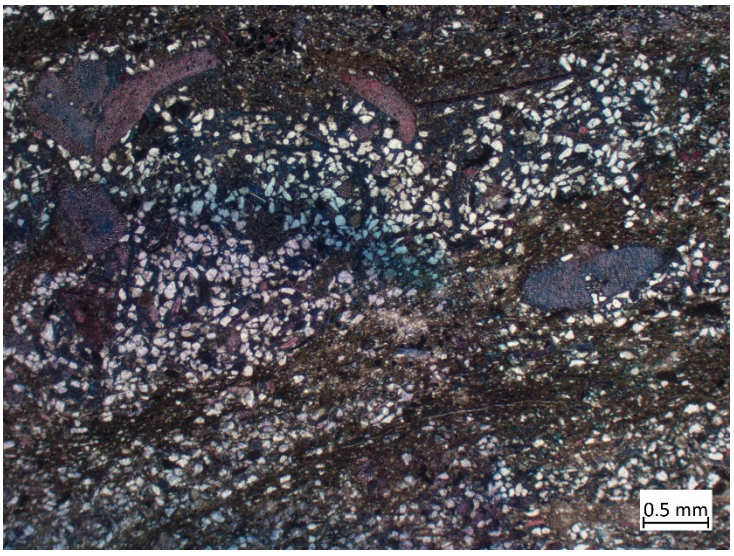

Fig. B-5:

Sandy marl (biodetritic):
big echinoderm skeletal elements (lilared) and quartz fine-grained with clay matrix and calcite cement

Thin section photo,
TS stained for calcite = red

MAR1-1-623.07
Opalinus Clay

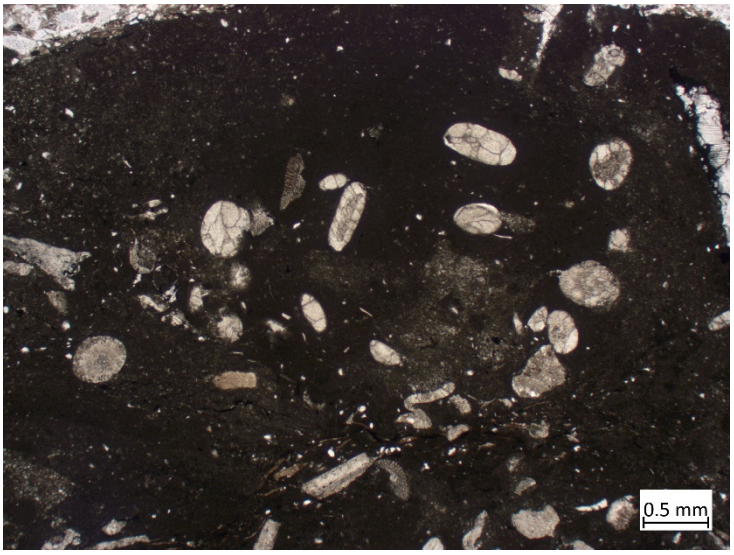

Fig. B-6:

Hardground:
limestone (iron-oolitic, sideritic), iron-ooids are replaced by calcite

Thin section photo

MAR1-1-609.64
Opalinus Clay

Selected photos of microfacies from Opalinus Clay

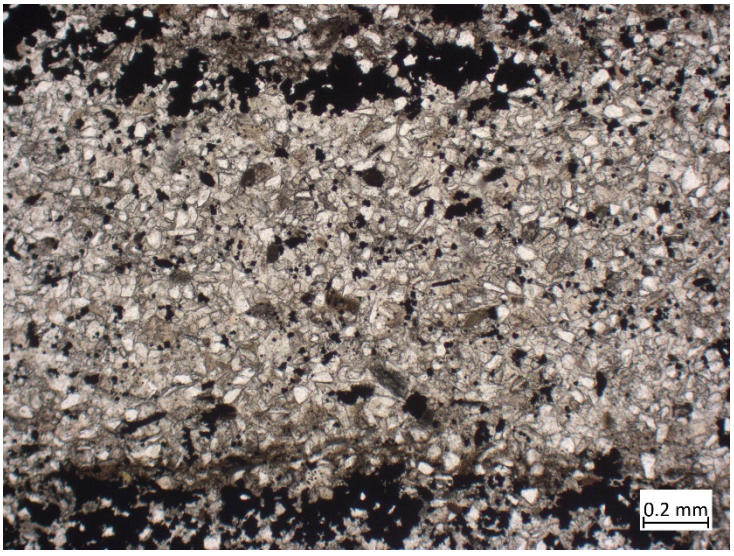	**Fig. B-7:** Silty-sandy facies: silty-sandy layer consisting of sand-sized biogene components and silt-sized quartz grains, as well as some pyrite crystals, all cemented by calcite cement. The pyrite crystals are mainly aligned in thin layers. Thin section photo MAR1-1-602.01 Opalinus Clay
	**Fig. B-8:** Hardground: biogene components, mainly echinoderm skeletal elements, and iron-ooids, with micritic, sideritic matrix and "stellate cement" Thin section photo MAR1-1-600.50 Opalinus Clay
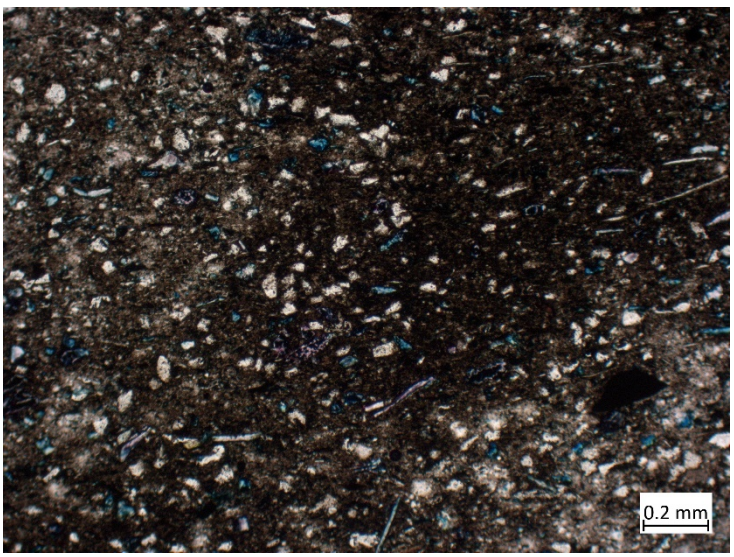	**Fig. B-9:** Clay-rich facies: some silt-sized quartz-grains (white) and small bioclasts (bluish) sedimented with an argillaceous matrix Thin section photo TS stained for calcite = red MAR1-1-594.13 Opalinus Clay

Selected photos of microfacies from Opalinus Clay

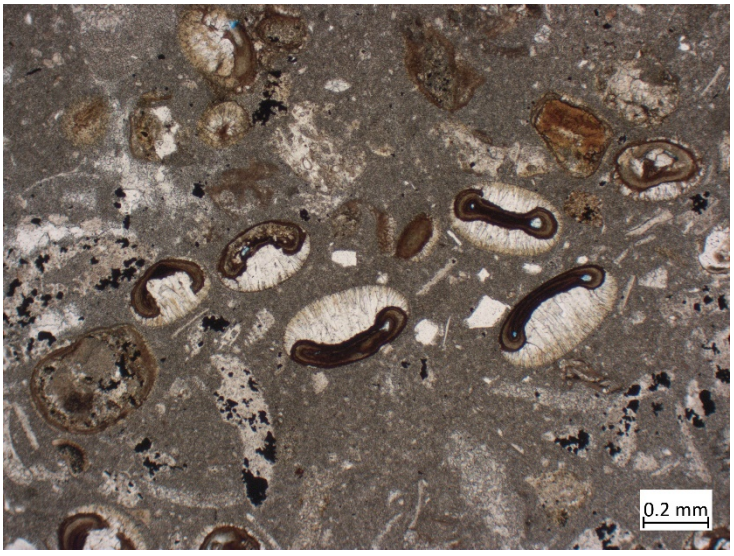

Fig. B-10:

Limestone (iron-oolitic): special iron-ooids, partly replaced by calcite, and bivalves with pyrite crystals, all in micrite matrix

Thin section photo

MAR1-1-589.23
«Murchisonae-Oolith Fm.»

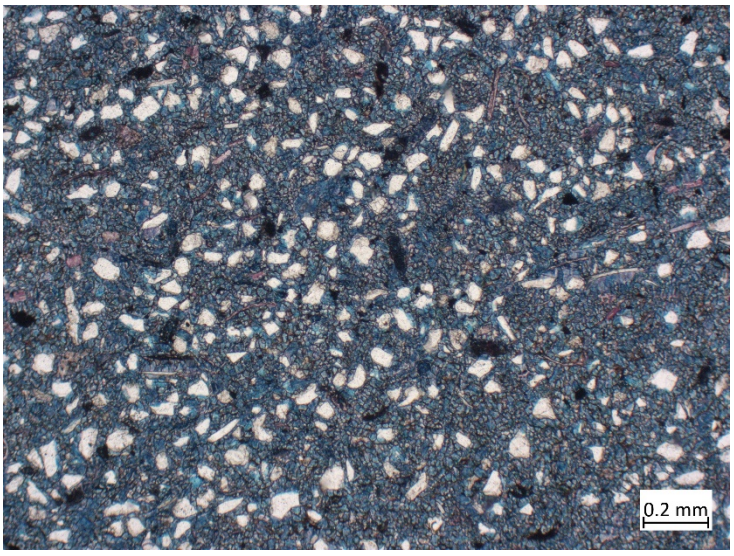

Fig. B-11:

Calcareous, quartz-rich bed: limestone (sandy, biodetritic): finely crystalline mosaic of small bioclasts, "stellate cement" and microsparite as well as quartz grains (white)

Thin section photo
TS stained for calcite = red

MAR1-1-582.17
Wedelsandstein Fm.

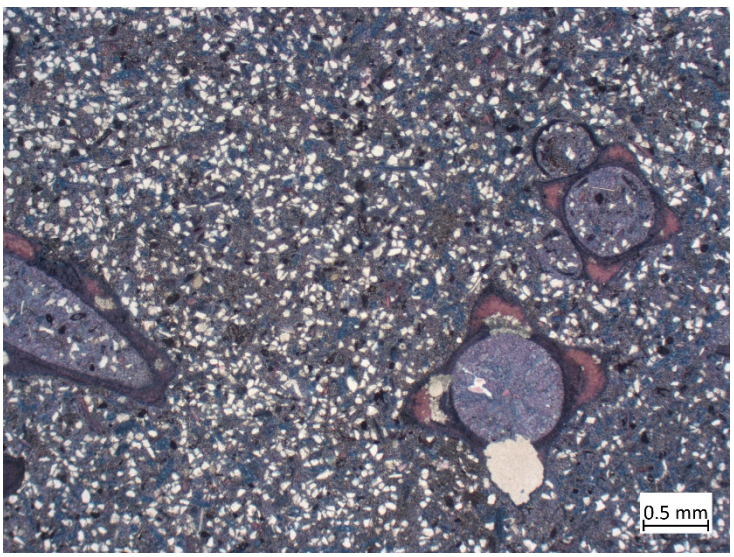

Fig. B-12:

Calcareous, quartz-rich bed: limestone (sandy, biodetritic): big serpulid tubes in a similar microcrystalline calcite mosaic as in MAR1-1-582.17. The lowest serpulid tube shows an edge replaced by chalcedon (white)

Thin section photo
TS stained for calcite = red

MAR1-1-569.18
Wedelsandstein Fm.

Selected photos of microfacies from «Murchisonae-Oolith Fm.» and Wedelsandstein Fm.

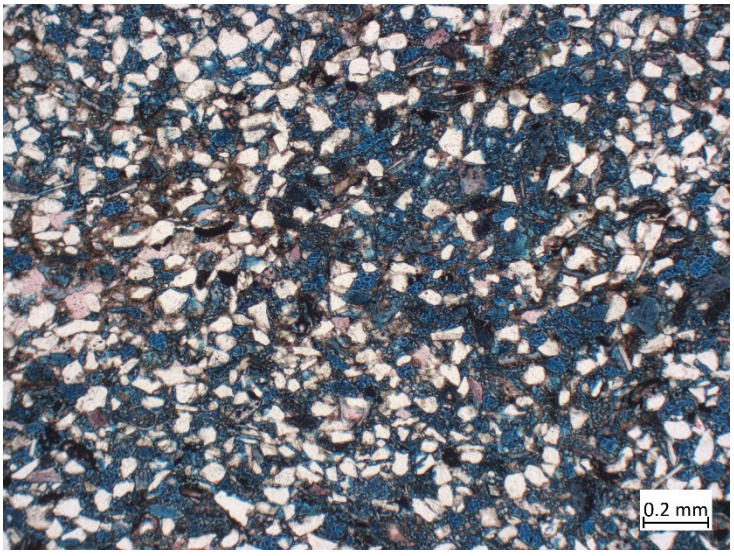

Fig. B-13:

Calcareous, quartz-rich bed: sandy limestone (biodetritic): biogene components (echinoderms, bivalves) and quartz grains, cemented by calcite

Thin section photo
TS stained for calcite=red

MAR1-1-565.73
Wedelsandstein Fm.

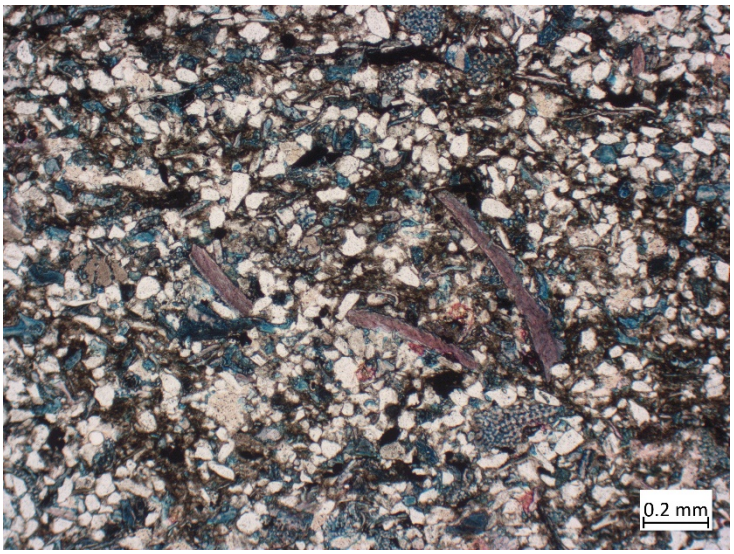

Fig. B-14:

Sandy marl (biodetritic): bivalves and echinoderm skeletal elements with quartz sand in marly matrix

Thin section photo
TS stained for calcite=red

MAR1-1-558.47
Wedelsandstein Fm.

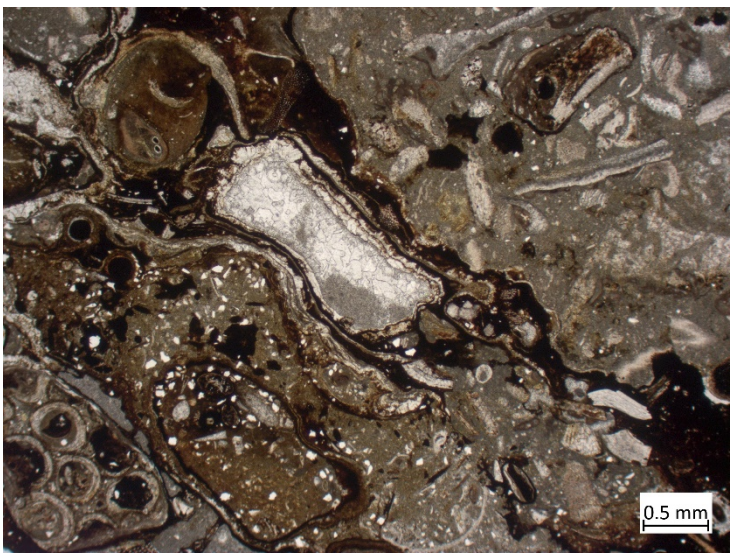

Fig. B-15:

Hardground:
limonitic biomicrite with iron-stromatolitic layers and limonitic biodetritus

Thin section photo

MAR1-1-555.12
«Humphriesioolith Fm.»

Selected photos of microfacies from Wedelsandstein Fm. and «Humphriesioolith Fm.»

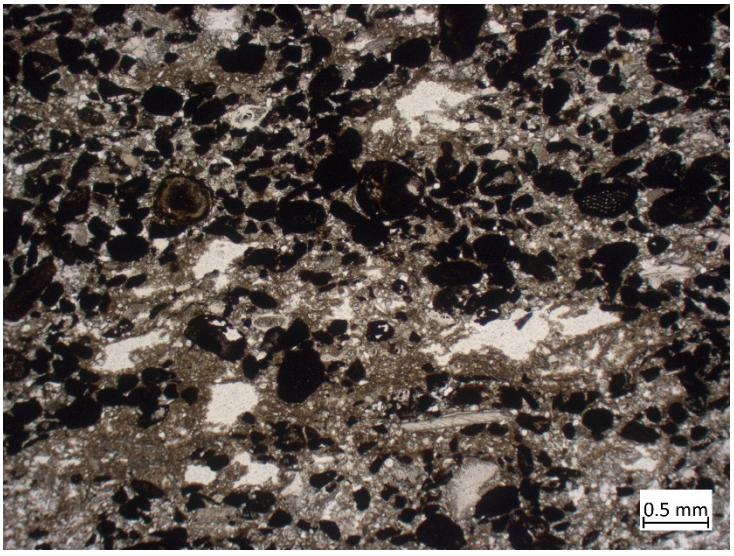

Fig. B-16:

Calcareous marl (iron-oolitic):
iron-ooids, limonitic pellets, some others limonitic grains and biogene components sedimented in marly matrix

Thin section photo

MAR1-1-550.47
«Humphriesioolith Fm.»

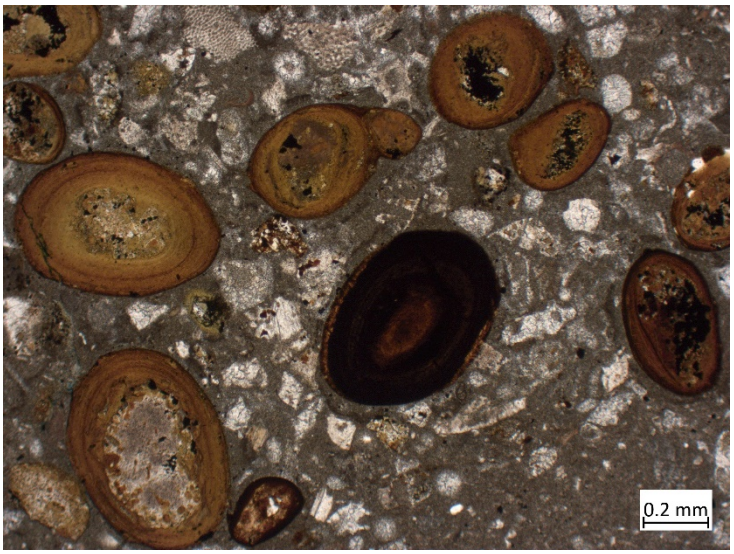

Fig. B-17:

Limestone (iron-oolitic): chamosite iron-ooids and biogene components in micrite matrix

Thin section photo

MAR1-1-547.75
«Humphriesioolith Fm.»

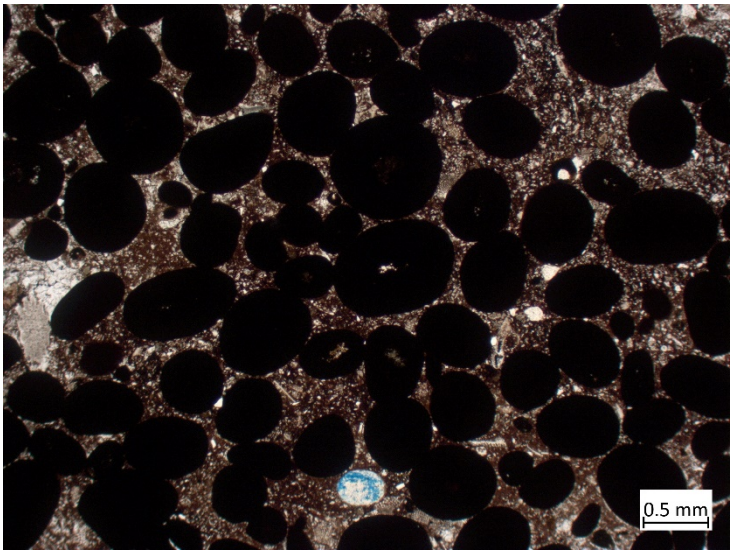

Fig. B-18:

Iron-oolite (calcareous): iron-ooids with limonitic matrix (see Fig. B-19)

Thin section photo

MAR1-1-546.90
«Humphriesioolith Fm.»

Selected photos of microfacies from «Humphriesioolith Fm.»

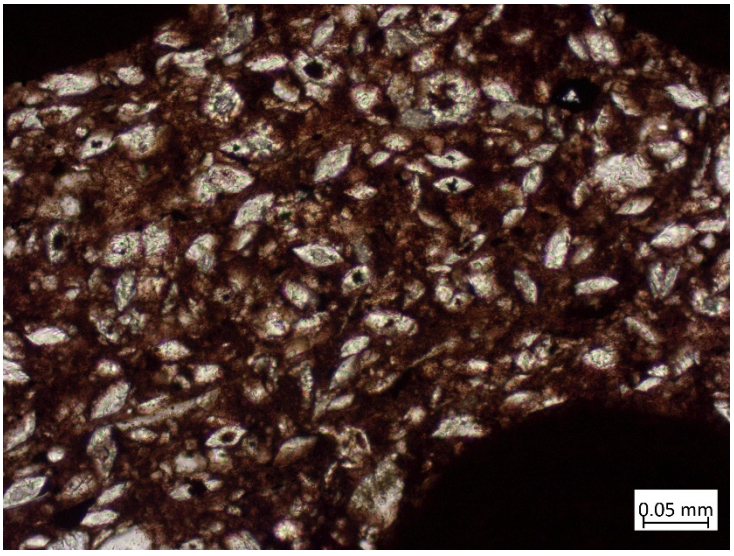

Fig. B-19:

Detail of Fig. B-18:
limonitic matrix with dolomite rhombohedrons with partly limonitic cores.

Thin section photo

MAR1-1-546.90
«Humphriesioolith Fm.»

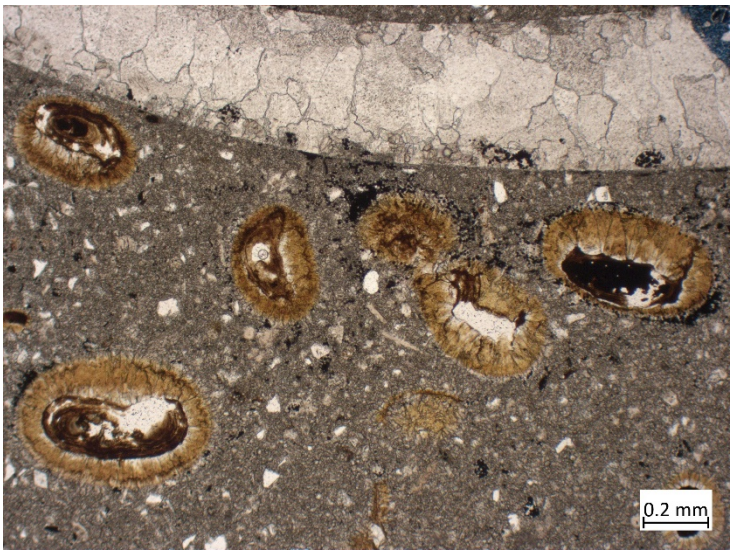

Fig. B-20:

Limestone (biodetritic, iron-oolitic):
iron-ooids, partly replaced by limonitic calcite, and a bivalve, sedimented in micrite

Thin section photo

MAR1-1-544.48
«Parkinsoni-Württembergica-Sch.»
(most probably «Parkinsoni-Oolith»)

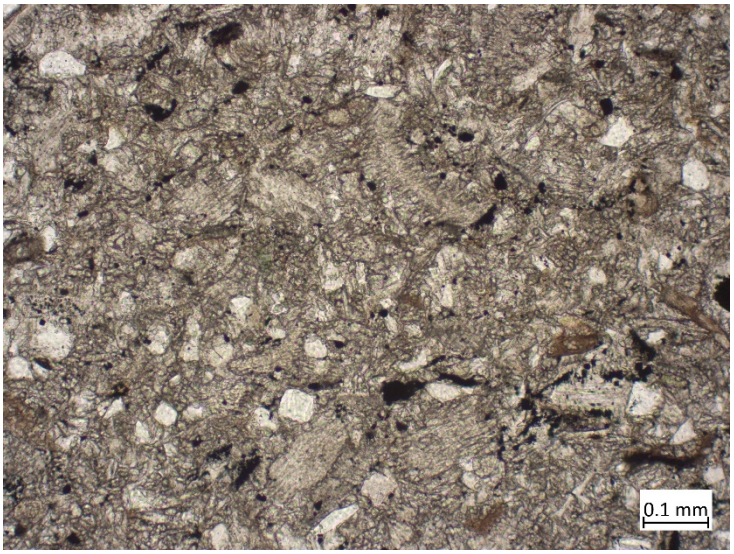

Fig. B-21:

Calcareous, quartz-rich bed: biodetritic limestone (silty): small bivalves and echinoderms as well as quartz silt, with micro-crystalline matrix and "stellate cement"

Thin section photo

MAR1-1-526.04
«Parkinsoni-Württembergica-Sch.»

Selected photos of microfacies from «Humphriesioolith Fm.» and «Parkinsoni-Württemb.-Sch.»

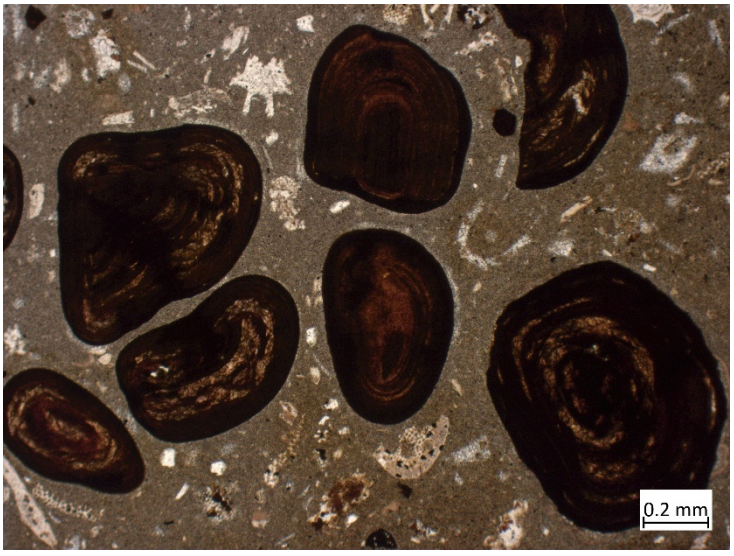

Fig. B-22:

Limestone (iron-oolitic): iron-ooids and small biodetritus, sedimented with micrite matrix

Thin section photo

MAR1-1-503.60
Wutach Fm.

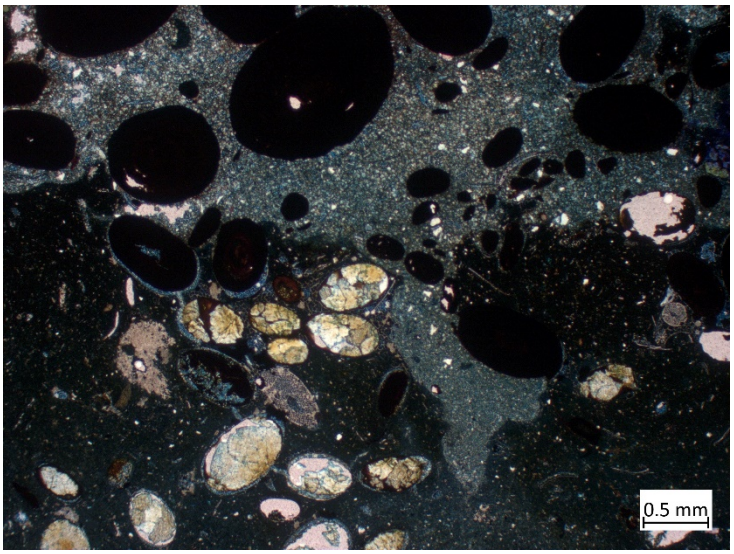

Fig. B-23:

Iron-oolite (marly): iron-ooids and iron-oolitic (now calcitic) intraclasts, sedimented with marly matrix

Thin section photo

MAR1-1-502.33
Wutach Fm.

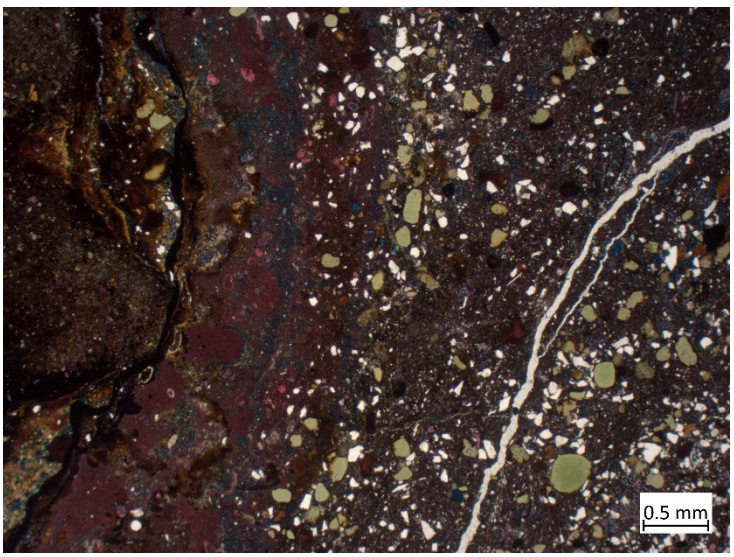

Fig. B-24:

Calcareous marl (sandy): glauconite grains (green), together with sand-sized quartz grains and a limonitic encrusted oncoid (to the left)

Thin section photo

MAR1-1-501.51
Wildegg Fm. («Mumienkalk Bed»)

Selected photos of microfacies from Wutach Fm. and «Mumienkalk Bed»

Appendix C: Plates of ammonites

Plate I MAR1-1 (723.40 – 705.04 m)

Fig. 1: *Amaltheus* ex. gr. *margaritatus* (de Montfort, 1808), depth: 723.40 m, Staffelegg Fm. (Rickenbach Mb.), Margaritatus Zone.
Fig. 2: *Grammoceras* sp., depth: 710.20 m, Staffelegg Fm. (Gross Wolf Mb.), Thouarsense Zone.
Fig. 3: *Pseudogrammoceras* ex gr. *fallaciosum* (Bayle, 1878), depth: 708.90 m, Staffelegg Fm. (Gross Wolf Mb.), Thouarsense Zone, Fallaciosum Subzone?
Fig. 4: *Dumortieria* sp., 3 fragments, depth: 708.23 m, Staffelegg Fm. (Gross Wolf Mb.), Levesquei Zone.
Fig. 5: *Pleydellia* ex gr. *buckmani* (Maubeuge, 1947), depth: 705.78 m, Staffelegg Fm. (Gross Wolf Mb.), Aalensis Zone, Torulosum Subzone.
Fig. 6: *Leioceras* ex gr. *subglabrum* (Buckman, 1902), depth: 705.04 m, Opalinus Clay, Opalinum Zone, Opalinum Subzone.

Most of the figures are illustrated in original scales; otherwise black bars indicate 1 cm.

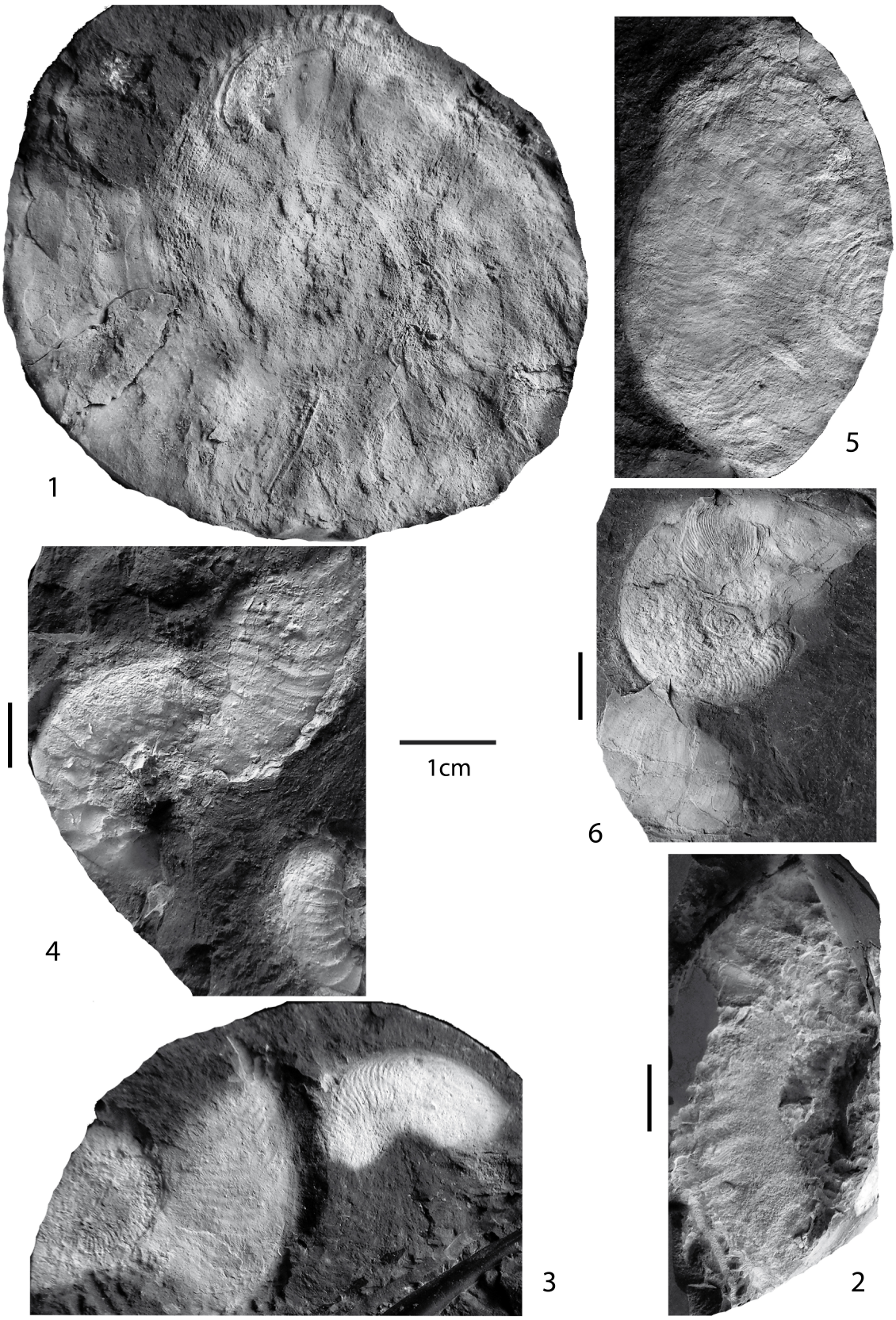

Plate I: MAR1-1 (723.40 – 705.04 m)

Plate II MAR1-1 (696.13 – 555.03 m)

Fig. 1: *Leioceras opalinum* (Reinecke, 1818), Microconch, depth: 696.13 m, Opalinus Clay, Opalinum Zone, Opalinum Subzone.

Fig. 2: *Leioceras* sp., depth: 597.85 m, Opalinus Clay, Opalinum Zone, probably Bifidatum Subzone (former «Comptum» Subzone).

Figs. 3a, b: *Staufenia* ex gr. *staufensis* (Oppel, 1858), depth: 589.19 m, «Murchisonae-Oolith Fm.», Bradfordensis Zone, Bradfordensis Subzone. 3a: lateral view, 3b: cross section.

Figs. 4a, b: *Emileia* sp., depth: 555.03 m, «Humphriesioolith Fm.», Sauzei Zone?. 4a: lateral view, 4b: cross section.

All figures are illustrated in individual scales; black bars indicate 1 cm.

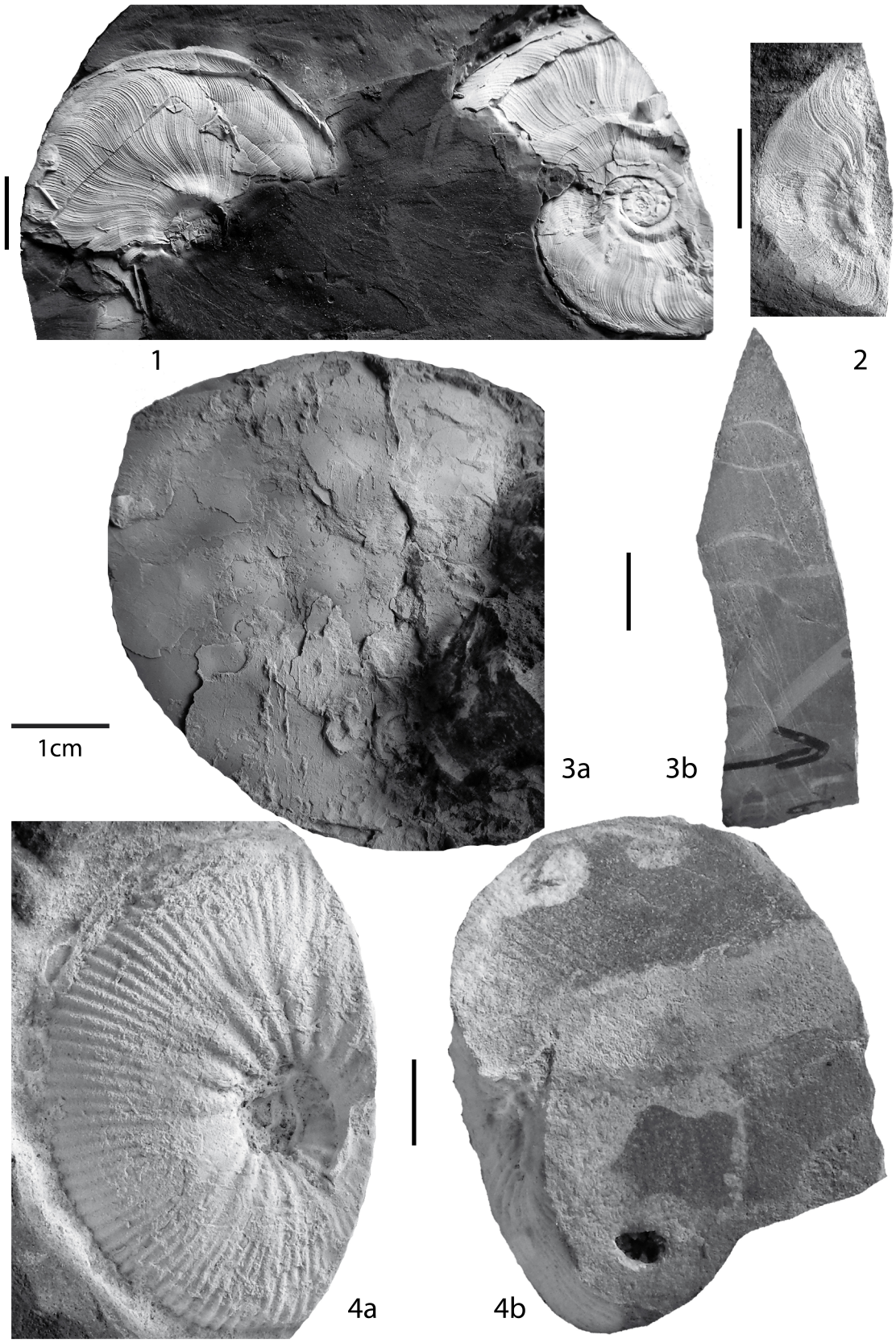

Plate II: MAR1-1 (696.13 – 555.03 m)

Plate III MAR1-1 (548.21 – 537.10 m)

Figs. 1a, b: *Chondroceras* ex. gr. *gervillii* (Sowerby, 1818), depth: 548.21 m, «Humphriesioolith Fm.», Humphriesianum Zone, Humphrisianum Subzone, *gervillii-cycloides* faunal horizon. 1a: lateral view, 1b: cross section.

Figs. 2a, b: *Stephanoceras* sp., depth: 547.66 m, «Humphriesioolith Fm.», Humphriesianum Zone, Humphrisianum Subzone. 2a: lateral view, 2b: cross section.

Figs. 3a, b: *Parkinsonia* ex gr. *subarietis-rarecostata*, Microconch, sharply ripped, depth: 544.39 m, «Parkinsoni-Württembergica-Schichten» (most probably «Parkinsoni-Oolith»), Parkinsoni Zone, Acris Subzone. 3a: lateral view, 3b: ventral view.

Fig. 4: *Parkinsonia* sp., Macroconch, depth: 544.28 m, «Parkinsoni-Württembergica-Schichten» (most probably «Parkinsoni-Oolith»), Parkinsoni Zone.

Fig. 5: *Parkinsonia* sp., Macroconch, depth: 543.61 m, «Parkinsoni-Württembergica-Schichten» (probably also «Parkinsoni-Oolith»), Parkinsoni Zone.

Fig. 6: *Parkinsonia* ex gr. *schloenbachi* (Schlippe, 1888)?, depth: 537.10 m, «Parkinsoni-Württembergica-Schichten», Parkinsoni Zone, Bomfordi Subzone?.

Most of the figures are illustrated in original scales; otherwise black bars indicate 1 cm.

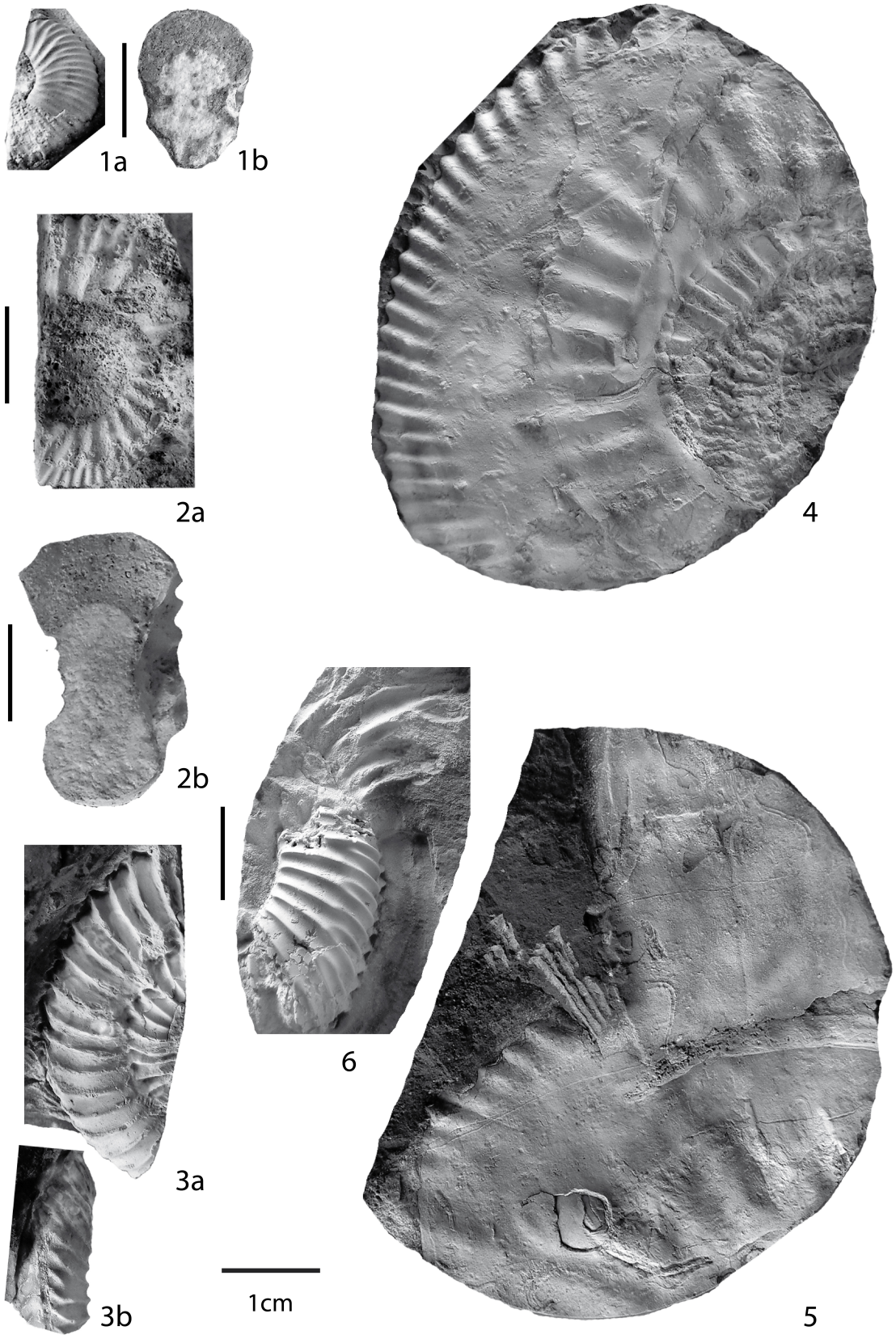

Plate III: MAR1-1 (548.21 – 537.10 m)

Plate IV MAR1-1 (518.36 – 494.27 m)

Fig. 1: *Oecotraustes* ex gr. *decipiens* (de Grossouvre, 1919), depth: 518.36 m, «Parkinsoni-Württembergica-Schichten», Early Bathonian.

Figs. 2a, b: *Macrocephalites* sp., depth: 502.87 m, Wutach Fm., Late Bathonian to early Middle Callovian, Early Callovian?. 2a: lateral view, 2b: cross section.

Fig. 3: *Ochetoceras* ex gr. *canaliculatum* (von Buch, 1831), depth: 501.52 m, Wildegg Fm. («Mumienkalk Bed»), Transversarium Zone?.

Fig. 4: *Euaspidoceras* ex gr. *oegir* (Oppel, 1863), depth: 494.27 m, Wildegg Fm. (Effingen Mb.), Transversarium to Early Bifurcatus Zone.

All figures are illustrated in individual scales; black bars indicate 1 cm.

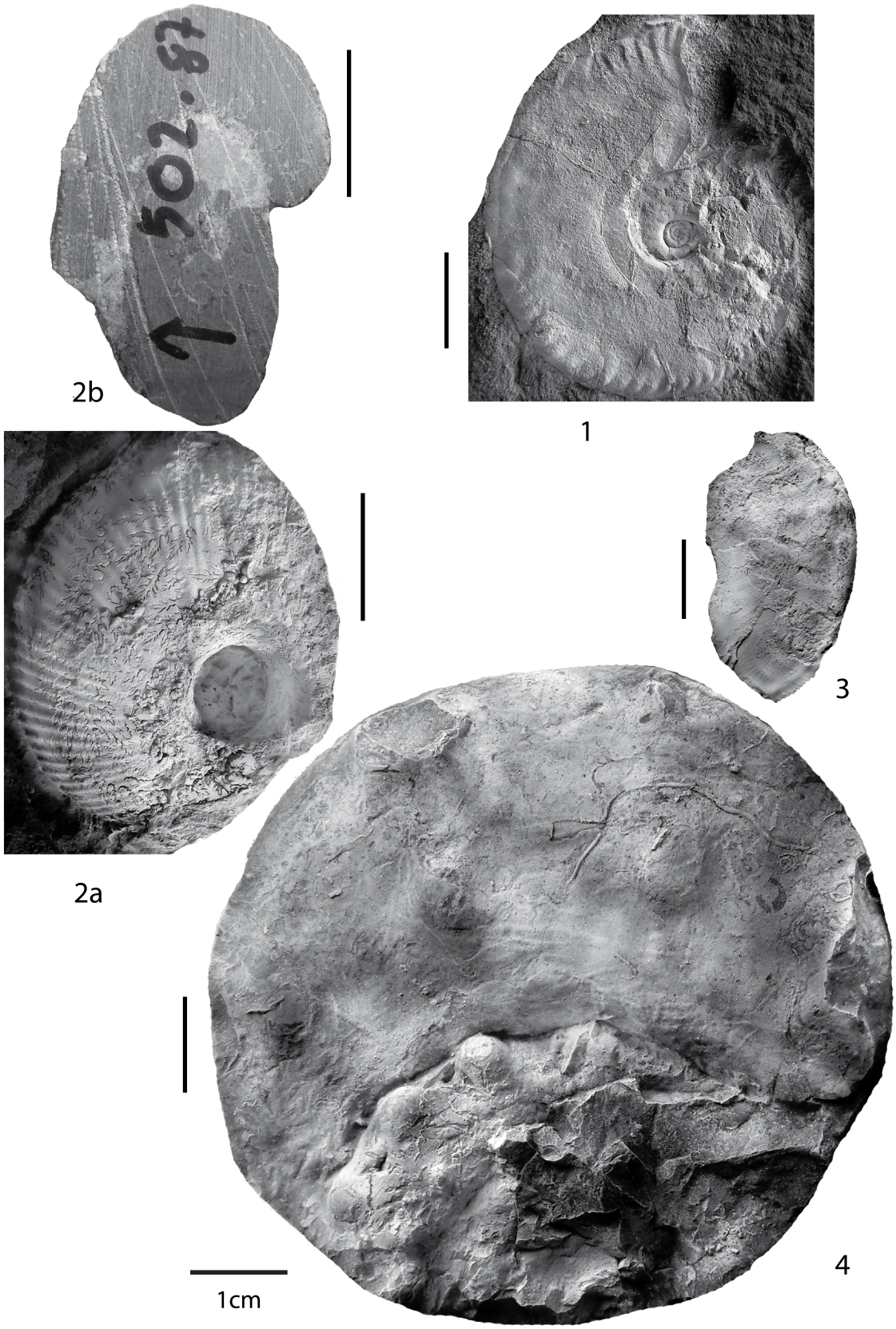

Plate IV: MAR1-1 (518.36 – 494.27 m)

Appendix D: Palynostratigraphy

Appendix D1: Range Chart: Quantitative stratigraphic distribution of Middle Jurassic palynomorphs in the Marthalen-1-1 borehole

Appendix D2: Depth/Age plot: Marthalen-1-1 borehole

Note: The appendices are only included in the digital version of this report (PDF) and can be found under the paper clip symbol.

Appendix E: Chemostratigraphy

Appendix E1: List of all geochemical samples and results mainly drilled from specific calcareous beds in the Opalinus Clay and its confining units

Data are discussed in Section 3.4 and partly illustrated in Fig. 3-4 (part of the data points lie outside the presented scale for the $\delta^{13}C_{carb}$): CC: drilled from a calcareous concretion, SC: drilled from a sideritic concretion, SN: drilled from a septarian nodule, MF: drilled from macrofossil, TS: drilled directly from thin section sample (see microfacies description in Section 3.1); The driftwood sample at 719.43 m is an organic measuremend ($\delta^{13}C_{org}$).

Depth [m]	**Description of sample**		**TS**	**$\delta^{13}C_{carb}$** [‰ VPDB]	**$\delta^{18}O_{carb}$** [‰ VPDB]	**Carbonate** [wt.-%]
510.08	Ammonite aptychus	MF		-0.81	-2.18	99.1
531.15	Belemnite	MF		-0.38	0.55	99.5
546.55	Belemnite	MF		1.49	1.01	104.3
548.04	Belemnite	MF		2.73	0.82	90.8
584.45	Belemnite	MF		1.39	0.24	101.4
589.22	Belemnite	MF		0.35	-0.48	101.9
589.23	Limestone (iron-oolitic)		×	0.28	-3.12	76.8
590.32	Iron-oolite with calcareous matrix		×	0.44	-4.79	79.3
591.01	Sideritic concretion	SC		-1.00	-0.49	35.5
595.06	Sideritic concretion	SC		-3.56	0.04	51.3
597.33	Calcareous Marl			-3.71	-4.98	56.4
600.44	Belemnite	MF		0.56	-0.94	103.9
600.50	Hardground		×	-2.04	-4.72	79.5
600.57	Hardground			-1.35	-1.36	84.0
603.69	Bioclastic marl		×	-4.96	-3.20	37.3
603.85	Septarian nodule	SN		-16.93	-1.30	78.8
603.85	Calcite vein from septarian nodule	(SN)		-5.66	-2.22	96.8
609.27	Sideritic layer, Fe-Ooids (calcitic)	SC	×	-3.00	-1.14	63.4
609.33	Sideritic concretion	SC		-6.37	-2.87	70.9
609.50	Calcareous marl			-4.87	-2.49	64.0
609.64	Hardground: calcareous concretion	CC	×	-3.81	-5.98	57.2
609.67	Belemnite	MF		1.53	-3.48	85.6
609.69	Hardground: calcareous concretion	CC		-18.06	-3.60	62.2
616.65	Sideritic concretion	SC		-0.18	-1.51	51.4
629.24	Hardground: calcareous concretion	CC	×	-16.99	-4.45	76.7
674.99	Sideritic concretion	SC		4.05	-0.35	54.9
695.13	Calcareous nodule	CC		-25.65	-2.11	80.2
695.22	Calcareous nodule	CC		-27.30	-1.52	93.0
705.27	Belemnite	MF		-0.17	-0.57	96.4
706.57	Belemnite	MF		1.50	-1.91	97.4
708.37	Belemnite	MF		0.48	-1.20	103.5

(continued)

Depth [m]	**Description of sample**		**TS**	**$\delta^{13}C_{carb}$** [‰ VPDB]	**$\delta^{18}O_{carb}$** [‰ VPDB]	**Carbonate** [wt.-%]
709.48	Belemnite	MF		0.56	-0.95	106.5
710.39	Belemnite	MF		0.53	-1.13	101.7
712.00	Belemnite	MF		0.86	-1.44	101.3
712.54	Belemnite	MF		0.79	-1.04	110.2
713.11	«Monotisbank» (Rietheim Mb.)			-0.99	-5.56	90.3
714.01	Belemnite	MF		1.33	-1.20	106.8
715.59	Belemnite	MF		1.19	-2.02	105.7
718.25	«Oberer Stein» (Rietheim Mb.)			-0.28	-6.37	81.8
719.25	«Homog. Kalkbank» (Rietheim Mb.)			-1.58	-4.03	94.1
719.43	Driftwood (organic sample)	MF		-26.84		
719.85	«Unterer Stein» (Rietheim Mb.)			-6.27	-3.30	94.3
720.00	«Unterer Stein» (Rietheim Mb.)			-2.05	-4.35	99.1
720.91	Belemnite	MF		2.50	-0.86	110.1
721.58	Belemnite	MF		1.30	-0.96	109.6
721.94	Belemnite	MF		0.36	-0.43	103.7